

# MASS PRODUCTION OF THIN FOIL LASER TARGETS FOR USE ON NEXT GENERATION LASER FACILITIES

*Chris Spindloe, S. Tomlinson, M. Tolley*

*Central Laser Facility, Science and Facilities Technology Council*

*G. Arthur*

*Scitech Precision Ltd, Rutherford Appleton Laboratory*

*S. Astbury*

*York Plasma Institute, Department of Physics, University of York*



Science & Technology  
Facilities Council

# OVERVIEW

- Background to high rep rate requirements
- Current Facility Requirements for HPL Targets
- The first RAL high rep rate experiment
- Developments in target mass production
- The Nano-positioning wheel
- First fabrication runs
- Flexibility vs. target numbers
- Finalised design and next stages.



# SCOPE

2008 - high power laser shots < targets available

2010 - high power shots >> targets available

What to do with extra shots?

How do we delivery targets to these shots?

Applications based experiments – security,  
medical, IFE?



The increasing number of high rep-rate, high power laser systems in the world can run at rates of up to 10Hz.

For 10 Hz it may be necessary to use (established) real-time target delivery techniques

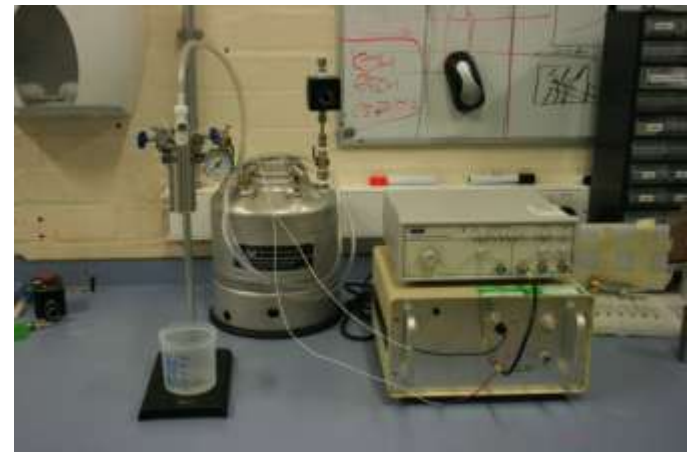
- Tapes (including multilayer)
- Structured tapes
- Droplets
- Gas jets



Tape speed ~ 5mm/sec

Tape substrates - Copper, PE, Al, PET (Mylar)

R&D Programme to produce multi-layer tapes



In continuous operation at 16Hz one IFE reactor will require:

~ 1 500 000 targets per day

Future systems such as ELI will be running in the kHz regime.

Targets for these experiments cannot be produced using current techniques and so new technologies need to be implemented.

One possible solution to this is to use MEMS technology integrated with injection/insertion systems.

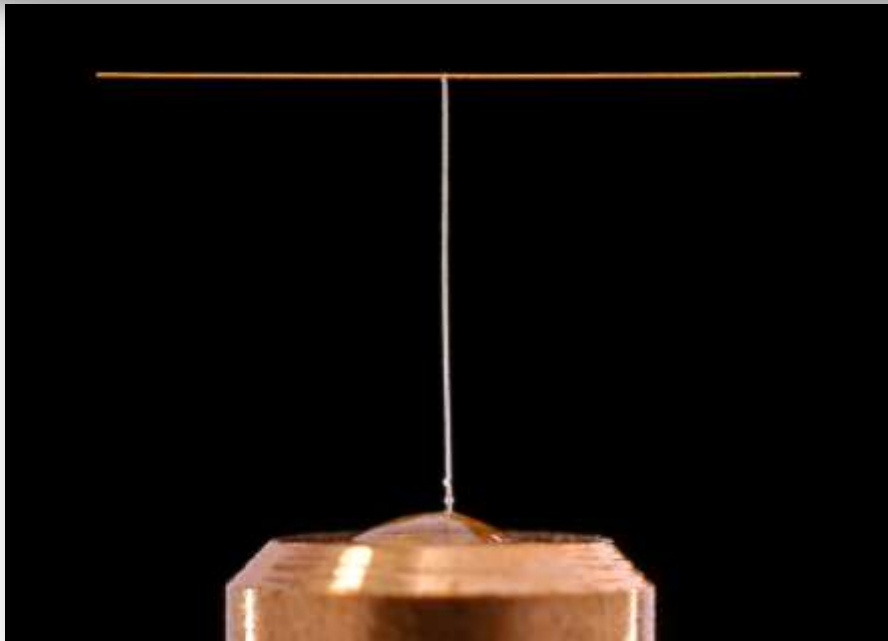
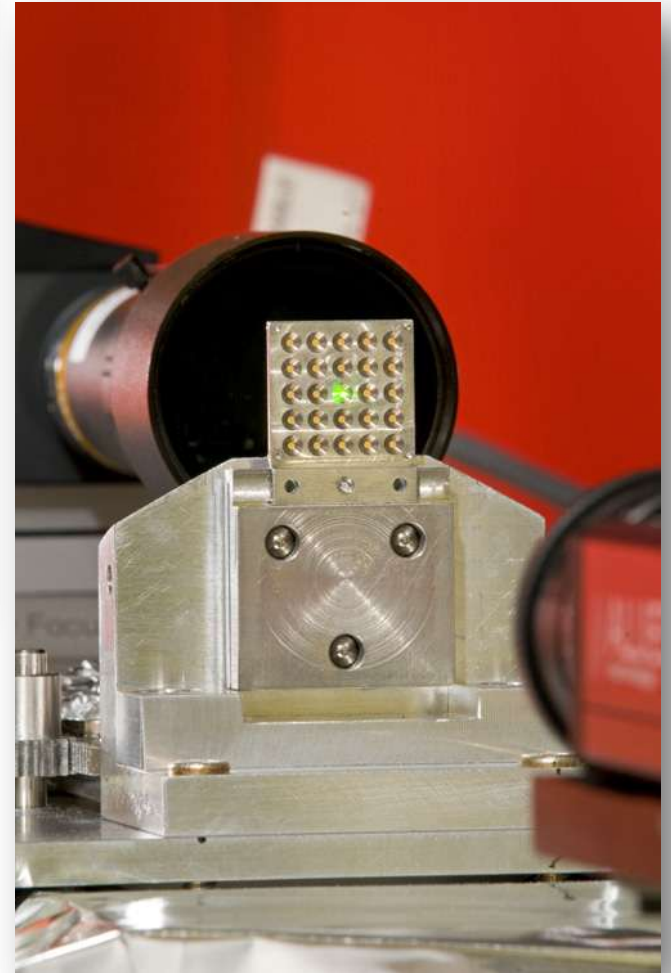
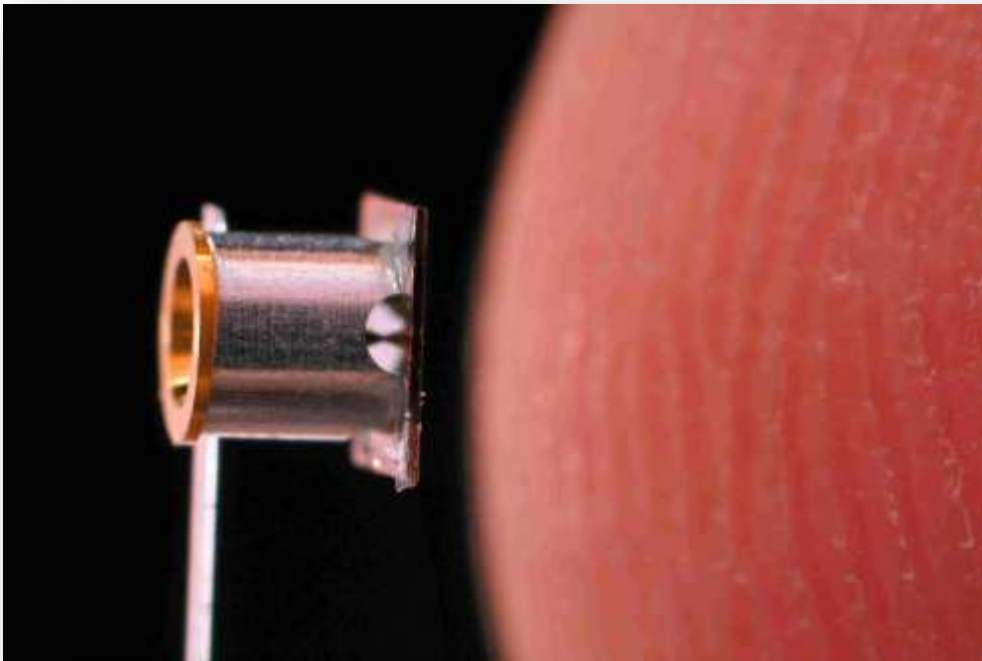


# GENERAL TARGET TYPES

It is difficult to define categories or groups for high power laser targets as they are inherently different for each type of experiment. However they can be loosely grouped into the following.

- Simple Thick Foil Targets ( $>1\mu\text{m}$ )
- Thin Foil Targets (20nm-1 $\mu\text{m}$ )
- Ultra Thin Foils ( $<20\text{nm}$ )
- Multi-layer or complex films
- Single component 3D targets
- Multi-component 3D targets
- Multi-target arrays





# APPLICATIONS BASED TARGETS

The first HRR solid target experiment at RAL shot over 3000 targets, most of these were thick but the interesting science is carried out using the ultra thin foils, using thin foils for statistical data and using more complex targets.

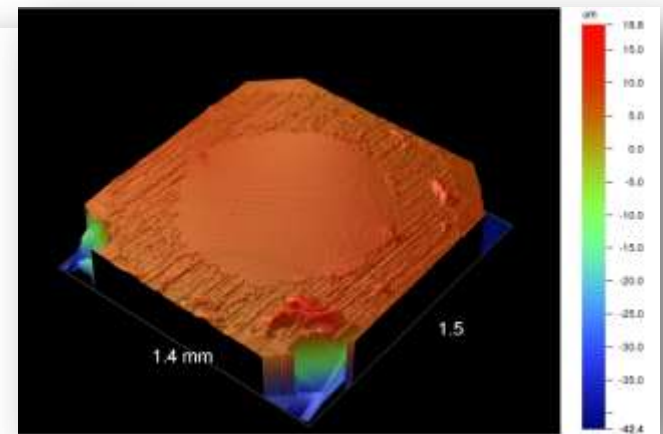
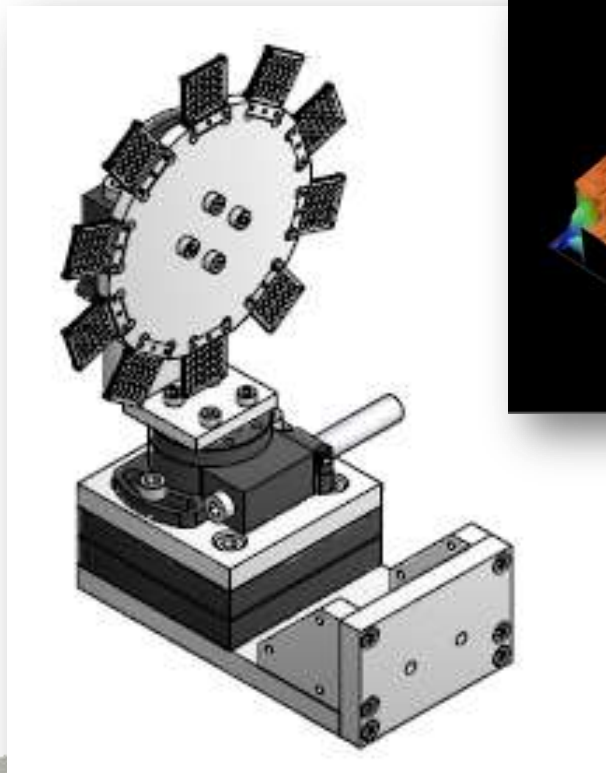
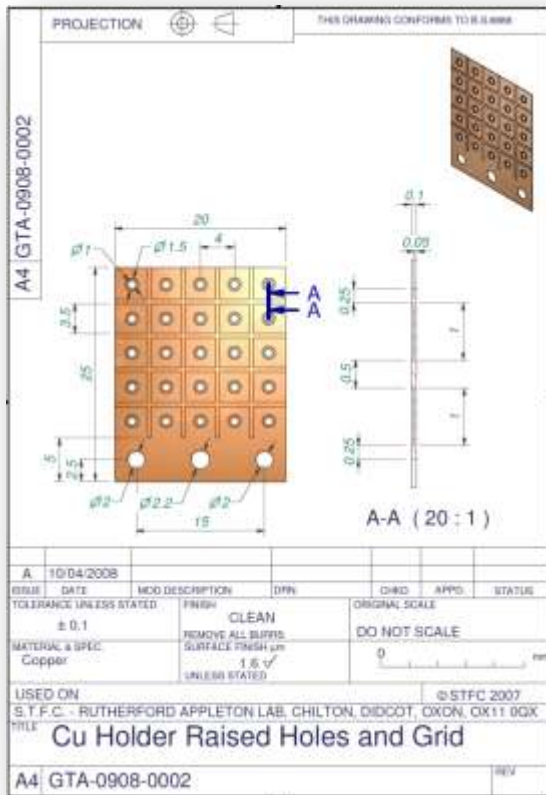
These complex targets are possible to make but are more difficult to fabricate for higher rep-rates. Examples of these are:-

- Ultra thin foils
- Ultra thin foams
- Micro-spoke targets
- Wire arrays
- Limited mass (100um x 100um squares).





The first HRR experiments were delivered using a 'puck' and wheel arrangement. This is labour intensive to deliver as each foil has to be floated onto a mount, characterised logged and then attached to the wheel. While the quality of the foils was good, there are a limited number of shots that are available to the user group and as you move to thinner foils (<20nm) the yield of the targets on a 'puck' is low.



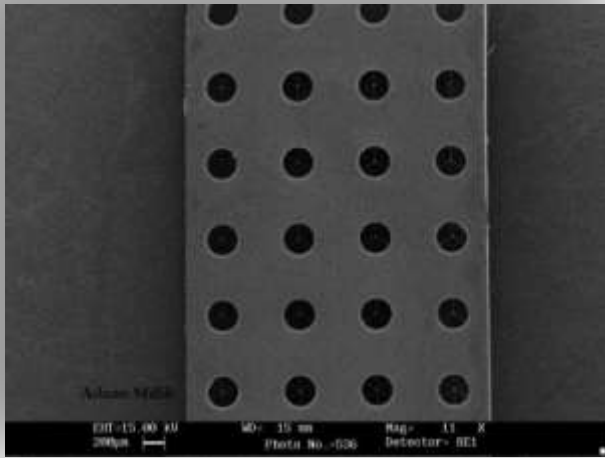
# MASS-PRODUCTION DEVELOPMENTS

There have been a number of developments in mass-production of targets, including using CNC milling machines to batch produce parts.

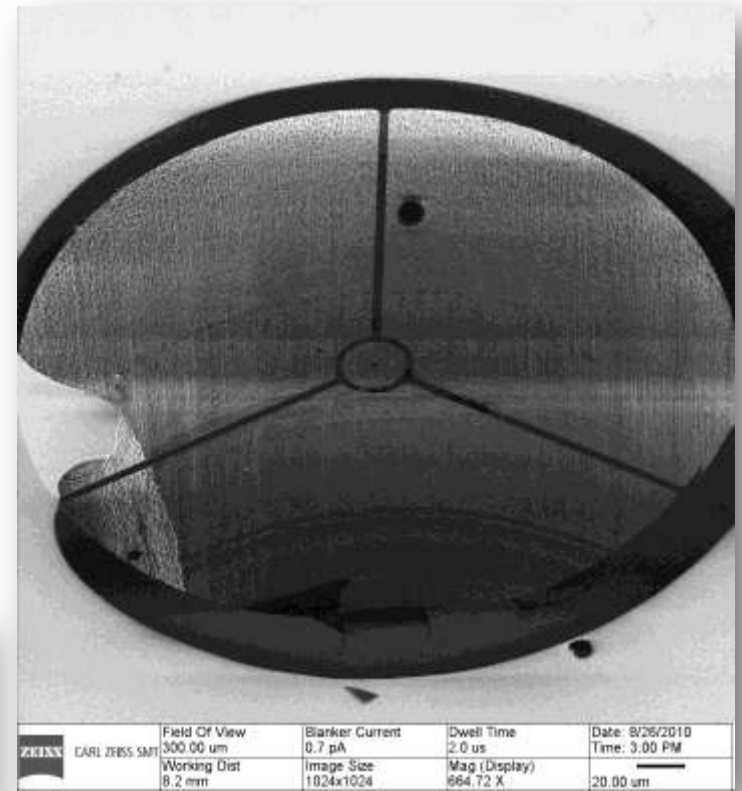
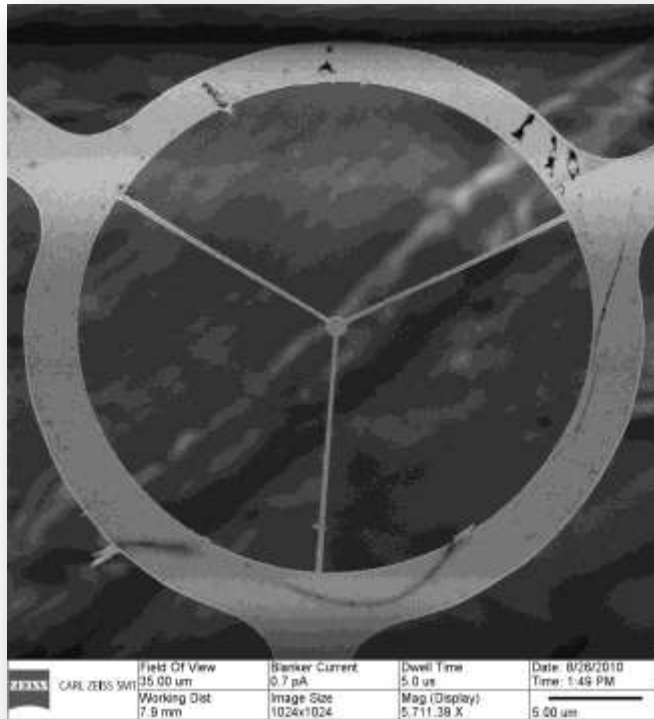
However, the only realistic way of producing targets for the HRR laser systems of the future is to use MEMS (Micro-electro-mechanical systems). This has advantages of large volume manufacture with high based fabrication yields and allows targets that cannot be conventionally machined to be fabricated

RAL has produced 2D and 2½ D components in the past using these techniques and this could be developed to provide a targetry stream for all HRR laser systems that is cost effective.





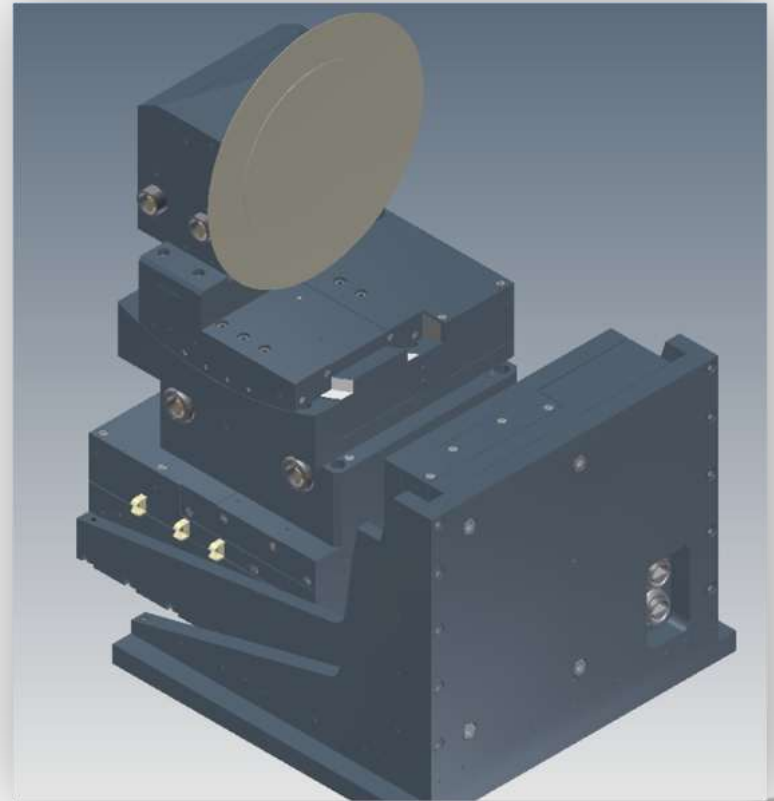
Membrane targets - 32um diameter, 40nm thick  
SiN membranes supported on 1µm wide, 40nm  
thick arms



# NANO-POSITIONING WHEEL

A design for a high specification target wheel with 6 axis translations a small footprint and high accuracy drives was produced. The wheel can hold 4" or 6" wafers.

- 3 Linear Translations
  - Travel = 60mm
- 3 Rotational Translations
  - 2 X Travel = 360°
  - 1 X Travel = 30°
- Small Footprint
  - 230mm x 260mm
- Encoded Resolution
  - 20nm



# NANO-POSITIONING WHEEL

The targetry solution for the wheel are designed to achieve the following aims.

- Standard design Si wafers can be used
- Standard geometries of target layout can be used
- Recipes for variation of hole separation etc.
- Recipes for variation of foil material and thickness.

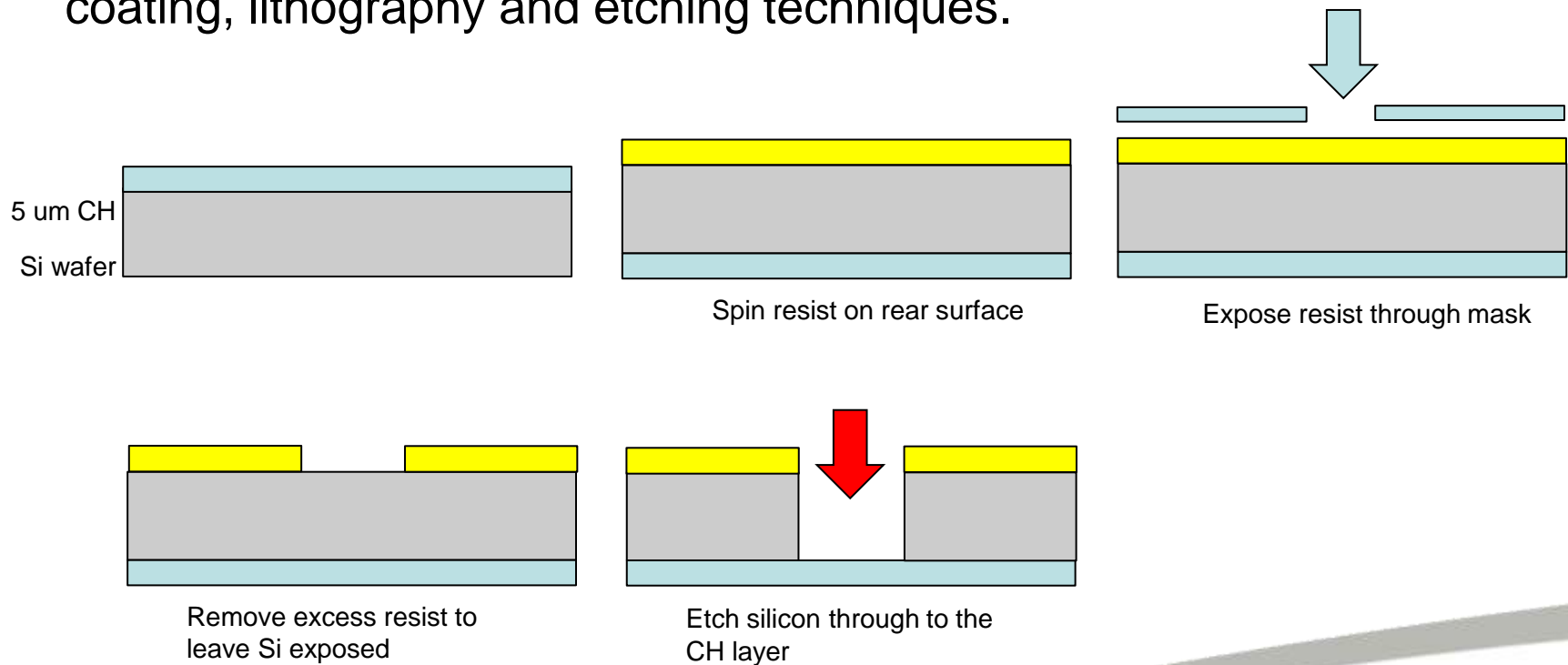
Essentially this is a 'off the shelf' target that can be used for a variety of both application and science based experiments.

It is also essential that 1000's of targets could be fielded onto a target wheel to take advantage of the high repetition rate of the latest generation lasers and also to make the wheel experimentally feasible.



# TARGETRY DEVELOPMENT

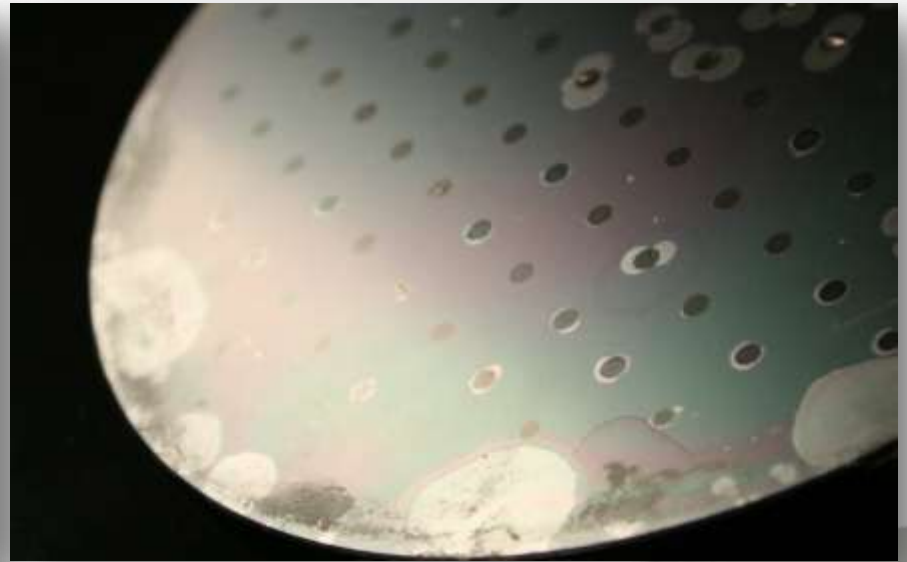
To deliver a robust targetry solution to the wheel 4" or 6" wafers need to be processed to delivery 1000's of targets on a single wafer. Using MEMS techniques a target can be produced on a wafer using coating, lithography and etching techniques.



# TARGETRY DEVELOPMENT

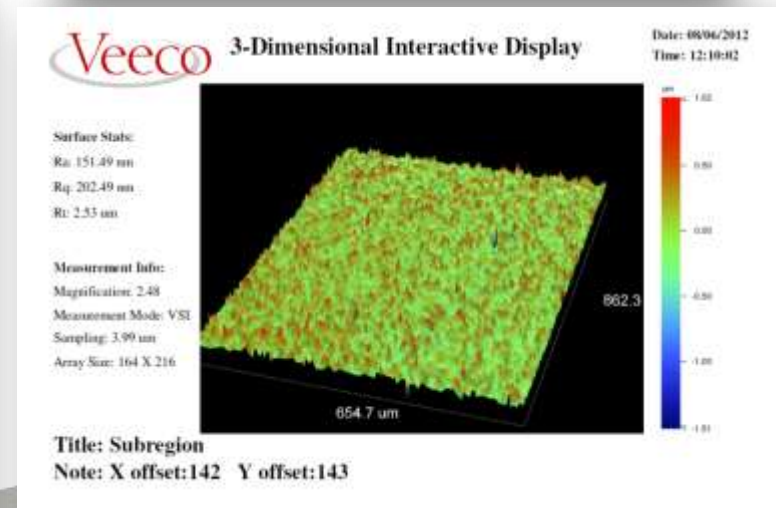
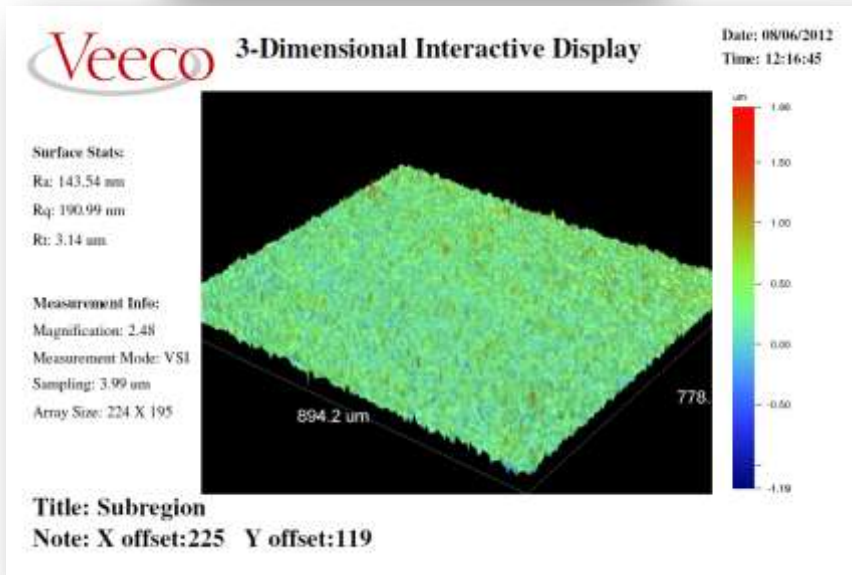
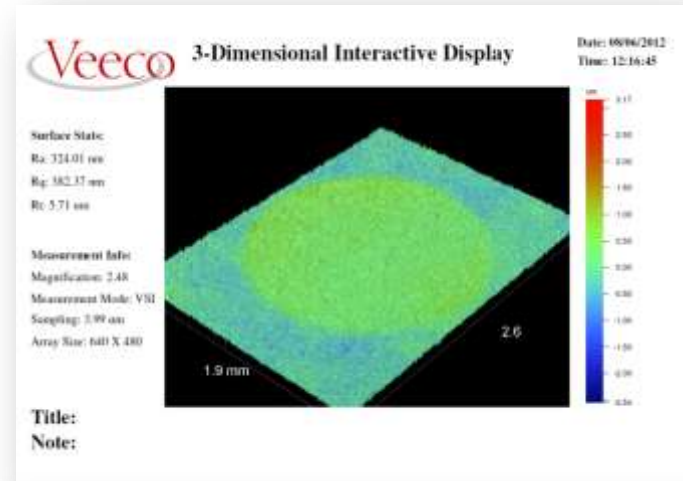
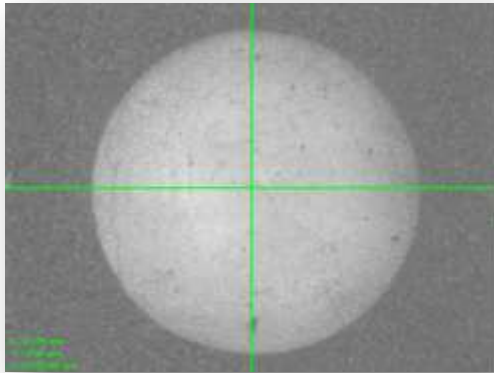
This technique was used to pattern a 100mm wafer with a number of holes. A 5um Parylene layer was used for the target foil.

A 100% yield was achieved with the foil produced exhibiting excellent flatness. (Dependent on the initial substrate roughness)



# TARGETRY DEVELOPMENT

The surface roughness of the film is similar to the surface roughness of the unpolished Si wafer.

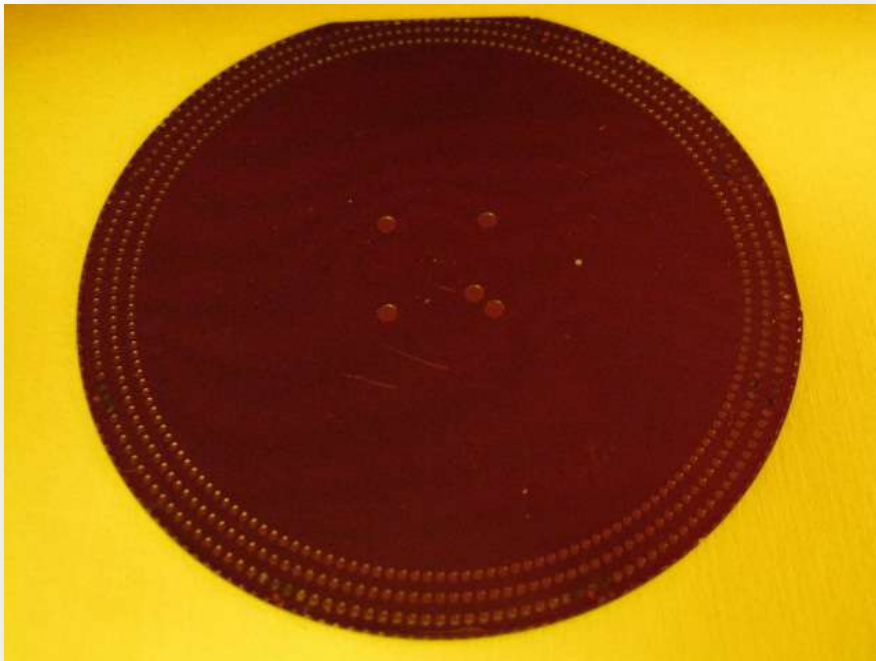




# TARGETRY DEVELOPMENT

A mask was produced to allow the wafer to be fitted to the wheel and also to pattern a large number of targets around the circumference. The material used for the target was 50nm SiN and a similar etching process was used to the previous targets.

Although successful the yield of the targets was low – due to etching variations across the diameter of the wafer.



- 3 concentric rings of ~500 thin film targets
- 50nm thick silicon nitride
- 500 $\mu$ m diameter
- 300 $\mu$ m thick wafer



# FLEXIBILITY VS. TARGET NUMBERS

There is an inherent problem with a single silicon target piece as a component for the wheel. This is that only one target type can really be supplied per wheel.

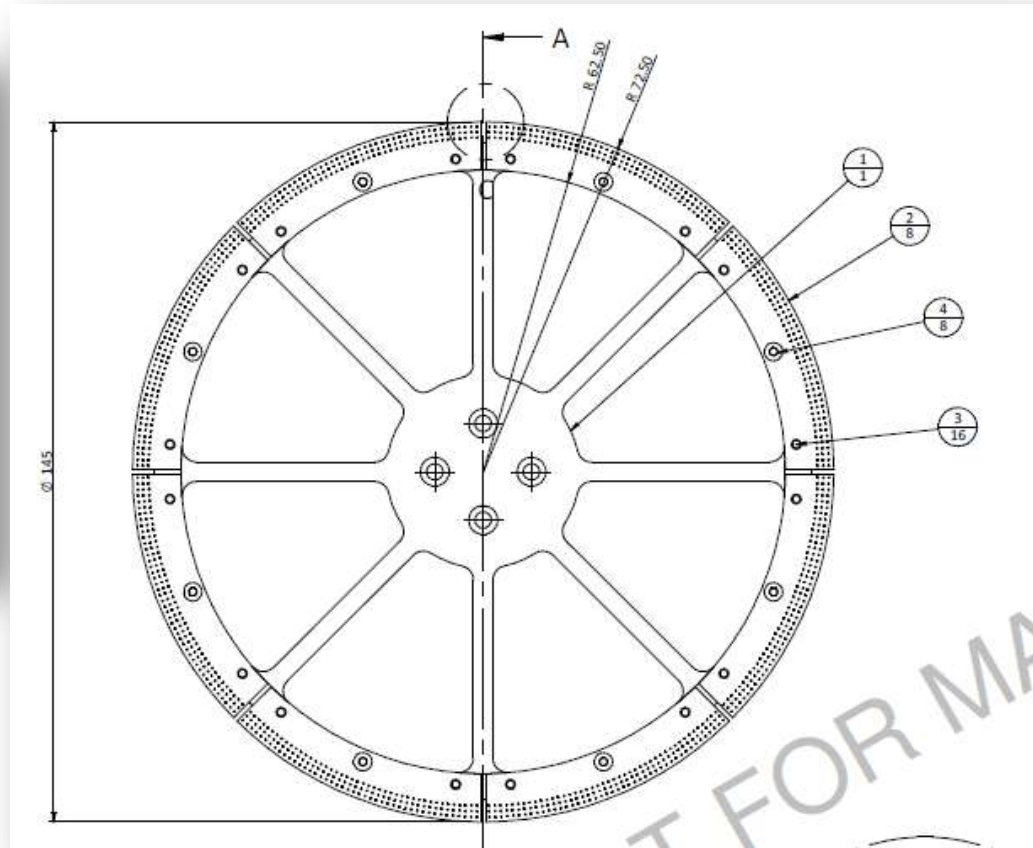
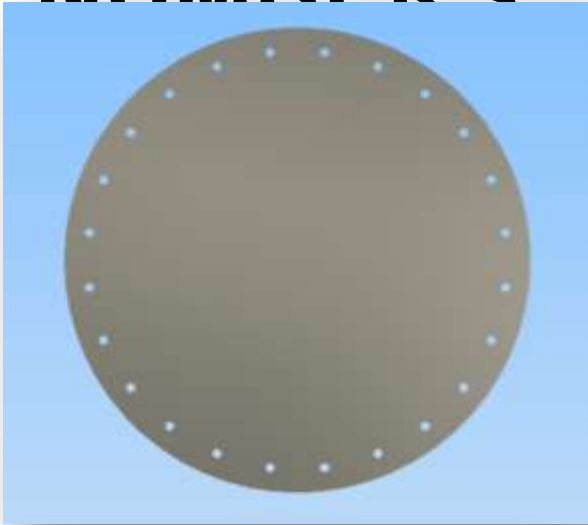
Experience has shown that the ideal experiment has a large number of targets but also variation in parameters such as material, foil thickness.

It was therefore decided to split the wheel into sections and to be able to deliver 'slices' of wafers onto a holding ring.

This approach still delivers a mass produced target that can be 'off the shelf' but gives experimental flexibility and will allow maximum use of laser time which can be up to 4x oversubscribed.



# FLEXIBILITY VS. TARGET NUMBERS



# COMPLETED WHEEL SECTIONS



The completed wheel sections

Protection layers are removed using a number of dry and wet etching techniques

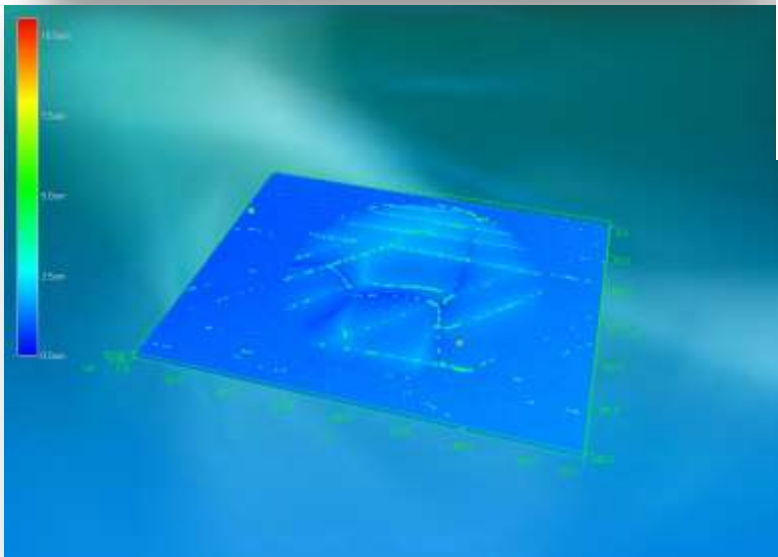
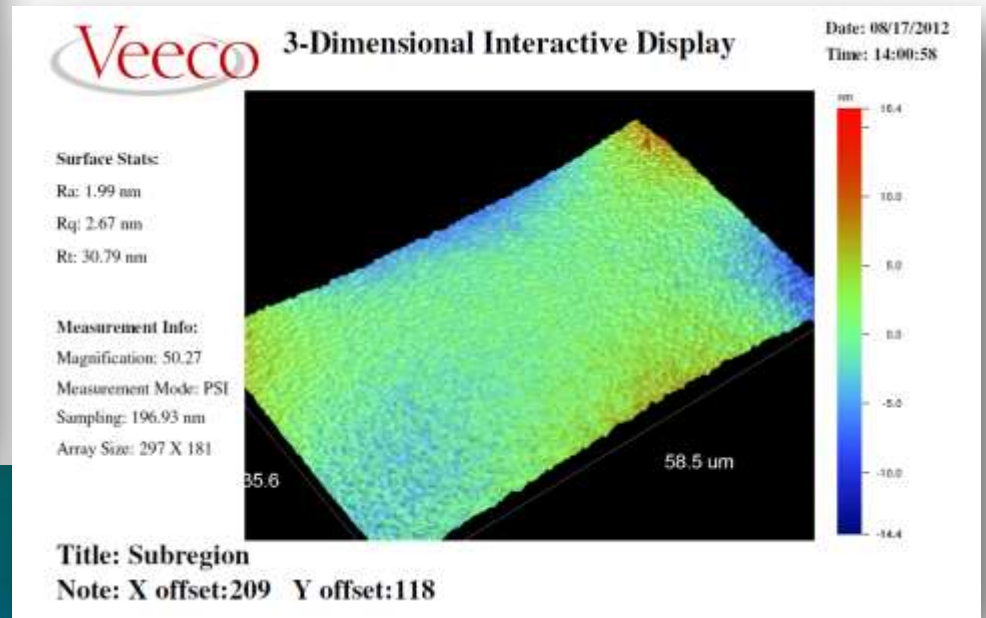
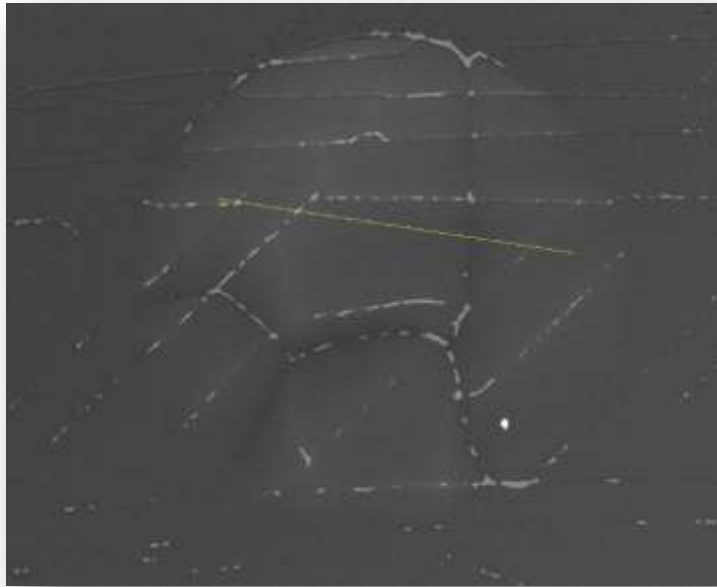
Yield from a 100mm wafer is almost 100% for 5um thick CH foils.

Foil roughness has been reduced to levels comparable to float off techniques.

Sections can be attached to the ring as required for each experiment.



# COMPLETED WHEEL SECTIONS



# COMPLETED POSITIONING WHEEL



# NEXT STAGES

Further work is required to establish production techniques to:

- Produce thinner films
- Measure wheel repeatability
- Investigate shock damage
- Integrate more complex targets

However initial trials have shown that simple thin foil targets can be produced in high numbers and the nano-positioning wheel has the ability to be a flexible method of delivering these targets to an experiment.



# THANK YOU

M. Tolley and S. Tomlinson,

*Central Laser Facility, Science and Facilities Technology Council*

G. Arthur

*Scitech Precision Ltd, Rutherford Appleton Laboratory*

S. Astbury

*York Plasma Institute, Department of Physics, University of York*

E. Barber, S. Serra





# Fabrication of Mass Produced Microdot Arrays for use as Micro- Targets on High-Repetition Rate Experiments.

**Graham Arthur<sup>1</sup>, Chris Spindloe<sup>2</sup>**

*<sup>1</sup> Scitech Precision Ltd., Rutherford Appleton Laboratory, Harwell  
Oxford, Didcot, Oxon. OX11 0QX, UK*

*<sup>2</sup> Central Laser Facility, Rutherford Appleton Laboratory, Harwell  
Oxford, Didcot, Oxon. OX11 0QX, UK*

# Outline

1. Background/Motivation

2. Target Design

3. Fabrication

- Basic processes
- Special Precautions
- Putting it all together

4. Conclusions

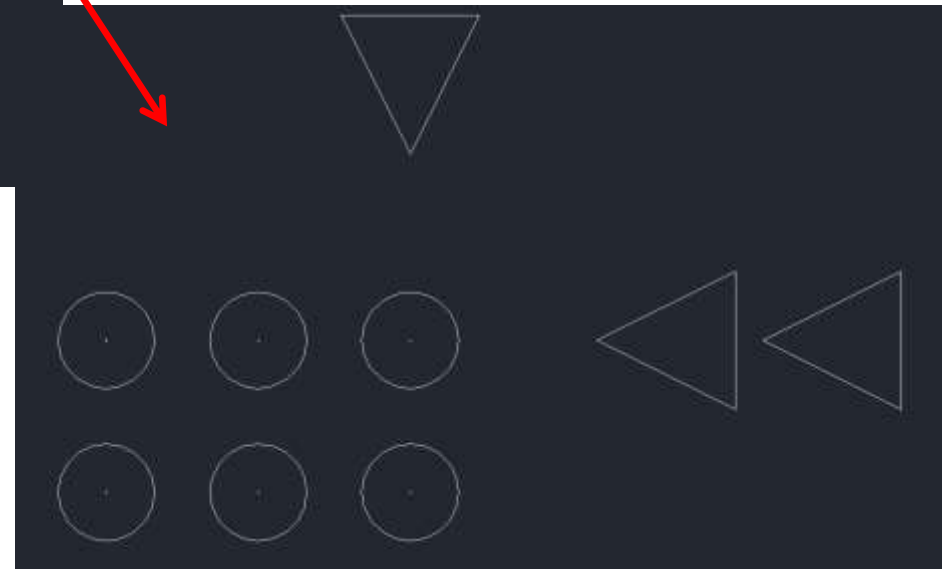
5. Questions

# Background

- Small target size
  - In cases where the is focused beam on a large target, the range of intensities may cover many orders of magnitude (e.g. FEL x-ray source)
  - Micro-scale target intercepts the beam at specific intensities
- Large arrays
  - Where high repetition rates are used
  - MEMS-based fabrication allows 10s – 1000s to be easily fabricated in precisely defined arrays

# Target Design

- Micro-dot size
  - Typically a few microns in diameter
  - Thickness up to a few microns – experiment/material dependent
  - Each dot is supported on a thin, low-Z (CH) membrane over a cavity in the support substrate
- Array size
  - Typically 40 x 40 (1600 dots)
  - Potentially could be much larger (e.g. 100 x 100 or more)



# Fabrication

- MEMS-based fabrication processes
  - **Substrate**
    - (usually) silicon wafer
  - **Patterning**
    - Microlithography (optical or e-beam)
  - **Deposition**
    - sputter, thermal evaporation, CVD, electro-deposition, spin/dip-coating
  - **Etching**
    - dry (plasma) etching, wet etching



Spin-coater



Mask aligner



E-beam



DRIE



RIE



Stepper

## Special Precautions

- Semiconductor manufacturers use a relatively limited range of materials
  - Silicon, aluminium, gold, chromium, copper, .....
- Laser Target Fabrication requires a much wider range of materials
  - Nd, Sm, Te, CsI, Sn, Au, Cu, Bi, Ag, Gd, Fe, etc, etc.
- To ensure compatibility during processing, it may be necessary to add extra masking layers, e.g.,
  - Standard Gold etch solution also etches iron
  - Adhesion of metallic coatings on polymers or Si



## Putting it all together

Example Fe microdots as laser targets

- **Fe dot targets on a suspended CH film**
  - Fe dots
    - Diameter = 5  $\mu\text{m}$  diameter
    - Thickness = 2  $\mu\text{m}$
  - CH film
    - Thickness = 1  $\mu\text{m}$
  - Substrate - Silicon
    - Cavity diameter = 350 $\mu\text{m}$
    - Array size = 40 x 40 (1600 targets)

Single-side polished silicon wafer. (~400um thick)



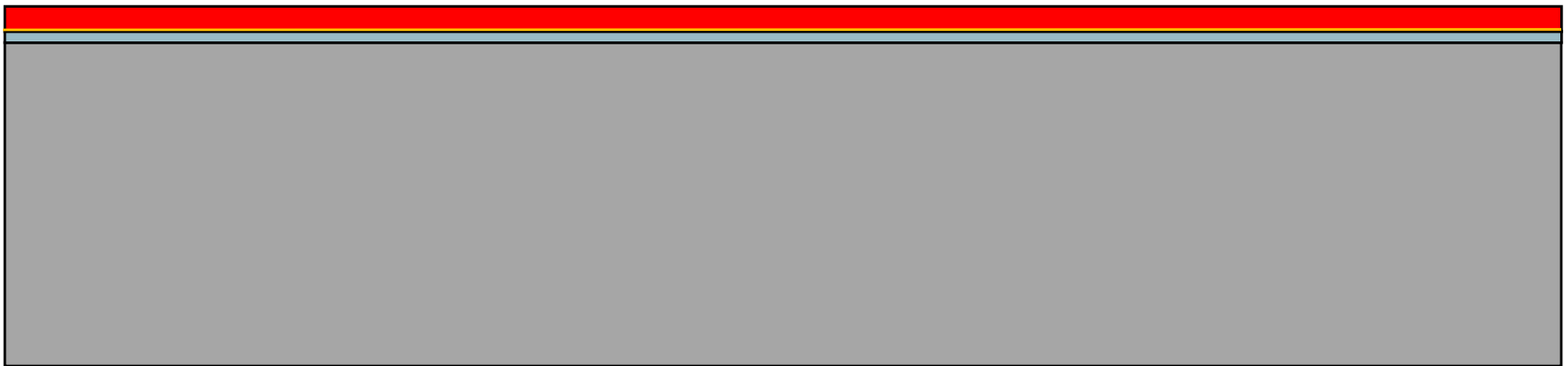
Deposit Parylene Layer (1 micron)



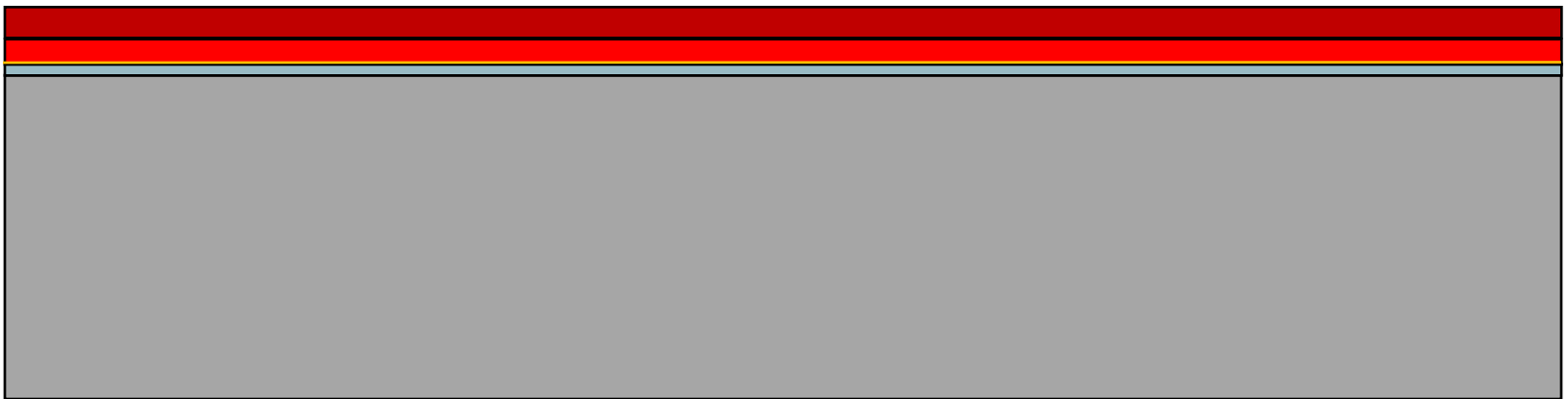
Deposit adhesion layer (approx 5nm)



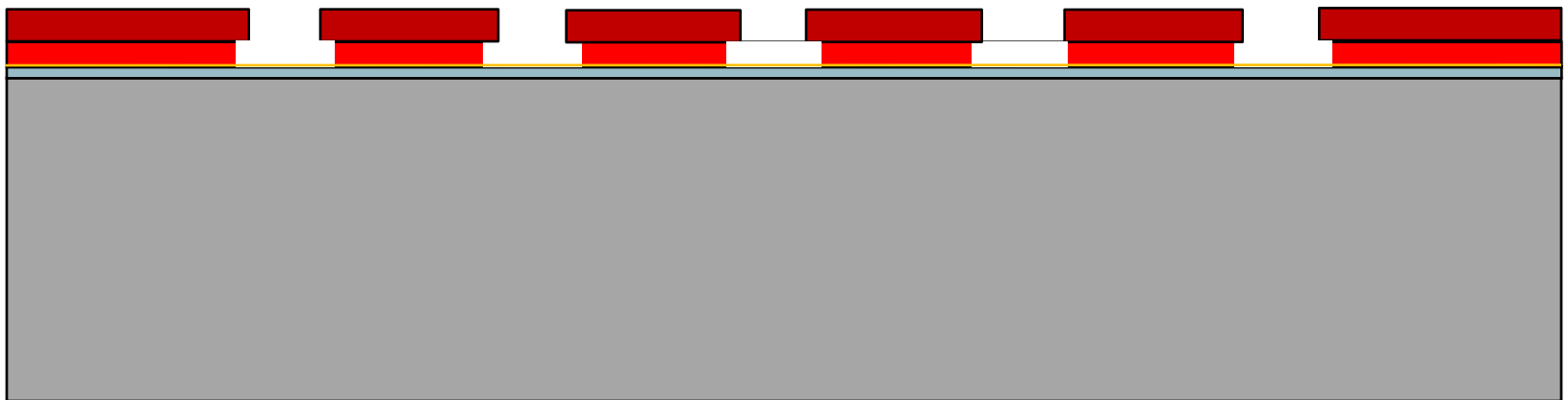
Deposit bottom LOR resist layer (thickness to suit dot thickness)



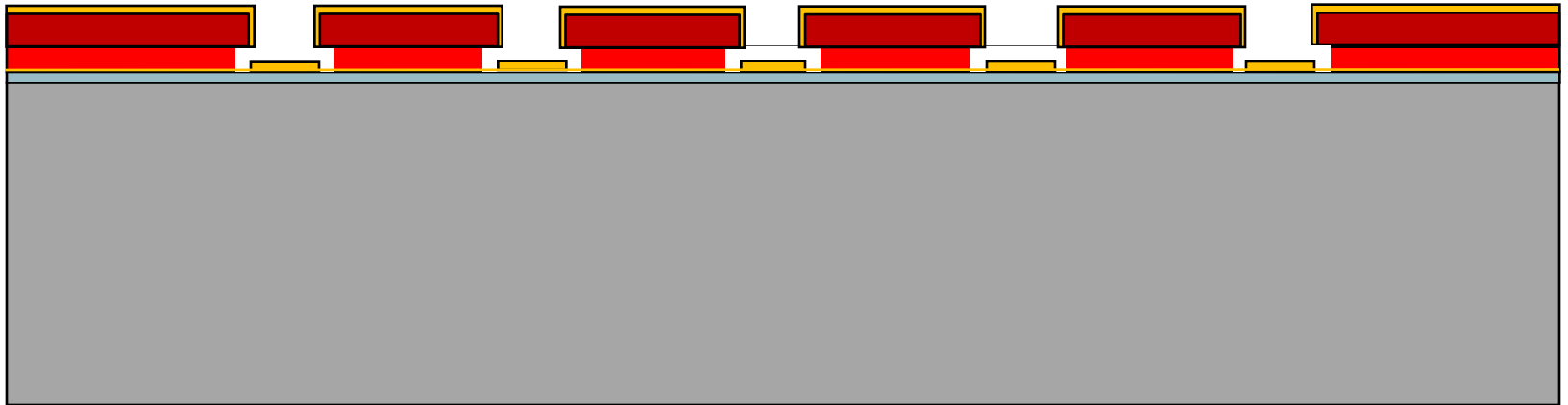
Deposit top imaging resist layer ( $\sim 1\mu\text{m}$ )



## Expose & develop bilayer holes

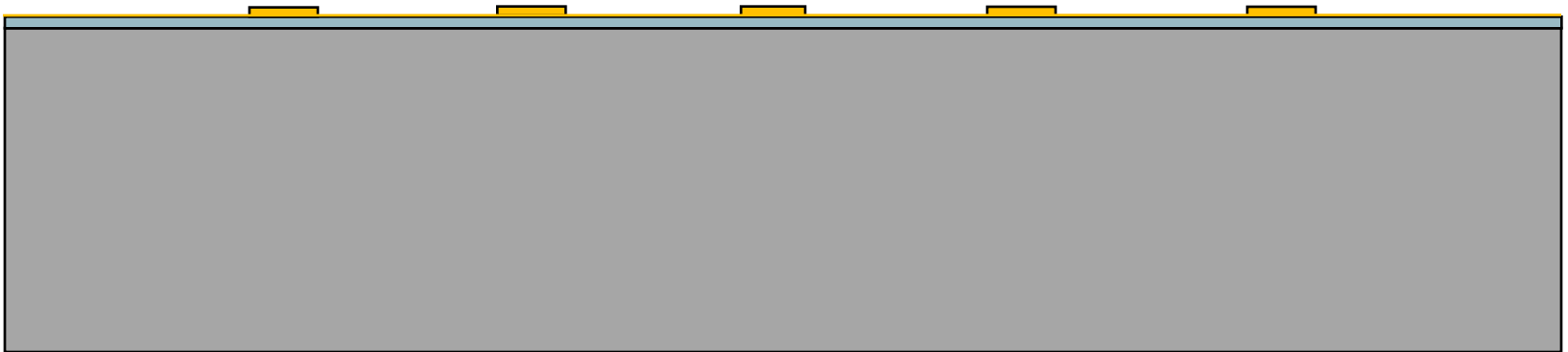


## Thermal deposition of Fe layer (1-2um)

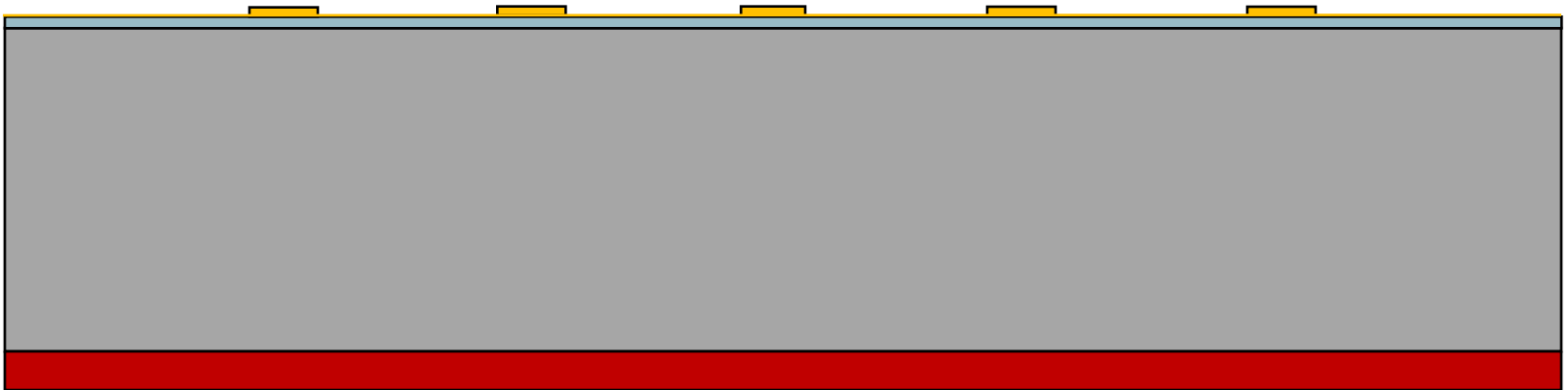




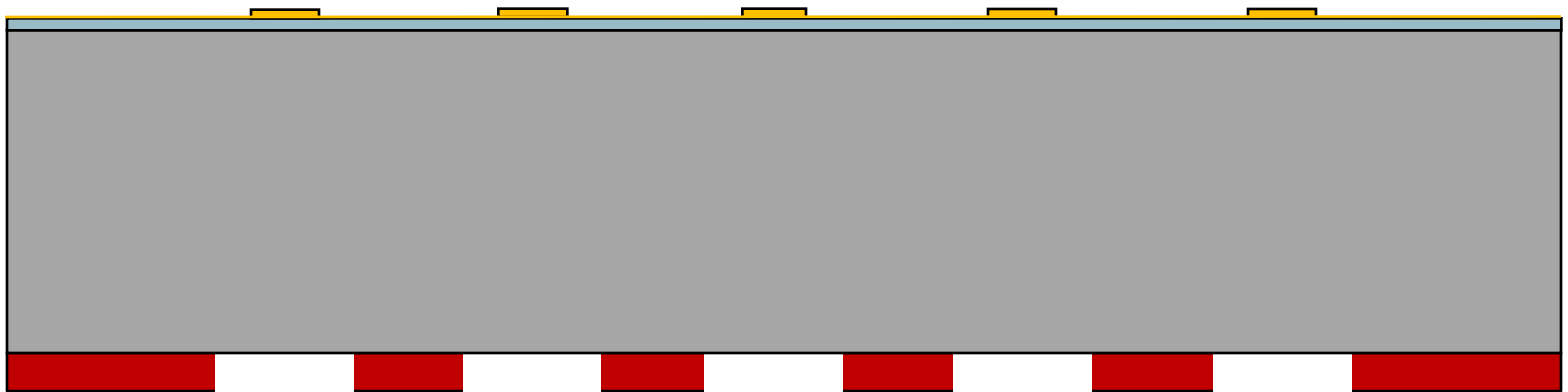
Lift-off resist to leave metal dots



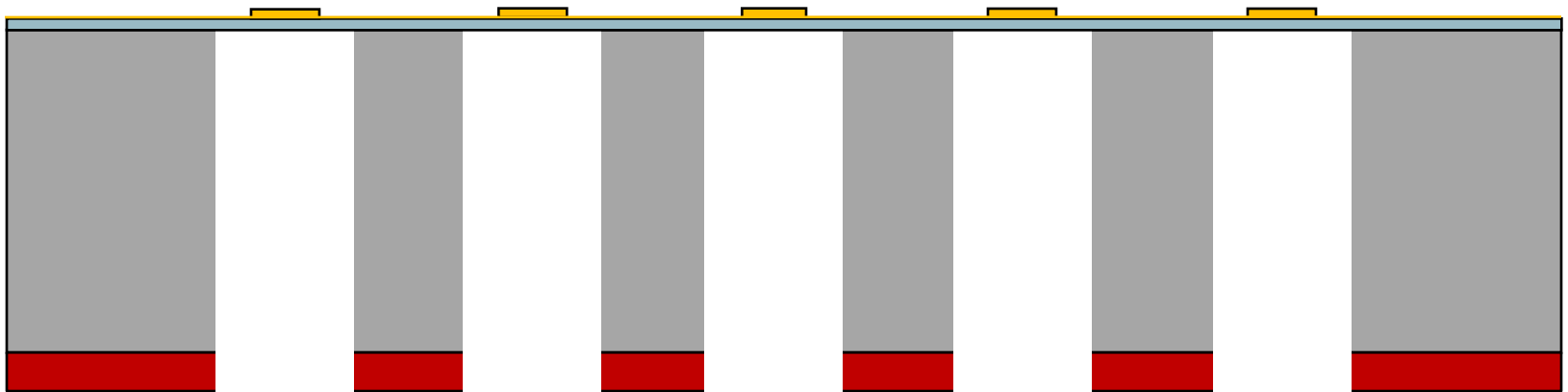
## Spin-coat DRIE resist on lower surface



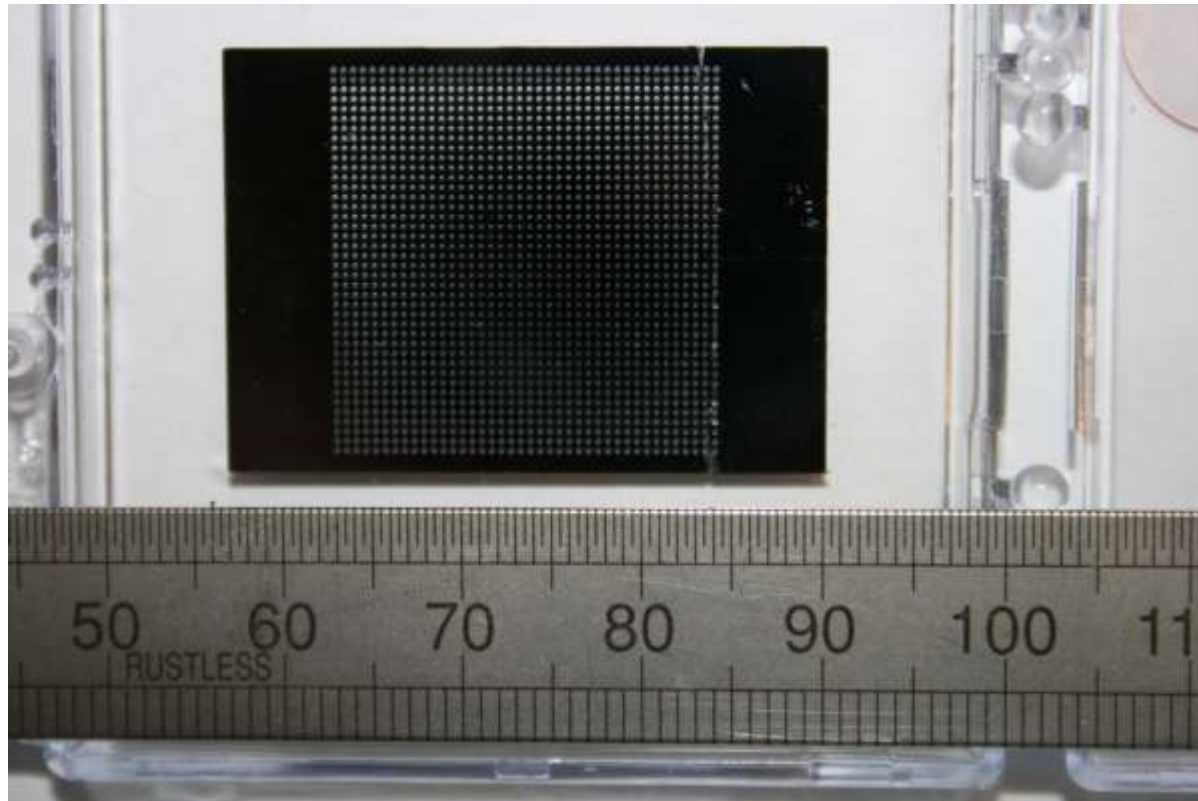
## Expose and develop resist



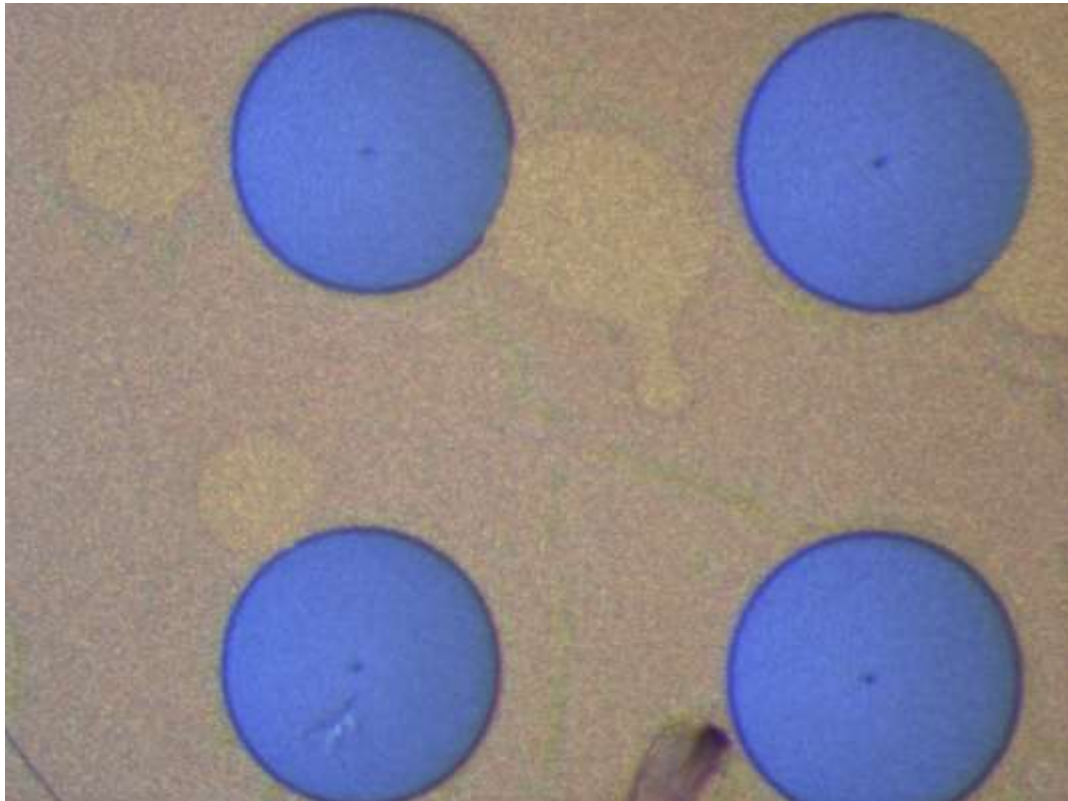
DRIE – Etch through to parylene (also dices substrate)



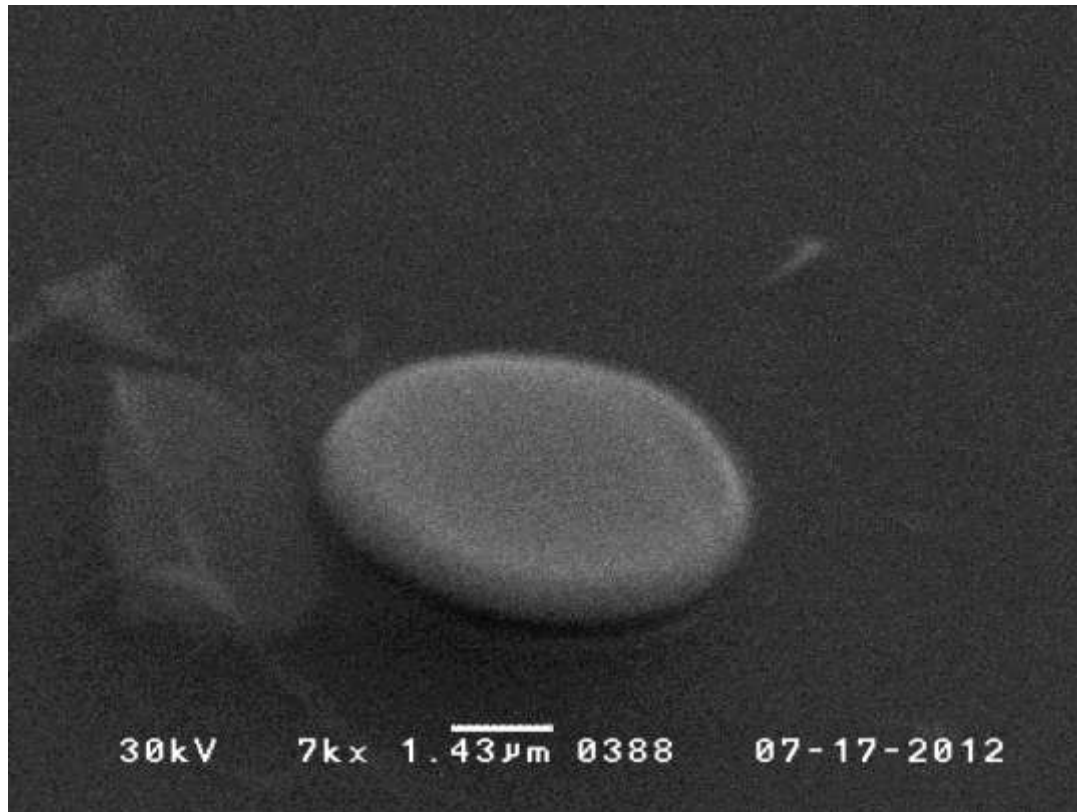
## Visual inspection



## Optical microscope inspection



## Scanning electron microscope inspection



## Conclusions

- MEMS-based fabrication processes have been used to successfully manufacture micro-dot laser targets
  - Good definition as individual targets
  - Good repeatability when used in high rep-rate arrays.
- Similar processes can also be used to fabricate other micron-scale structures such as backlighters, diagnostic filters and much more.



**THANK YOU**

[graham.arthur@scitechprecision.com](mailto:graham.arthur@scitechprecision.com)

# IFE TARGET FABRICATION

Martin Tolley

Target Fabrication Group

Central Laser Facility,  
Rutherford Appleton Laboratory

[martin.tolley@stfc.ac.uk](mailto:martin.tolley@stfc.ac.uk)



Science & Technology  
Facilities Council

# Thank You

C Spindloe, STFC, UK  
P Hiscock, STFC, UK  
N Sykes, Micronanics, UK  
M Beardsley, STFC, UK  
W Nazarov, St Andrews, UK  
I Sari, U Southampton, UK  
M Kraft, U Southampton, UK  
G Schaumann, TUD, Germany  
F ben Said, CEA, France  
O Legaie, CEA, France  
M Brookes, AWE, UK  
D Wyatt, STFC, UK  
S Serra, STFC, UK  
D Haddock, STFC, UK  
J Jiang, U Huddersfield, UK  
R Leach, NPL, UK

J-P Perin, CEA, France  
D Chatain, CEA, France  
N Alexander, GA, US  
E Koresheva, LPI, Russia  
J.M Perlado, UPM, Spain  
S Cuesta Lopez, UPM, Spain  
G Schurtz, CELIA, France  
D Guillaume, CEA, France  
I East, STFC, UK  
G Arthur, Scitech Precision, UK  
F Hall, Scitech Precision, UK  
D Barrow, U Cardiff, UK  
D Harding, LLE, US



# Overview

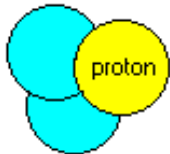
- IFE Targetry Requirements
- Shell target mass production
- Complex target mass production
- Target Factory
- Is it achievable?
- Summary

# IFE TARGETRY: REQUIREMENTS



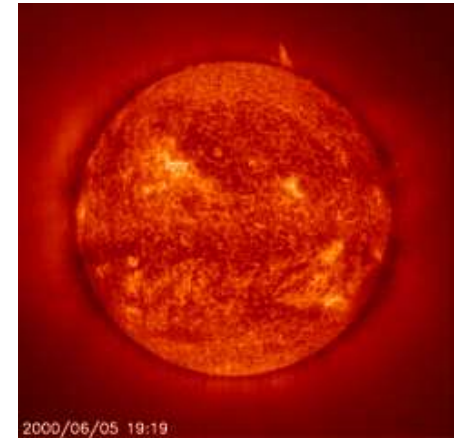


Deuterium molecule

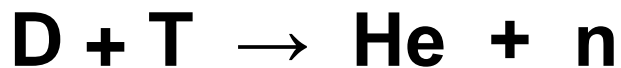


Tritium molecule

**The Sun:**  
a natural  
fusion  
reactor



**Core ~ 15 MK**  
**~ 150 g/cc**



**3.5 + 14.1 MeV**

This energy is ~ a million times greater than in chemical reactions

$$\mathbf{E = m c^2}$$

## A spherical, pulsed rocket



Hot spark formed at the centre of the fuel by convergence of accurately timed shock waves



Material is compressed to  $\sim 1000 \text{ gcm}^{-3}$

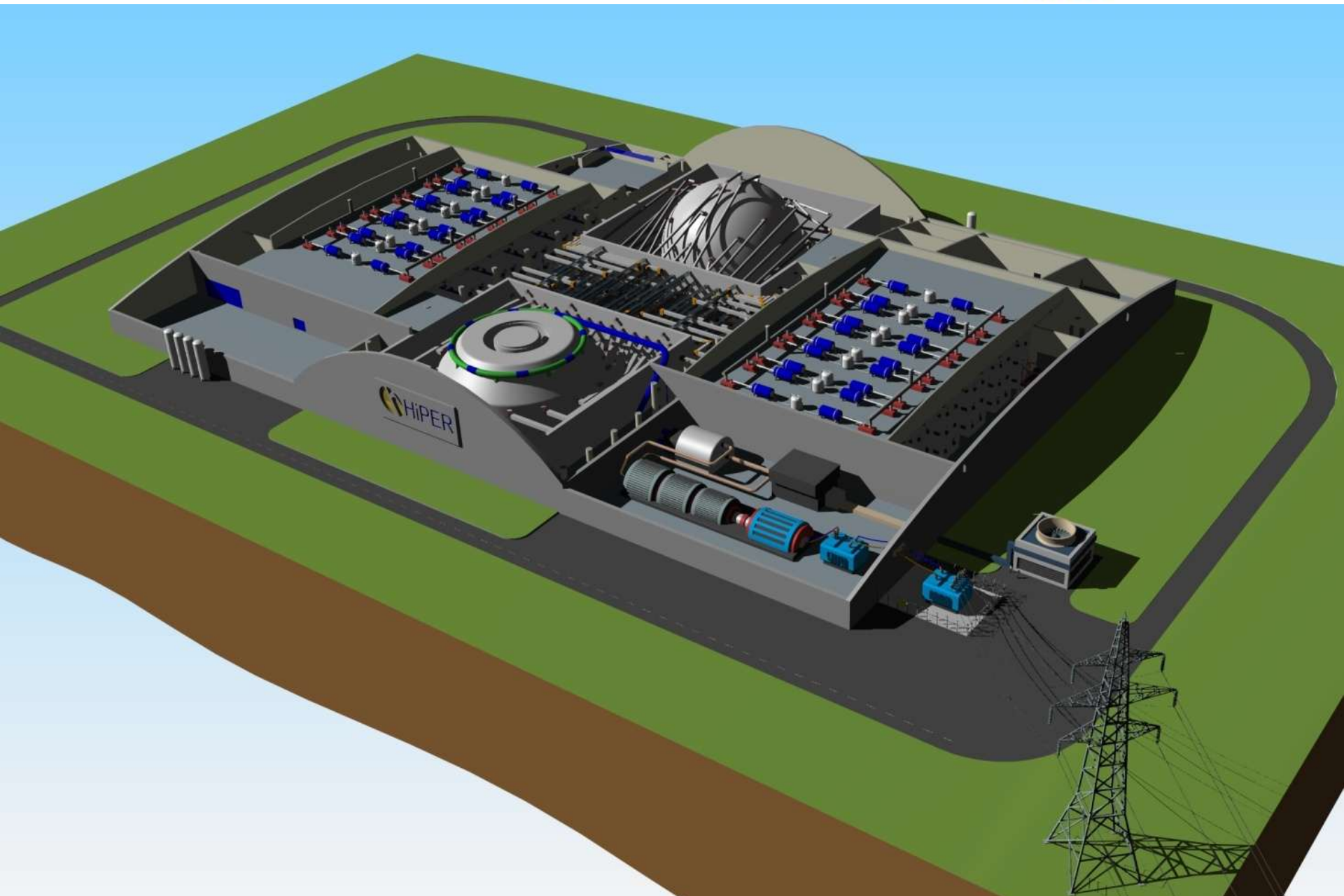


Hot plasma expands into vacuum causing shell to implode with high velocity



Lasers or X-rays symmetrically irradiate pellet

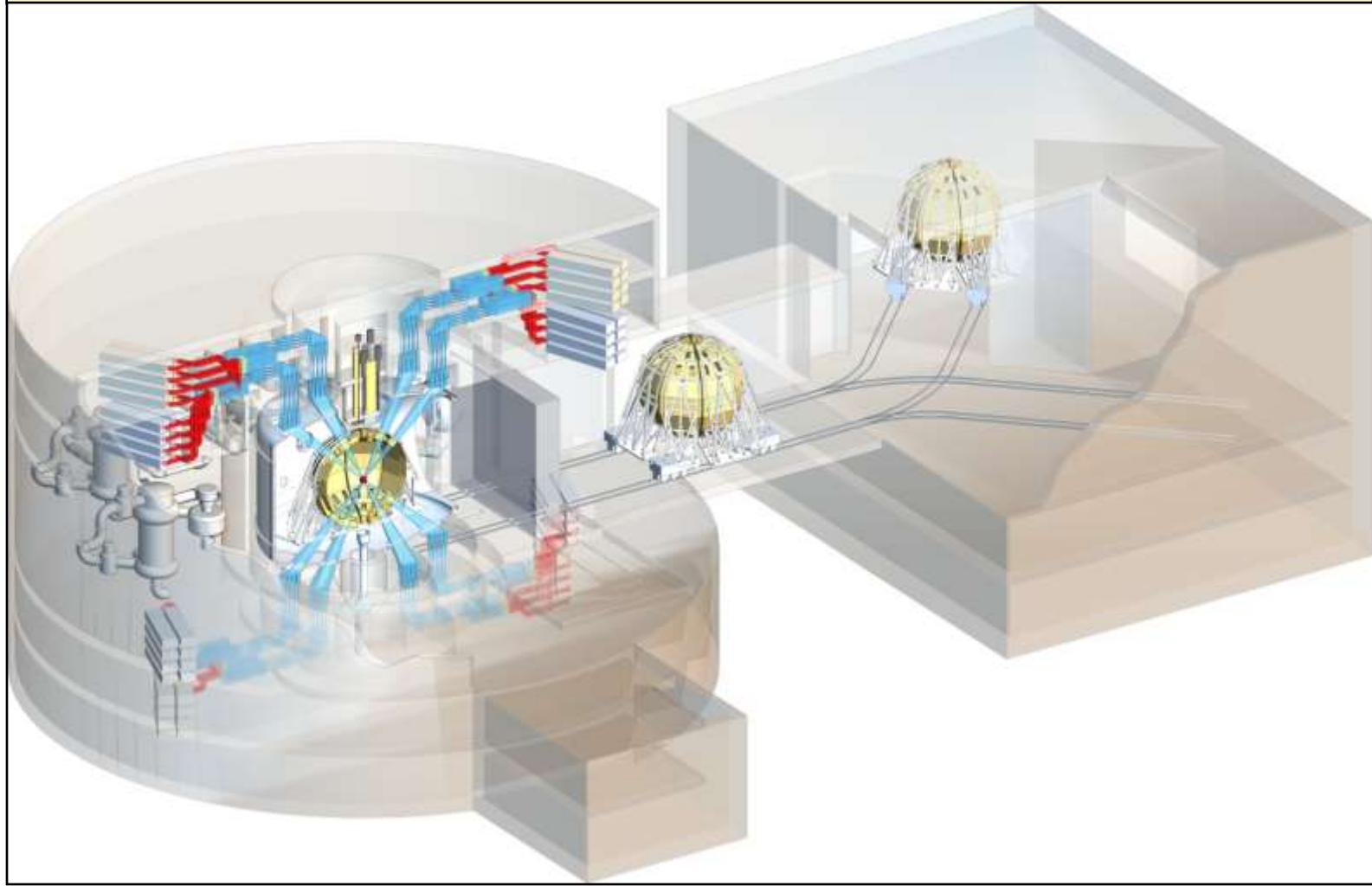
# Latest Facility Design





# The chamber system can be transported for maintenance or replacement

**Unsealed chamber, separate from the vacuum and optical systems**



# IFE Target Production Numbers

In continuous operation at 10Hz one IFE reactor will require:

~ **860 000** fuel capsules per day

In continuous operation at 16Hz one IFE reactor will require:

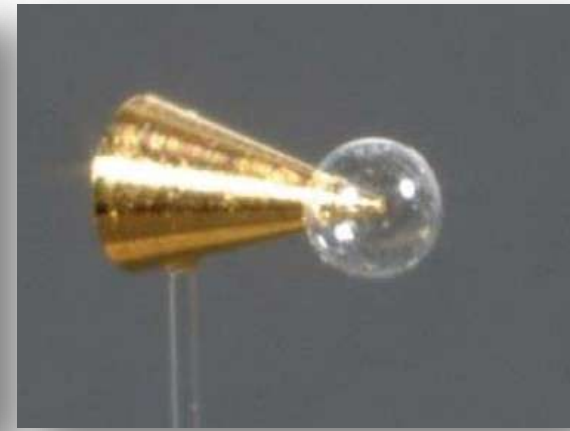
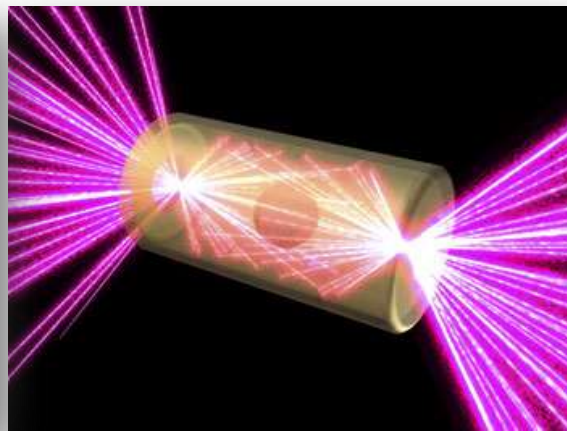
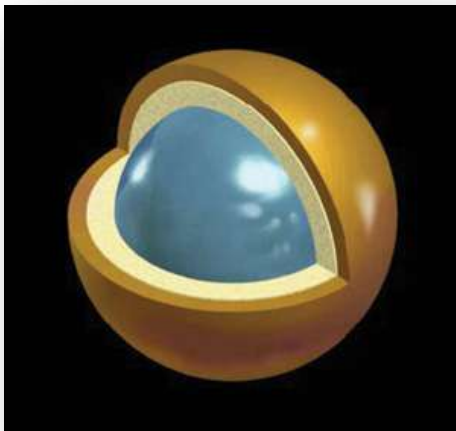
~ **1 380 000** fuel capsules per day

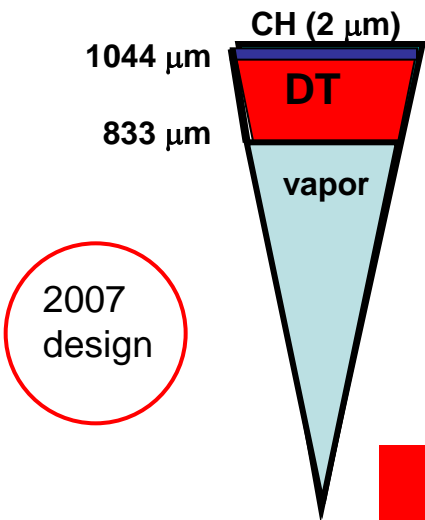


# IFE Target Types

Three main generic types currently being considered. Many shared microfabrication challenges.

1. Shock Ignition Targets – DT filled shell targets with a low Z ablator on the outside
2. Indirect drive targets – DT filled shell with ablator in a hohlraum.
3. Fast Ignition – DT filled shell with ablator (and re-entrant cone)

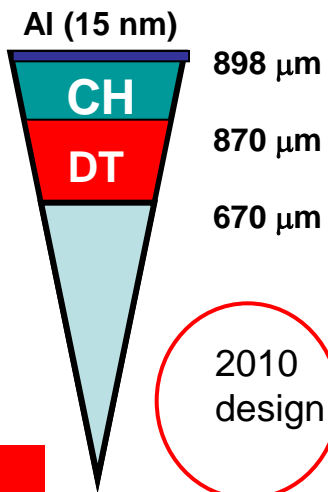




2007 design

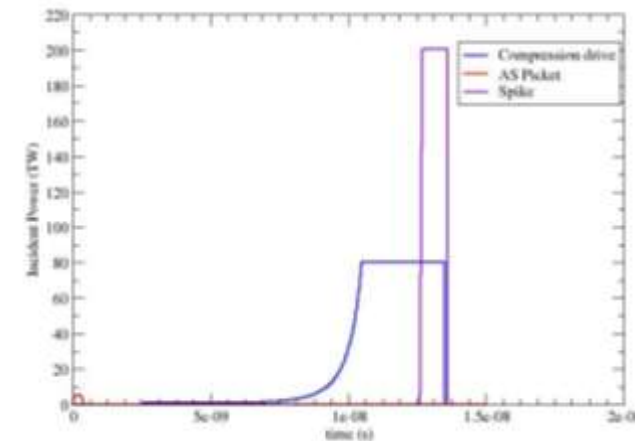


Lower AR and hydro efficiency → hydro robustness



2010 design

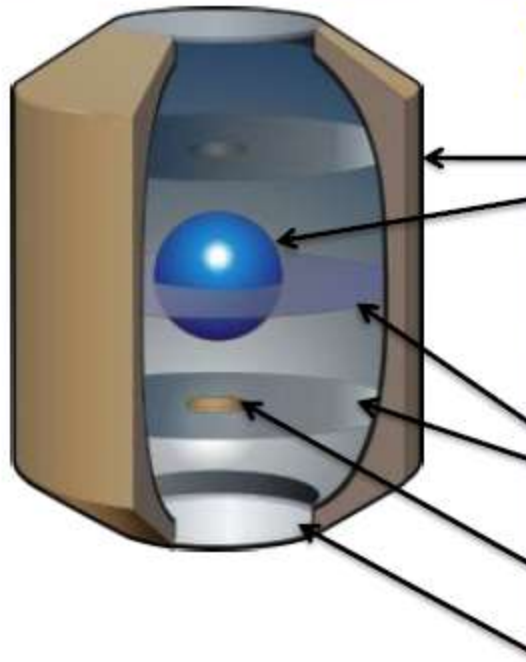
Outer surface Roughness ~ 10's nm



Inner ice Roughness ~ 1 μm

	IFAR 75% $r_0$	Mass	Compression	Vimpro	$\eta$ %	Spike	Gain
<b>ALL DT</b>	4.5 (t=0) 30 (75% $r_0$ )	.59 mg .29 fuel	180 kJ 50 TW 600 g/cc 1.5 g/cm <sup>2</sup>	280 km/s	9%	160 TW 80 kJ	Y = 20 MJ G ~ 76
<b>CH</b>	3.4 (t=0) 18 (75% $r_0$ )	.67 mg .38 mg fuel	260 kJ 80 TW 720 g/cc 1.83 g/cm <sup>2</sup>	240 km/s	5%	200 TW 150 KJ	Y = 32 MJ G ~ 80

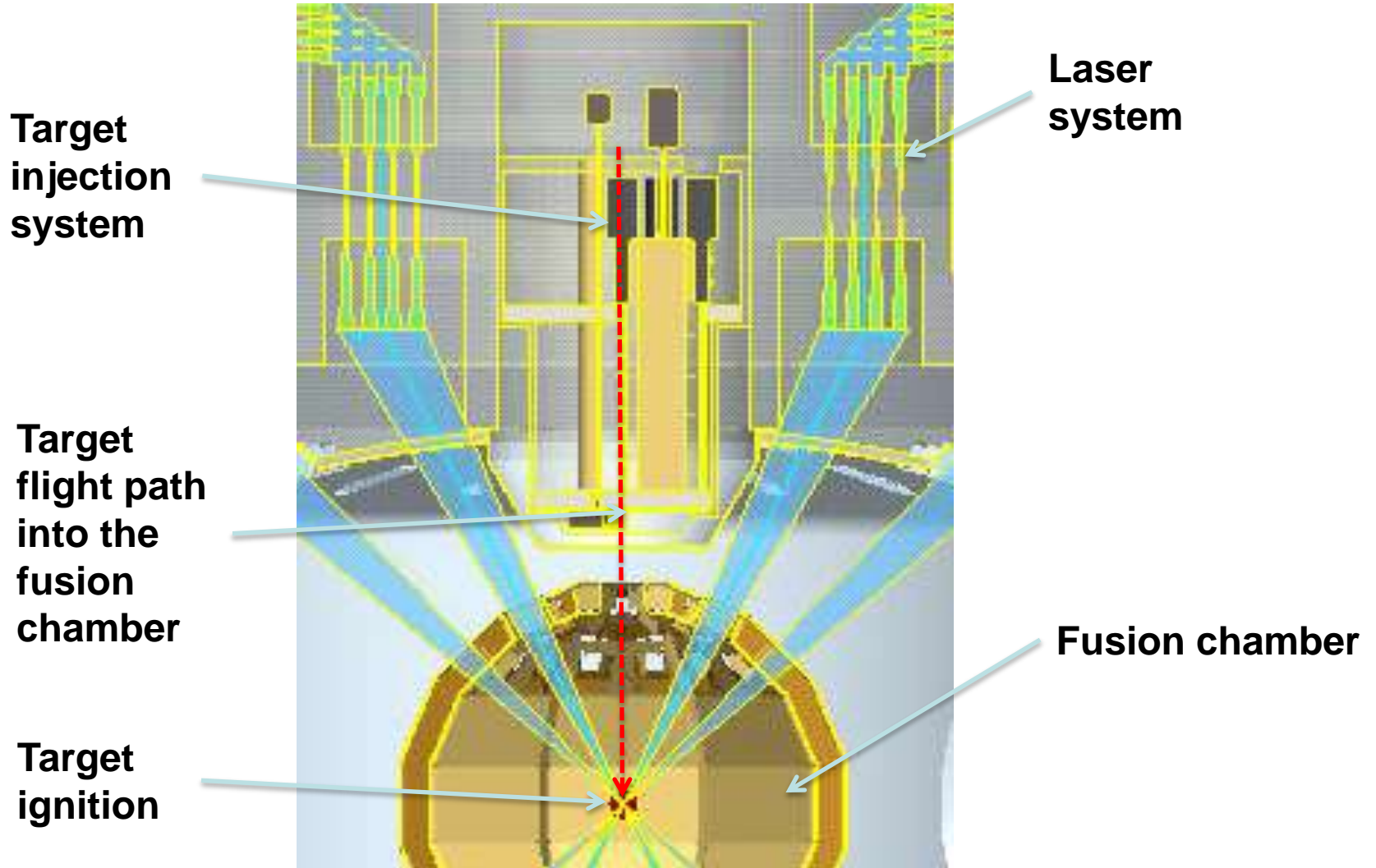
# LIFE exhaust characterization is essential for design of tritium systems



Component	Dimensions	Material	~Mass (mg)	Alternate materials
<b>Hohlraum Capsule</b>	Length = 1.54 cm ID = 0.89 cm Thickness = 0.05 cm	Pb; 5% Sn or Sb	2579	High-Z
<b>Ablator</b>	OD = 0.382 cm Thickness = 75 $\mu$ m	C	11.6	CH; Be, B
<b>Dopant</b>		Ta	0.0021	Ge
<b>Foam</b>	Thickness = 142 $\mu$ m	DCPD (< 20 mg/cc)	0.1389	SiO <sub>2</sub> (5 mg/cc)
<b>DT</b>	Thickness = 142 $\mu$ m	DT	1.3889	
<b>Support</b>	Thickness = 110 nm	C	0.0488	polyimide
<b>IR window</b>				
<b>Substrate</b>	Thickness = 400 $\mu$ m	C	0.2439	polyimide
<b>Metalization</b>	Thickness = 30 nm	Al	1.01E-05	Ag, Au
<b>P2 shield</b>	OD = 0.191 cm Thickness = 10 $\mu$ m	Pb; 5% Sn or Sb	6.50	High-Z
<b>LEH window</b>	Diameter = 0.45 cm Thickness = 500 $\mu$ m	C	0.2439	polyimide
<b>Total mass</b>			2599	

- Strong interface between target material choices and design of T systems
- Optimized LIFE target design eliminates CH substrate (no protium)
- Tritium per target < 1 mg (~ content in one EXIT sign)
- 0.5% chamber clearing ratio with partial gas recirculation facilitates T recovery

# Fusion targets are injected at high acceleration rates into a hot chamber



The target must arrive at chamber center in the correct configuration for ignition

# IFE Targetry – Key Challenges

**Target technology is one of the key challenges for IFE**

**The main IFE Target Fabrication challenges**

- **Scaling of processing and materials to micro-domain**
- **Industrial scaling for mass production**
- **Novel production processes and materials**
- **Tritium handling**
- **Fine control cryogenics/layering**
- **And all at ~ 25 – 30 €c per target !**

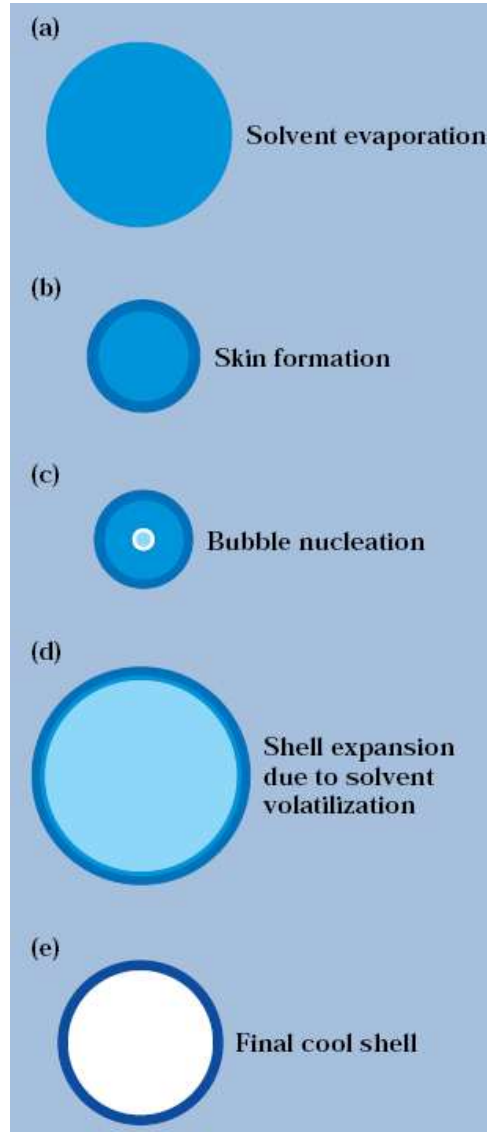
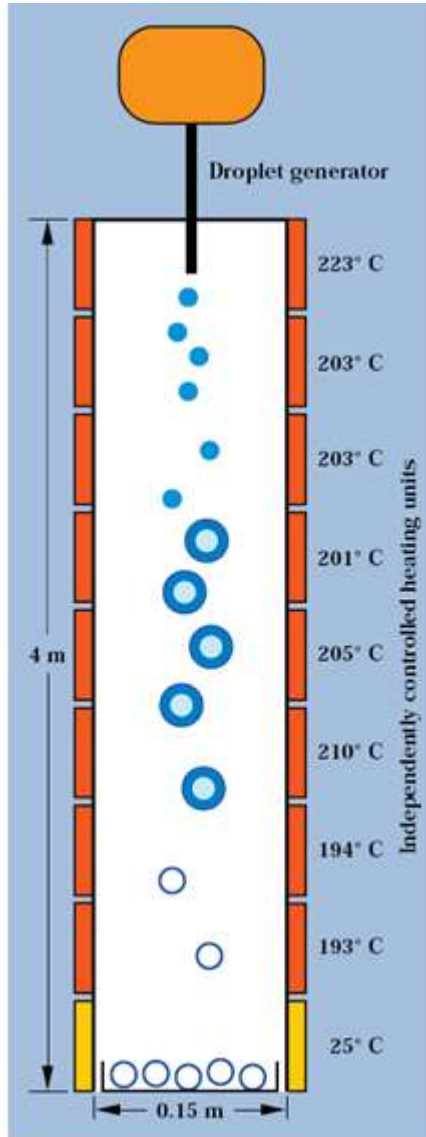


# **SHELL (MASS) PRODUCTION**





# 1. Drop Tower



1 - A double orifice generator injects a droplet of polymer solution into the tower.

2 - A polymer membrane skin forms at the surface due to solvent evaporation.

3 - When the droplet temperature exceeds its boiling point the shell inflates.

4 - The final size and quality will depend on the cooling rate and symmetry of the hot polymer shell.

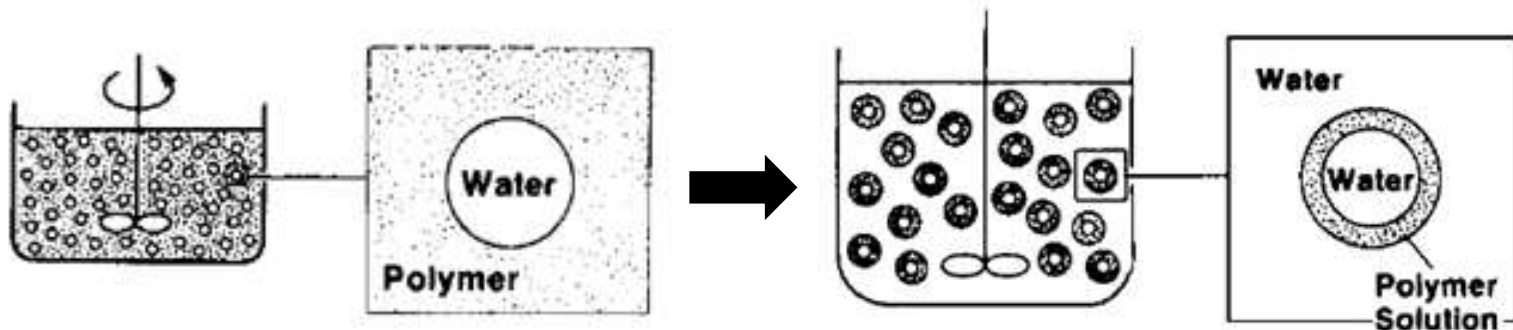
Requires expensive equipment.

**Robert Cook, Creating Microsphere Targets for Inertial Confinement Fusion Experiments, Lawrence Livermore National Laboratory.**



## 2. Microencapsulation: Double emulsion method

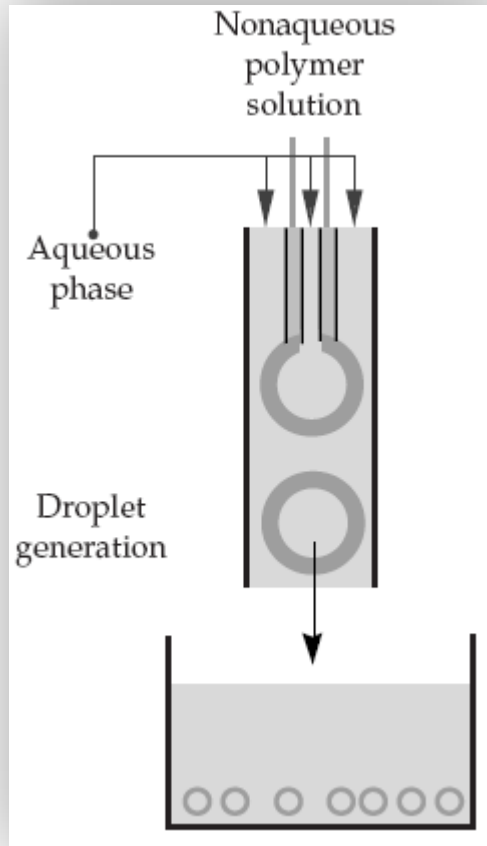
- 1 – Emulsify water into polymer solution (oil phase) with surfactants and mechanical agitation.
- 2 – Pour emulsion into second water phase while maintaining mechanical agitation
- 3 – Evaporate polymer solvent
- 4 – Remove microshells from second water phase
- 5 – Evaporate water from inside microshell



Guillermo Velarde, Yigal Ronen, José María Martínez-Val, Nuclear fusion by inertial confinement: a comprehensive treatise.



## 2. Microencapsulation: Triple orifice droplet generator



To form W/O/W emulsion droplets with reasonably constant diameters.

The smallest orifice flows water to the inner phase.

Around it, the second orifice flows the polymer solution.

The third orifice around it dispenses water and surfactant solution.

The droplets are dripped into a stirred beaker of water.

Adjusting the flow rates of the various solutions changes the outer diameter and shell thickness.

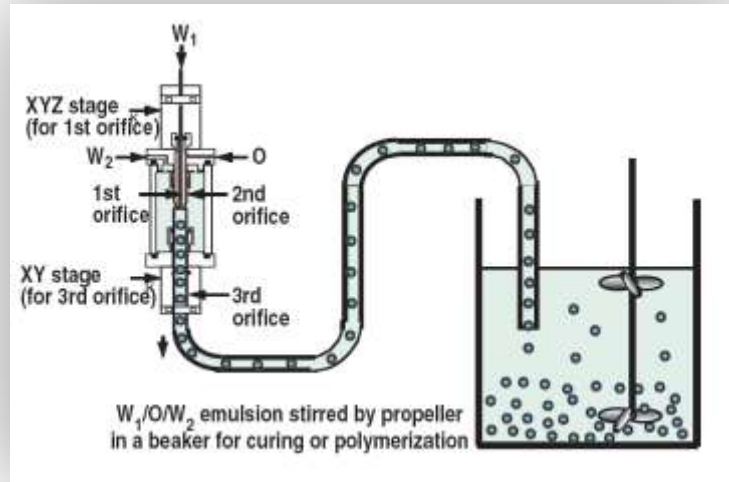
R. Cook, The development of plastic targets for NIF targets, *ICF Semiannual Report October 1999—March 2000, Volume 1, Number 1, LLNL*



Science & Technology  
Facilities Council

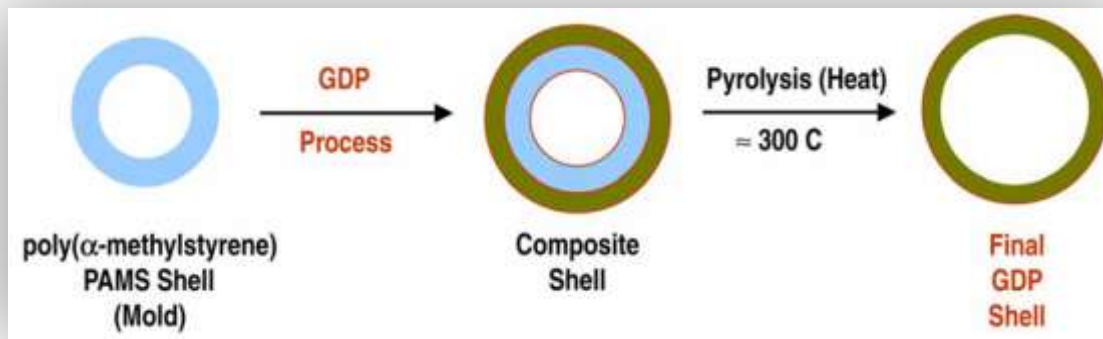
# 2. Microencapsulation: Depolymerisable Mandrel Technique

PAMS (Poly- $\alpha$ -methylstyrene) mandrels are produced using a microencapsulation process.



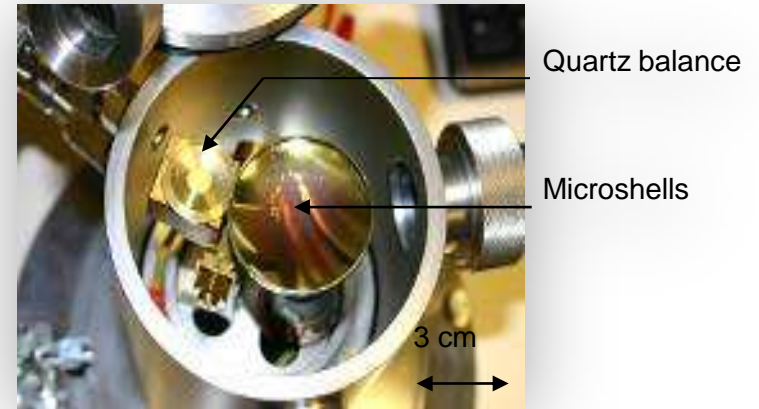
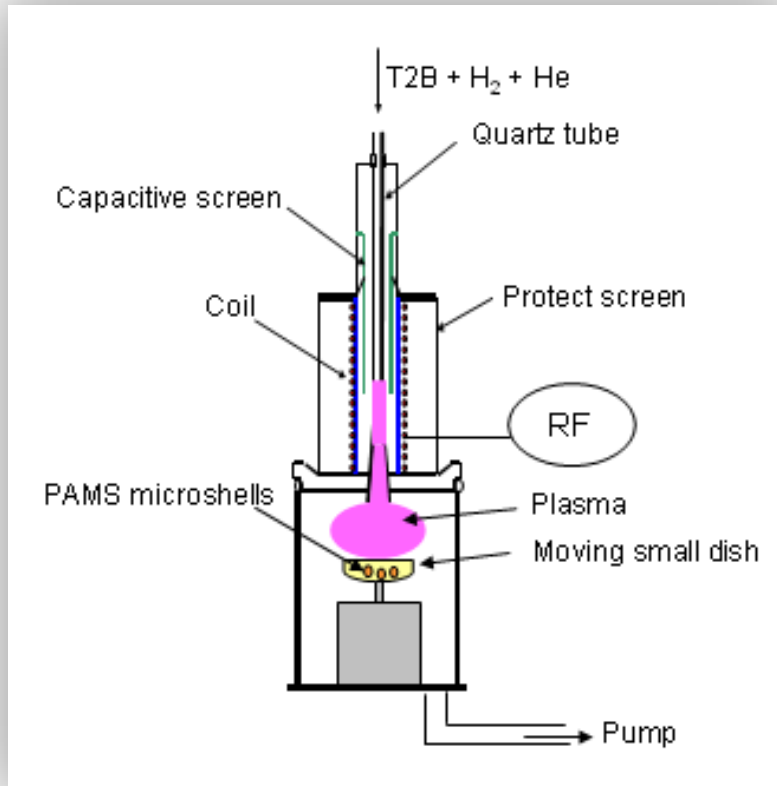
- W1 Water
- O 11%wt PAMS in Fluorobenzene
- W2 PVA solution 0.2%wt

When dried the PAMS mandrels are over coated with a Glow Discharge Polymer (GDP) to the desired thickness.



Evelyn M. Fearon, Adapting The Decomposable Mandrel Technique To Build Specialty ICF Targets, 11<sup>th</sup> Target Fabrication Specialists' Meeting Orcas Island, Washington September 8-12, 1996.

# Microballoon PAMS



Discharge polymerization coating schematic (left) and deposition chamber (right)

F. Bensaid  
(CEA-Valduc-DRMN-L.M.C)

# **SHELL (MASS PRODUCTION) FILL AND CRYOGENIC LAYERING**



# D-T Filling

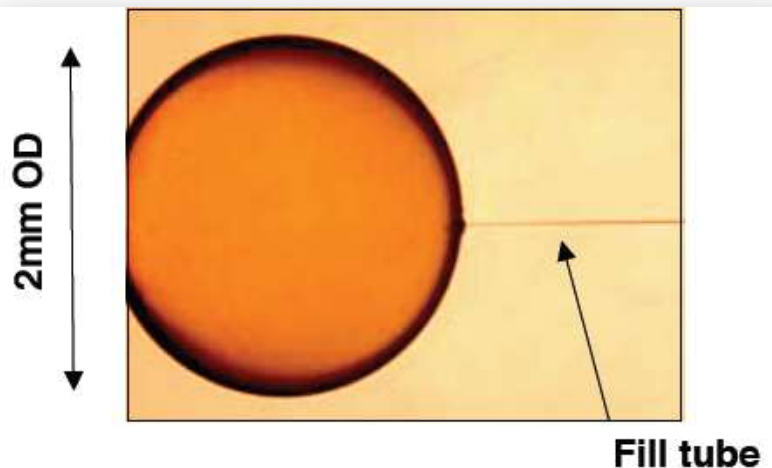
Filling of the shell with D-T fuel can be either carried out using a diffusion fill or where the ablator layer prevents this by drilling a small hole attaching a fill tube and introducing the cryogenic liquid through the tube.

## 1) Diffusion Fill

DT gas is permeated through the wall in a controlled manner to prevent buckling of the wall in a high pressure cell. The cell is then cooled to  $\sim 20\text{K}$  to condense the gas.

## 2) Fill Tube

A small hole is laser drilled about  $5\mu\text{m}$  in diameter and a tube is bonded into the shell. The shell is then cooled close to the triple point of the liquid and then the tube is used to introduce the fuel.



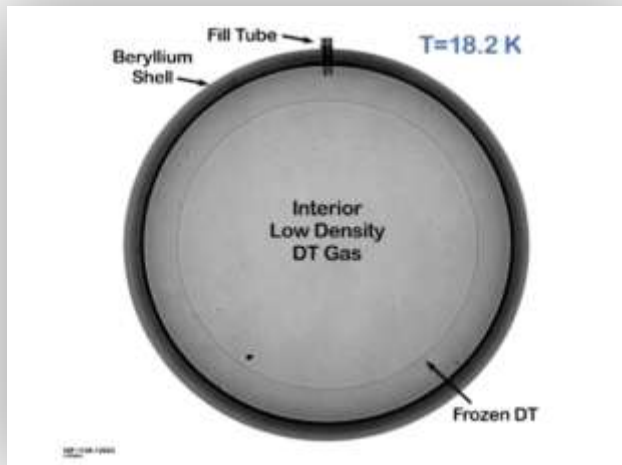
# Layering

1) If enough tritium is present in the shell can use **Beta layering**.

Nuclear decay of the tritium produces a beta particle that loses its energy to heat causing most redistribution from regions where layer is locally thickest.

2) If there is not sufficient tritium (e.g. H-D-T target) a **layering chamber** is used.

Filled shells are held in a cryogenic environment and repeatedly slightly heated (with an IR laser) and then cooled causing redistribution.



NIF capsule showing DT ice layer

Both layering processes typically take ~24 hours. Scalability to IFE?

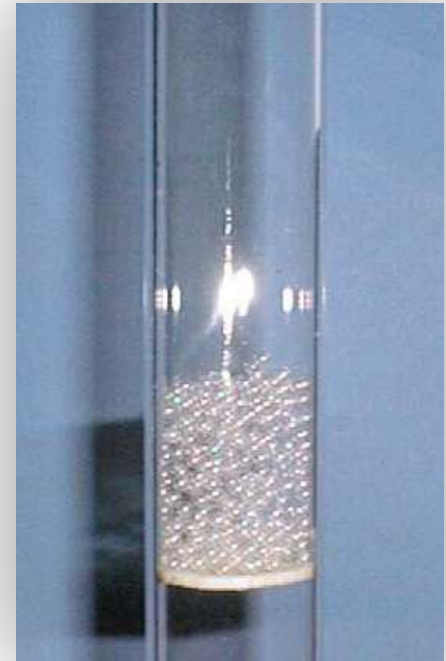




# Fluidized Bed Technique

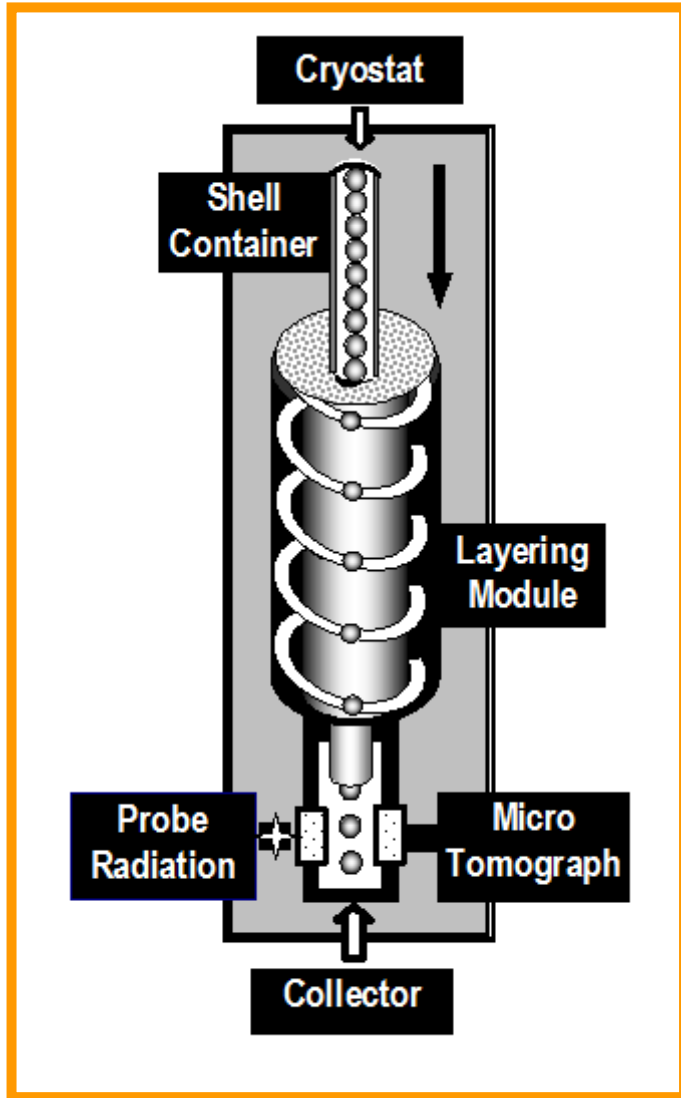
General Atomics (and Shafer) have proposed a fluidised bed technique for mass production layering.

- Possible issues with surface damage.
- Multiple nucleation sites so possible nanocrystallinity



Capsules layering in a fluidized bed

# LPI: D-T Fill and Layering



Layering Mechanisms – Free Standing Target (FST) Layering

Permeation fill of the shells in a cryostat.

Rolling of the shells down a layering channel

Characterisation of the layer at the end.

Issues

Fuel needs to be a single crystal layer?

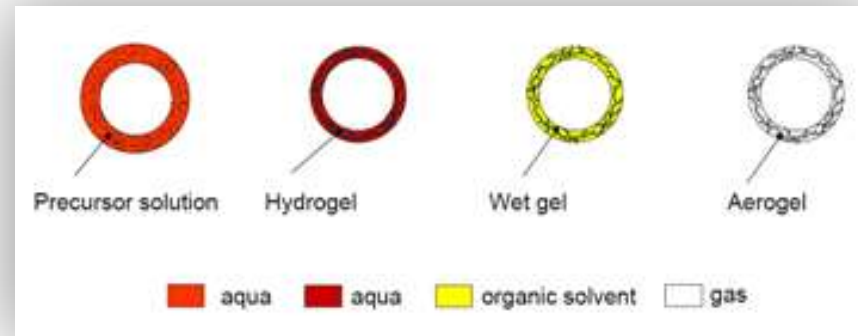
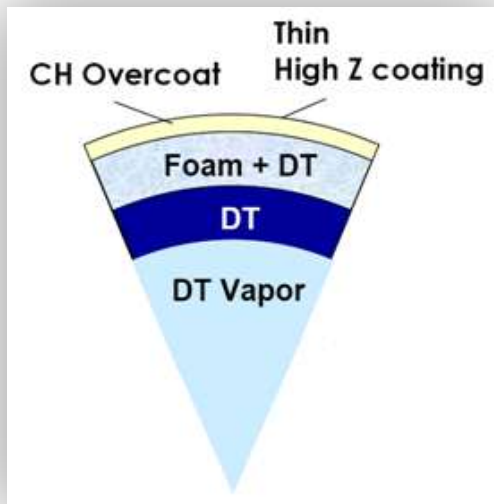
FST filling may give polycrystalline DT

- I.V.Aleksandrova, E.R.Koresheva, I.E.Osipov, *et al.* *Free-Standing Target Technologies for ICF*. 2000 Fusion Technology 38 No1 p.166
- I.V.Aleksandrova, S.V.Bazdenkov, V.I.Chtcherbakov *et al.* *An efficient method of fuel ice formation in moving free standing ICF/IFE targets*. J.Phys.D: Appl.Phys. **37**, 1-16, 2004

# Don't Layer – Use Foam Shells

Target designs including foam shells have been proposed for ICF. Potential foam materials include polystyrene (PS), resorcinol-formaldehyde (RF) and divinylbenzene (DVB).

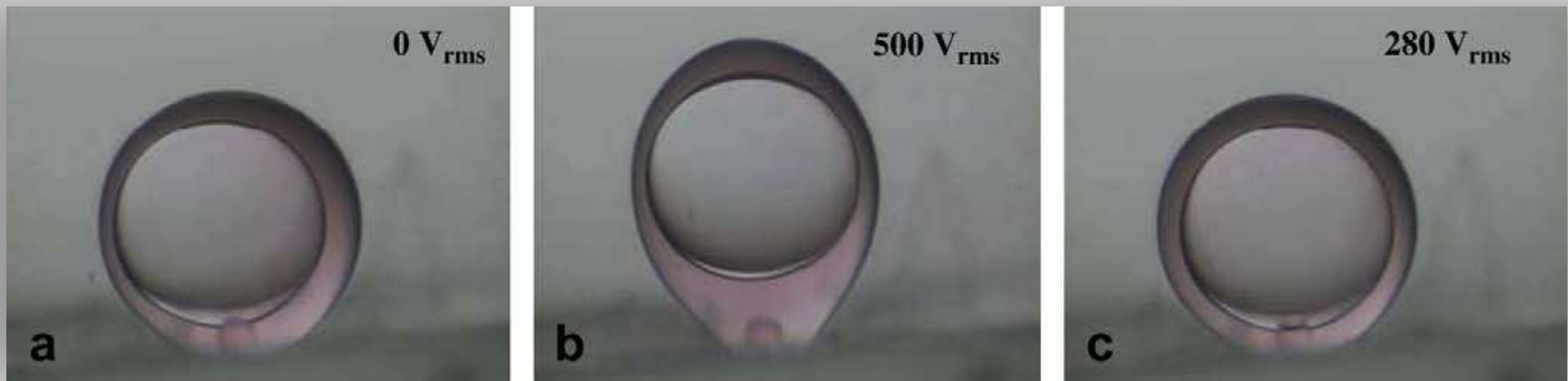
With a foam layer the DT fuel may wick into the foam thereby reducing/removing the issues associated with layering.



Keiji Nagai, et al., Foam materials for cryogenic targets of fast ignition realization experiment (FIREX), Nuclear Fusion 45 (2005) 1277–1283.

# Advanced Techniques: Microfluidics

- Harding\* has proposed a six phase programme to produce layered shells based on microfluidics.



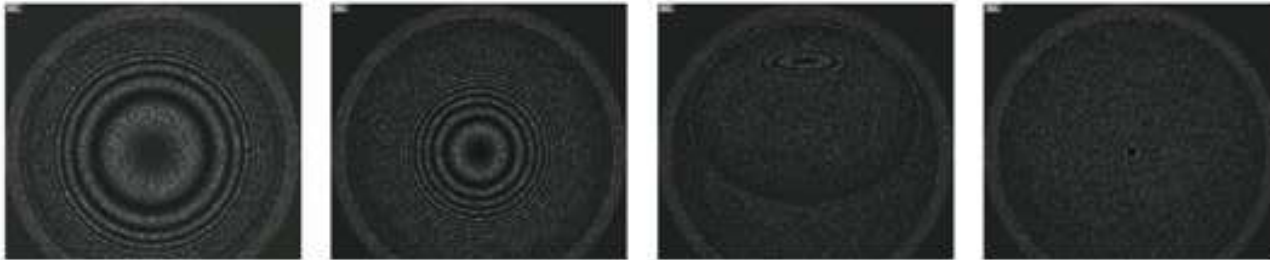
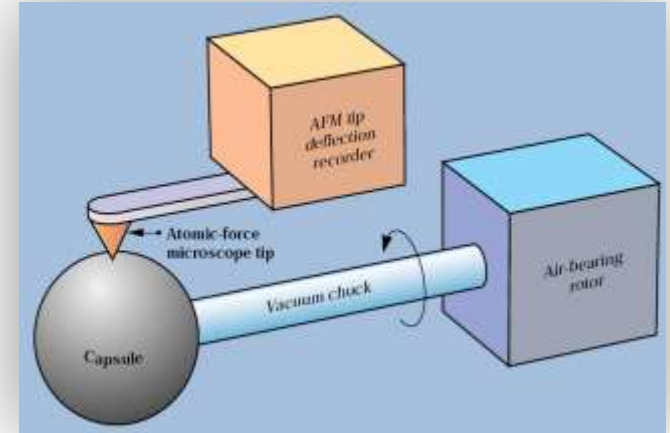
- \* 1) W. Wand et al, On-Chip Double Emulsion Droplet Assembly Using Electrowetting-On-Dielectric and Dielectrophoresis, *Fus. Sci. and Tech*, **59,1**, pp 240-249
- 2) Z.-M. Bei, et al., Forming concentric double-emulsion droplets using electric fields, *Journal of Electrostatics* (2009), doi:10.1016/j.elstat.2008.12.013



# Characterization Methods

Shells can be characterised for the outside wall roughness using an AFM.

Robert Cook, Creating Microsphere Targets for Inertial Confinement Fusion Experiments, Lawrence Livermore National Laboratory.



A. Iwamoto, K. Nagai, Development of the Foam Cryogenic Target for the FIREX Project, IF/P5-1

Optical interferometry /shadowgraphy used to characterize wall thickness and defects.



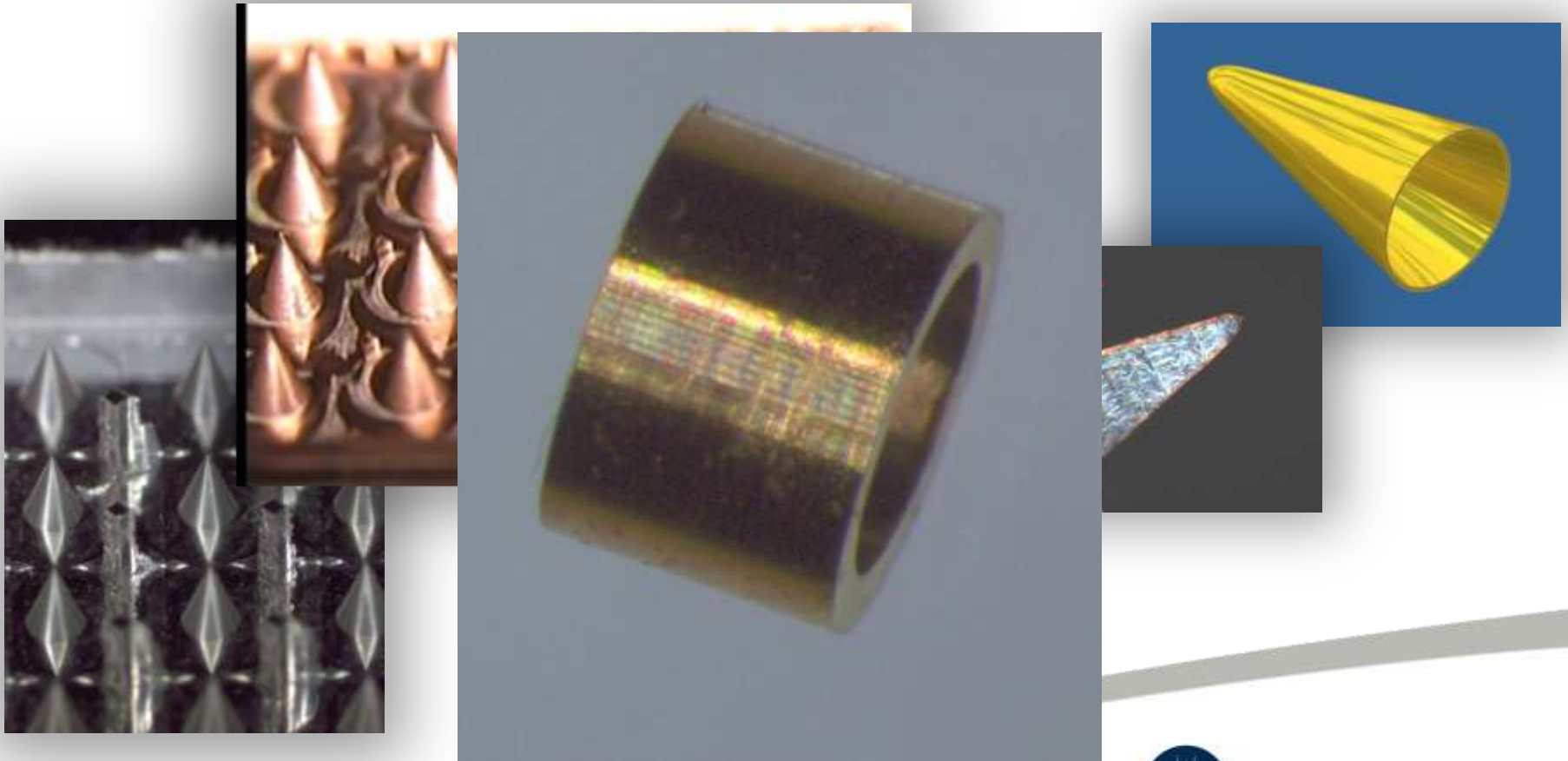
Science & Technology  
Facilities Council

# **HIGH ASPECT RATIO MICROCOMPONENT/ MICROTARGET MASS PRODUCTION**



# High Aspect Ratio Microcomponent Mass Production 1) Micromachining

Significant progress in production of 3D microcomponents

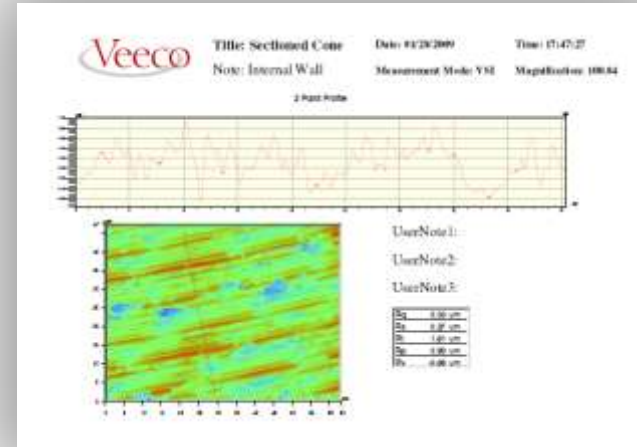


Show target



Science & Technology  
Facilities Council

# High Aspect Ratio Microcomponent Mass Production 1) Micromachining



Iteration between metrology and processing parameters is enabling improved quality, especially surface roughness. (Sub micron roughness achievable 0.25um Ra)

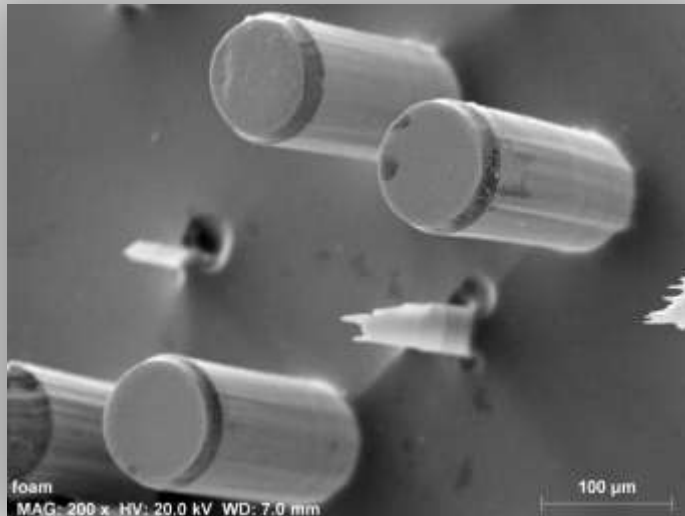
The specific CNC allows large area machining suitable for Pressing and Injection molding





# High Aspect Ratio Microcomponent Mass Production 2) MEMS

Advanced lithography techniques for production of high aspect ratio structures.



- Vertical side patterned halfraum production.
- Entire wafer processed in 1 lithography step



# 3) Emerging Techniques

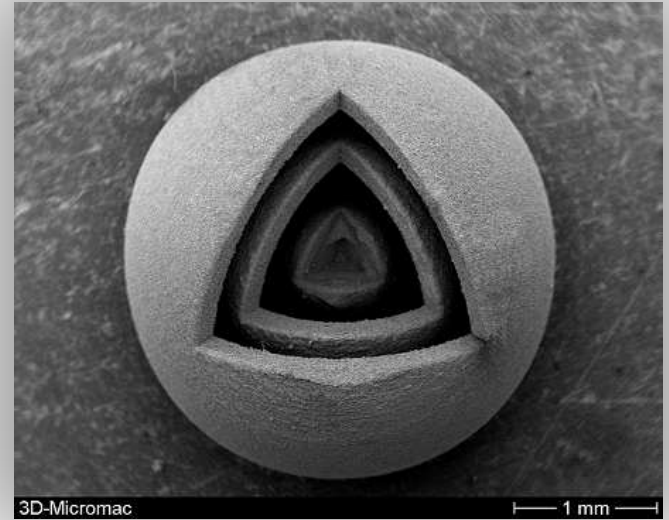
1) ALM – Laser Sintering

2) Injection Moulding

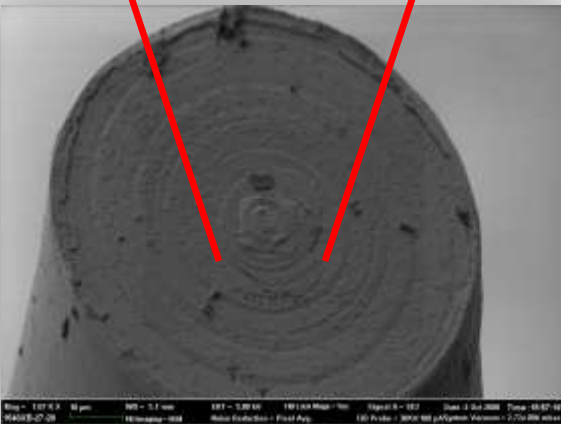
3) Pressing

4) Focussed Ion Beam

5) Atomic Layer Deposition



EOS Sphere (Mo) (Laser sintered)



# INJECTORS



# Target (Injection) Survivability

“We calculated the stress in DT target over a range of injector acceleration values up to  $10,000 \text{ m/s}^2$  for three target support methods; support on a hard flat surface, support within a cup in a low-density ( $50 \text{ mg/cm}^3$ ) foam, and on a flexible membrane.

Calculations showed that the DT would survive without yielding for the foam and membrane supports with  $10,000 \text{ m/s}^2$  acceleration, but would not survive acceleration on the flat plate for any useful value of acceleration.”

Information taken from report commissioned from General Atomics by HiPER:

Task 11.4.2: Modeling of Injector accelerated cryogenic layered targets and assessment of survivability

Task 11.4.3 Comparative analysis of injector designs (suitable for cryogenic targets injected into radiation environment)



# Injector Requirements

The 2010 HiPER-EU tender (direct drive targets) included the following very demanding specifications **which cannot be met by any current injector technology**

The injector shall introduce targets into the chamber at a **velocity of between 500m/s +/-10% to 1000m/s +/-10%** and at a repetition rate of between 5 and 10Hz.

The time between target arrivals shall be between 100ms and 200ms +/- 2ms, (this is dependent on selected repetition rate).

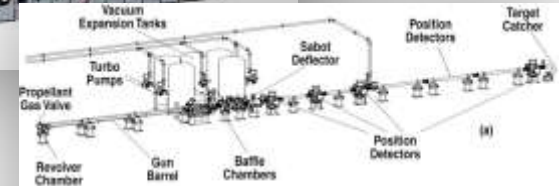
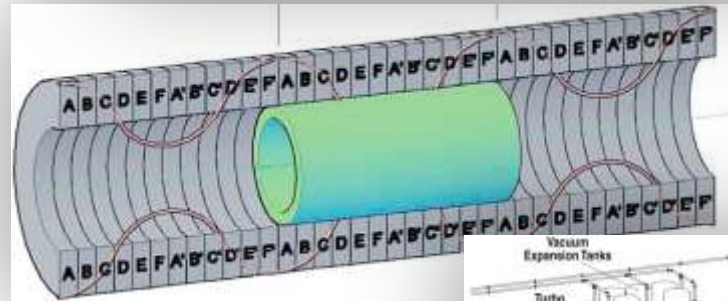
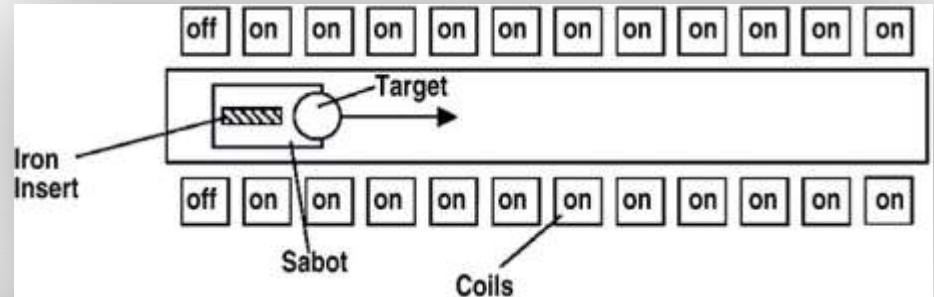
The injector should be capable of passing targets through the chamber centre **with an x,y,z accuracy of better than 10mm** at chamber centre point.



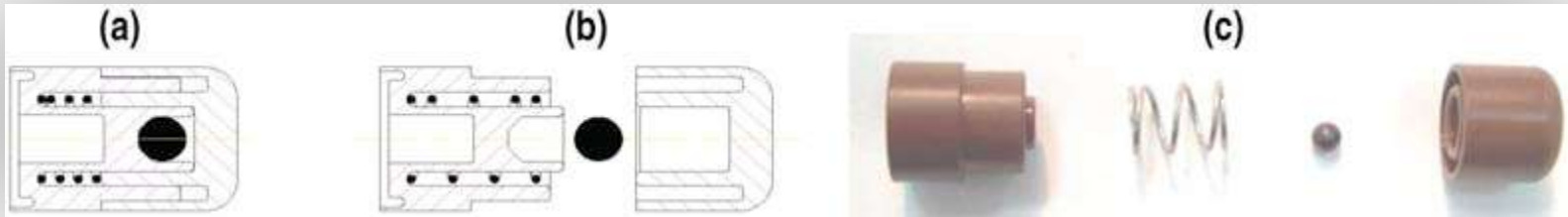
# Target Injector Types

## TARGET INJECTORS

1. Mechanical Injectors
2. The Magnetic Accelerator
3. The Gas Gun
4. The Electrostatic Accelerator
5. Magnetic Slingshot

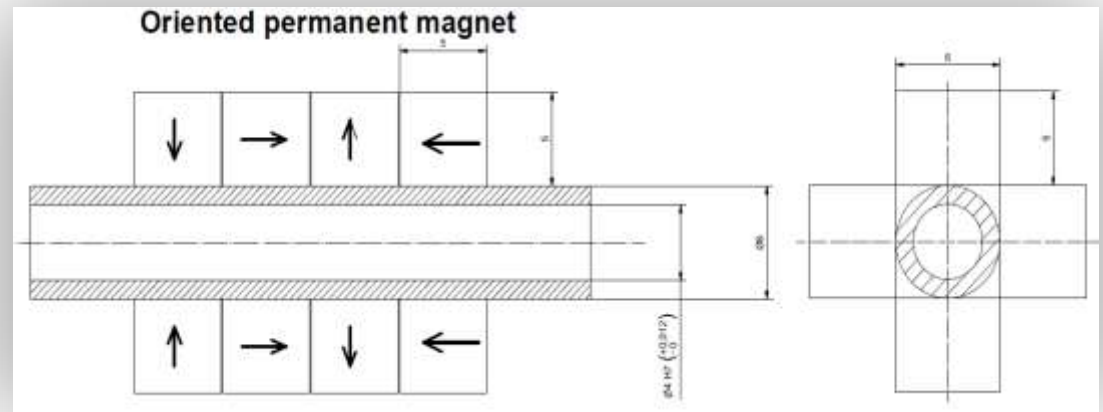
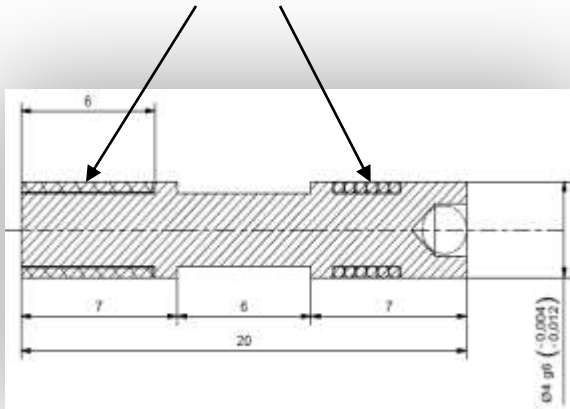


# Sabots and Sleights



Picture courtesy General Atomics

## Stabilization coils



## Magnetic bearing



# EU Tracking Tender (Dec 2009)

## 4.1 Target Tracking System Parameters (All Targets) (*Extract*)

- Velocity Measurement  $\pm 1\mu\text{m/s}$  over the range 400 to 1100m/s
- Positional measurement to within  $1\mu\text{m}$  x,y,z
- Positional Accuracy  $\pm 1\mu\text{m}$  x,y,z
- Timing Accuracy  $\pm 1\text{ns}$
  
- Confident that tracking both during acceleration and in chamber will be achievable
  
- Therefore if the injector cannot achieve accuracy then a combination of either steering of target, or the optics will allow engagement of the target



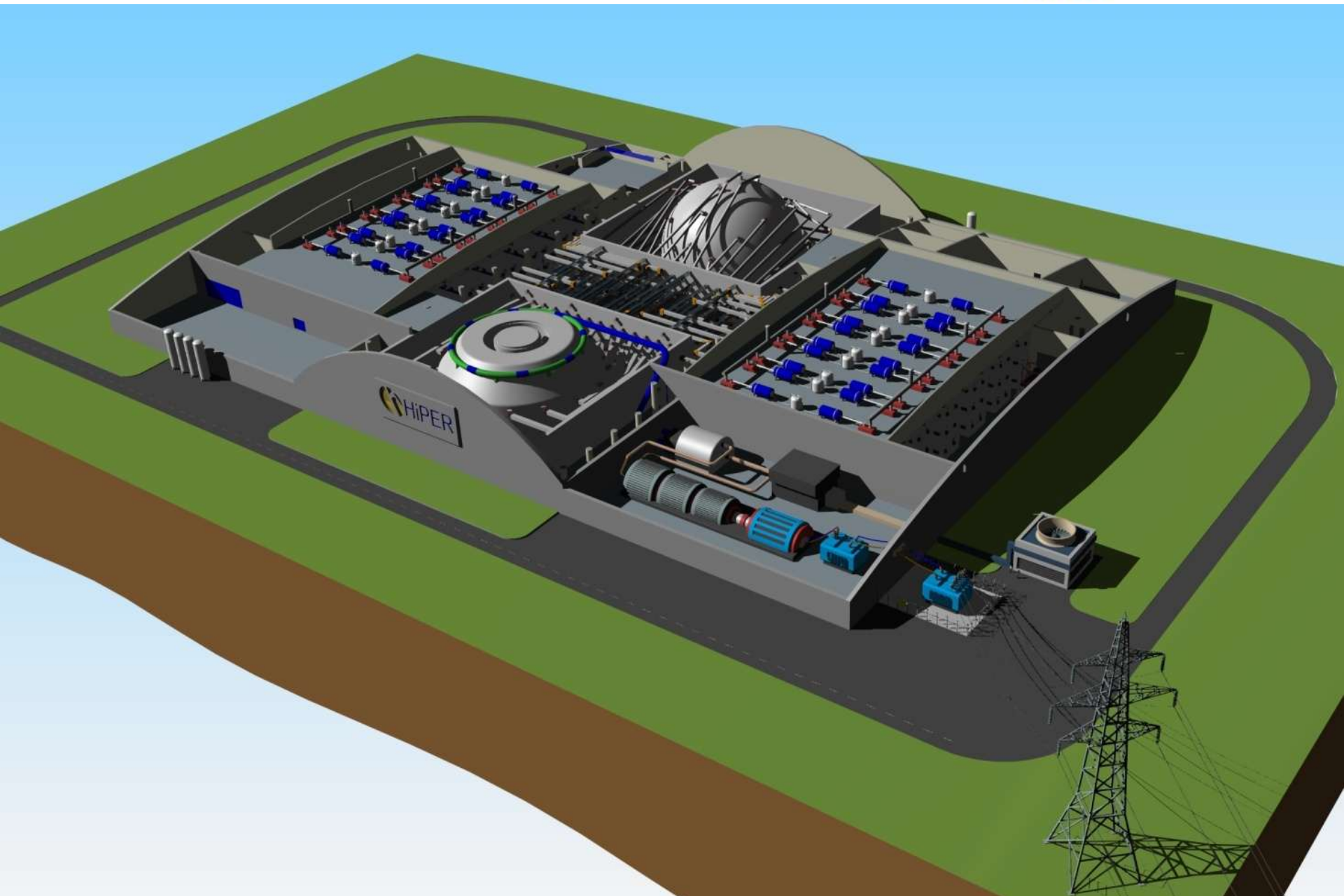


# TARGET FACTORY PRODUCTION LINE

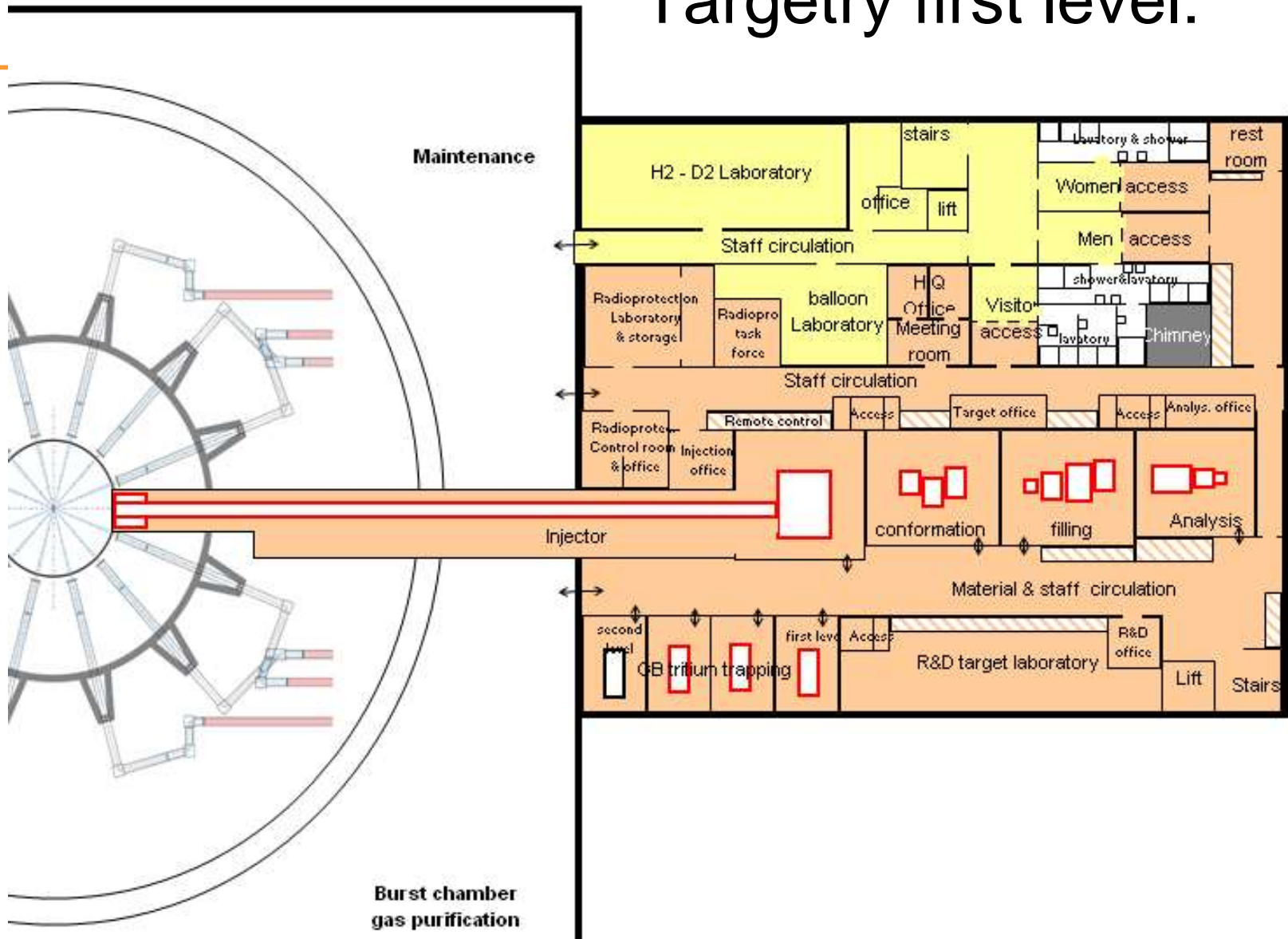


Science & Technology  
Facilities Council

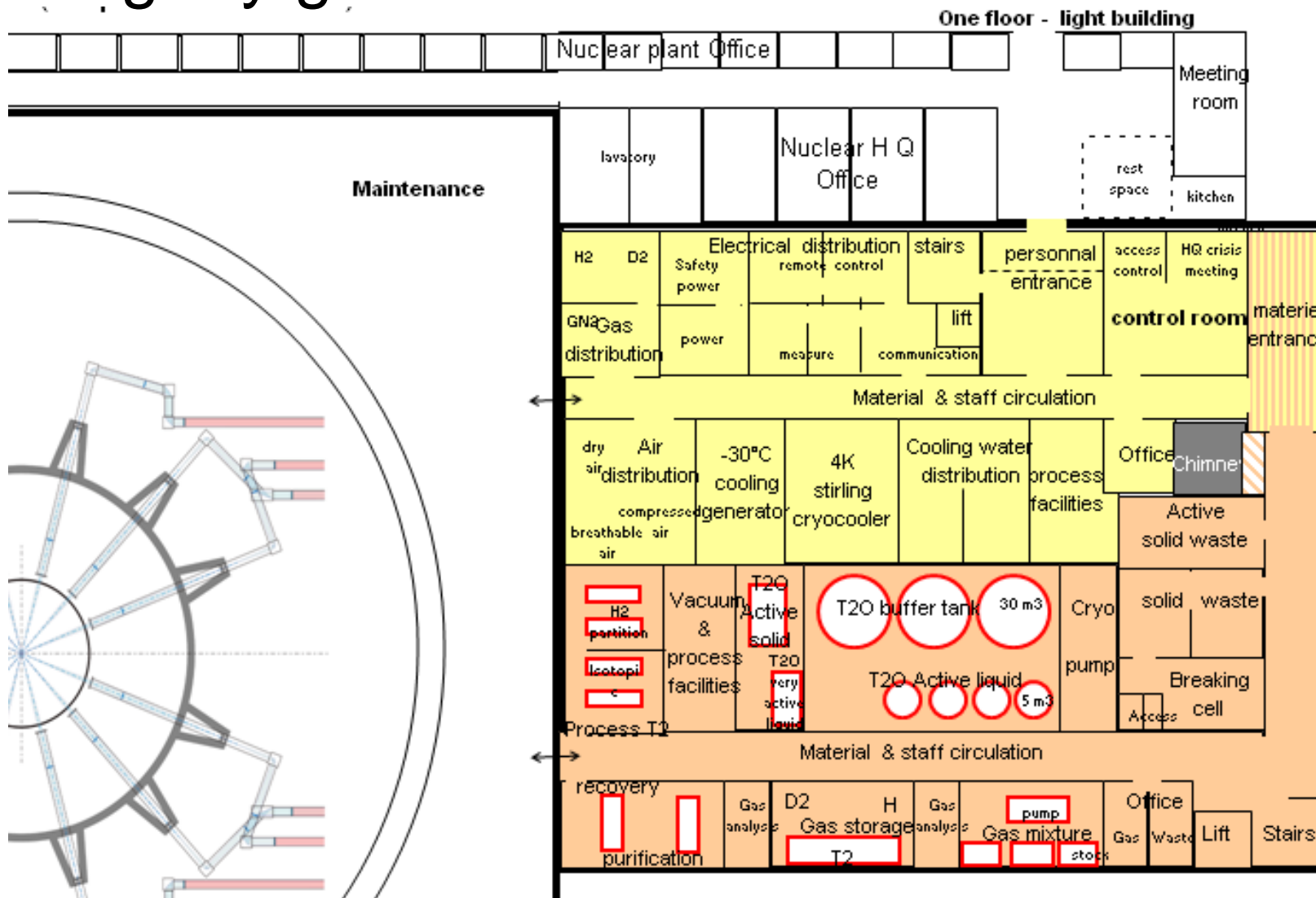
# Latest Facility Design



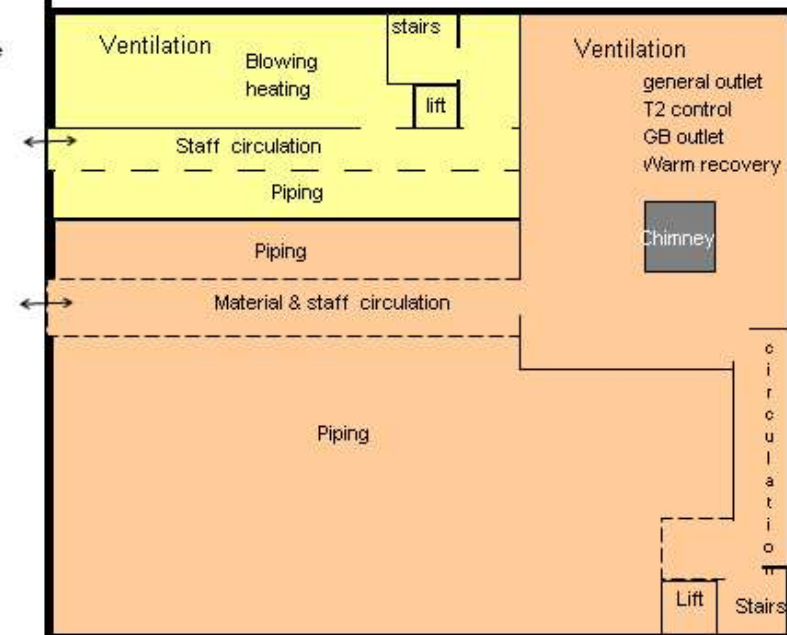
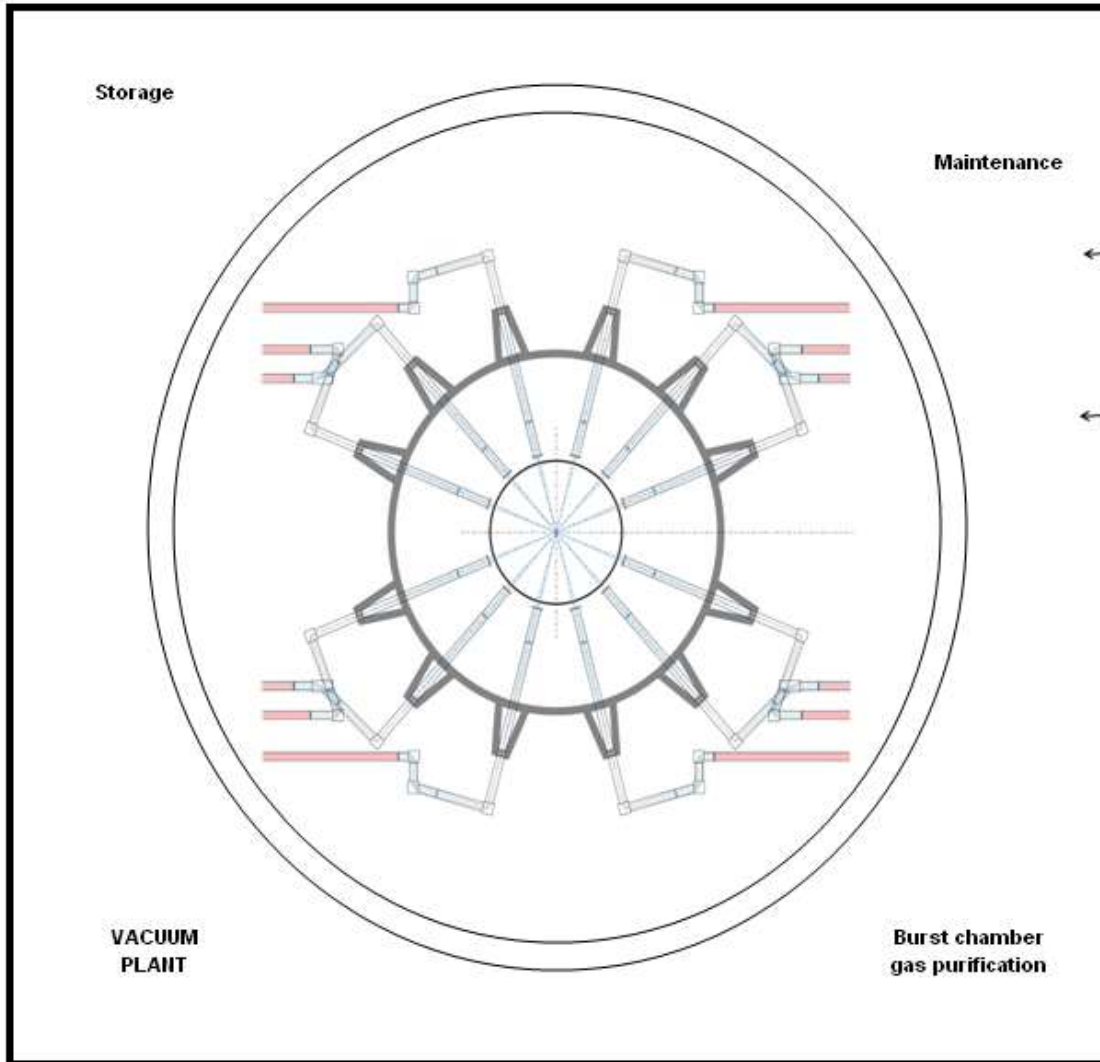
# Targetry first level:



# Targetry ground level:



# Targetry second level:



# Target Factory Operation: Integrating Advanced Target Technologies and Pragmatics of the Production Line

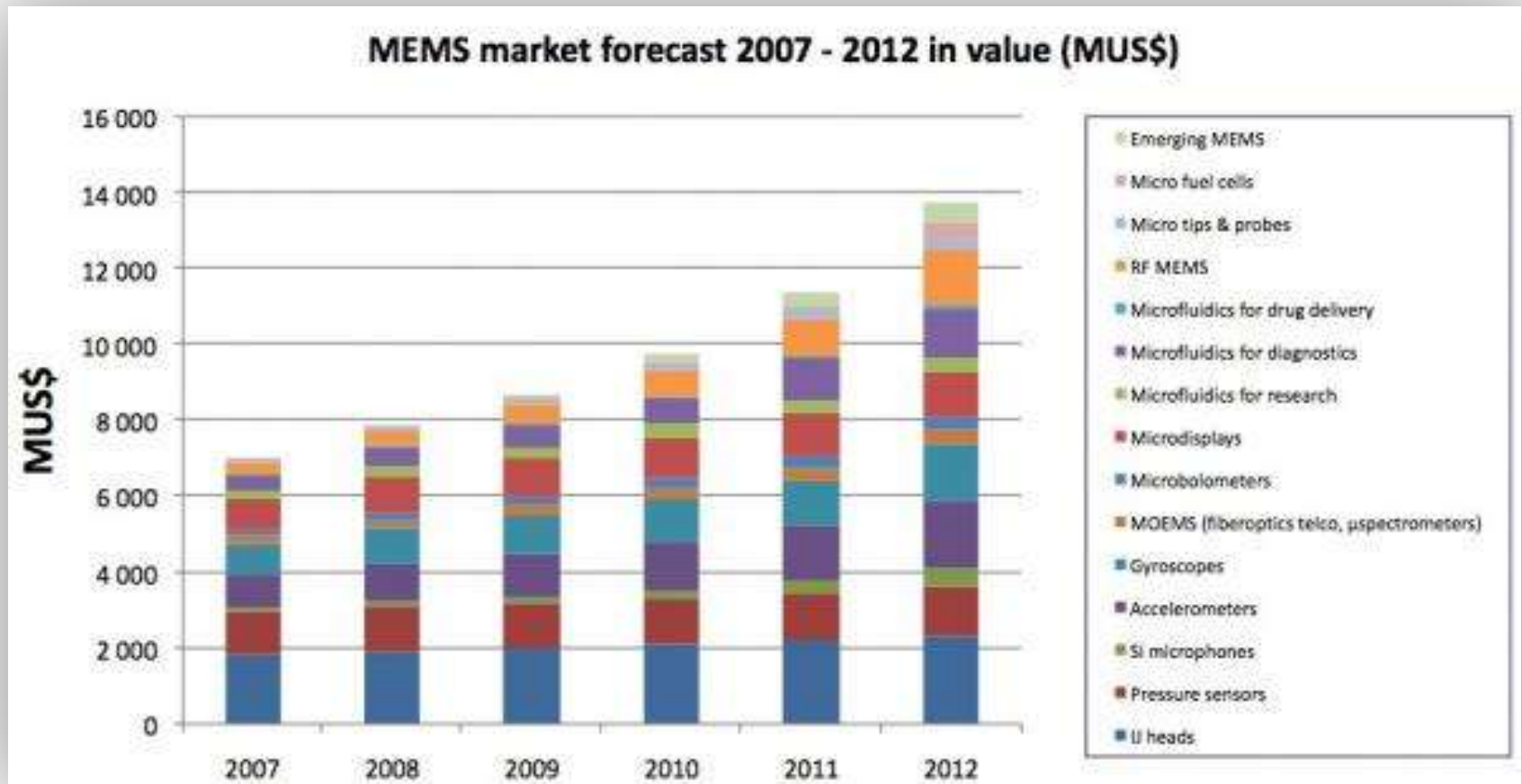
- Operating regime to be decided from economic analysis; six sigma aspiration, pragmatically 3-4 sigma.
- Sampling frequency and techniques to be decided.
- Highly automated with some ability for remote handling.
- On-line buffer period built in.
- Transfer technique: mechanical vs levitation.



# **IS COST-EFFECTIVE IFE MICROTARGET PRODUCTION ACHIEVABLE?**



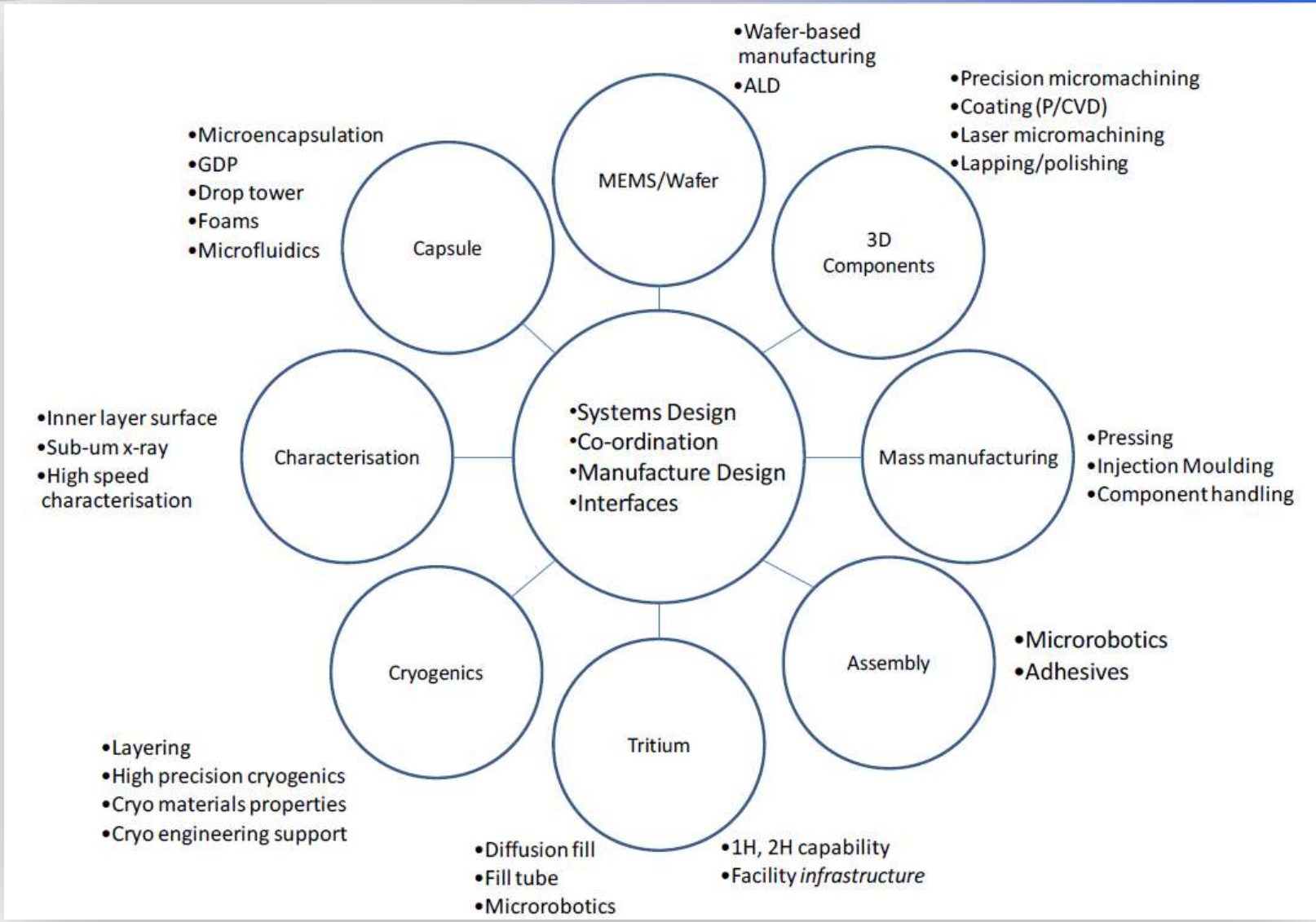
# Industrial Comparisons (1)



***Yole 2007-2012 global MEMS market forecast***







**8 key Capability Areas each with sub-capabilites**

# Summary

- Target technology is one of the key challenges for HiPER
- Considerable progress has been made in the Preparatory Phase in many areas of Targetry
- Building on this work a robust plan for Targetry has been written for the HiPER Business Case



# Development of repetition rate fusion target injection for HiPER

B. Rus<sup>1</sup>, P. Homer<sup>1</sup>, J. Polan<sup>1</sup>, M. Kozlová<sup>1</sup>, V. Kolařík<sup>2</sup>, T. Papírek<sup>2</sup>, P. Havlík<sup>3</sup>, M. Kopecký<sup>3</sup>,  
D. Neely<sup>4</sup>, M. Tolley<sup>4</sup>, N. Alexander<sup>5</sup>

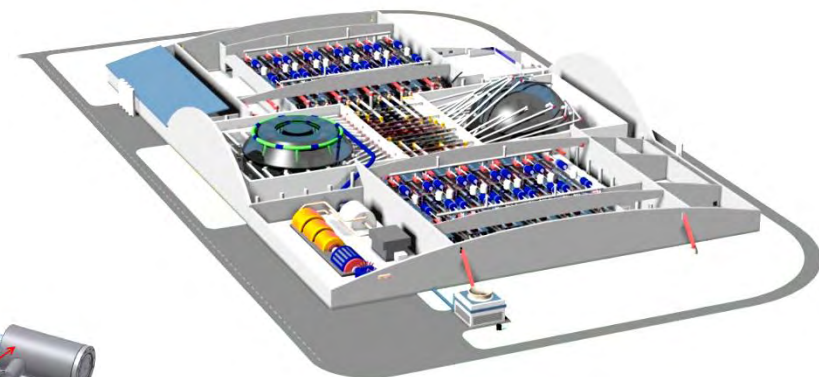
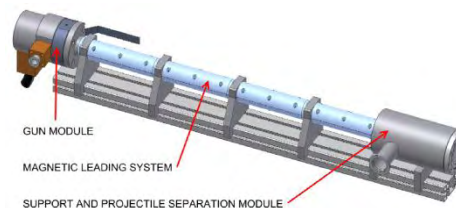
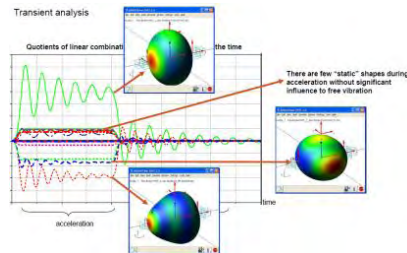
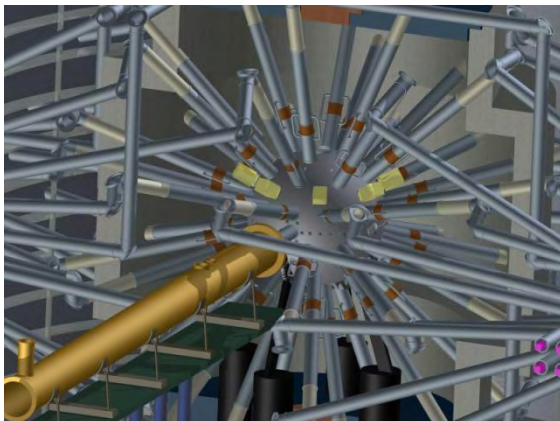
<sup>1</sup> *Institute of Physics v.v.i. / PALS Centre, 182 21 Prague 8, Czech Republic*

<sup>2</sup> *SWELL s.r.o., Hořice, Czech Republic*

<sup>3</sup> *Delong Instruments s.r.o., Brno, Czech Republic*

<sup>4</sup> *Scientific and Technology Facility Council, United Kingdom*

<sup>11</sup> *General Atomics, USA*

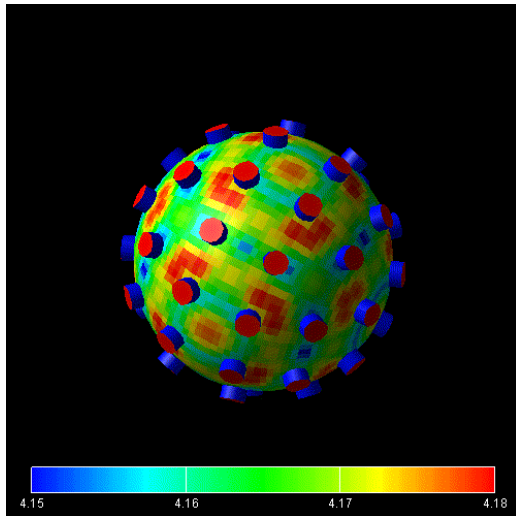


**Developed within activities of the Work Package 15 of HiPER including:**

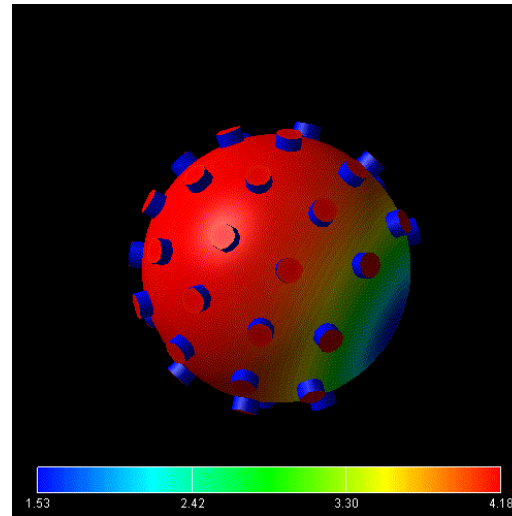
- 1. Fusion chamber conception**
- 2. Injector schemes and proposed solutions**
- 3. Studies of target integrity during acceleration phase**
- 4. Target chamber and target area shielding**
- 5. Remote handling**
- 6. Debris mitigation, ELMG deflector**
- 7. Time synchronisation between the injected target and laser pulse arrival**
- 8. Baseline target tracking solutions**
- 8. Vacuum system**
- 10. Implosion and fusion diagnostics**
- 11. Maintenance of final optics and diagnostics**

**48 beams:** perfectly symmetric configuration

## Shock ignition



## Fast ignition



$$I(\theta) = \frac{1}{\int_{-\pi}^{\pi} r d\varphi} \int_{-\pi}^{\pi} I(\theta, \varphi) r d\varphi$$

This can be expanded in Legendre polynomials :

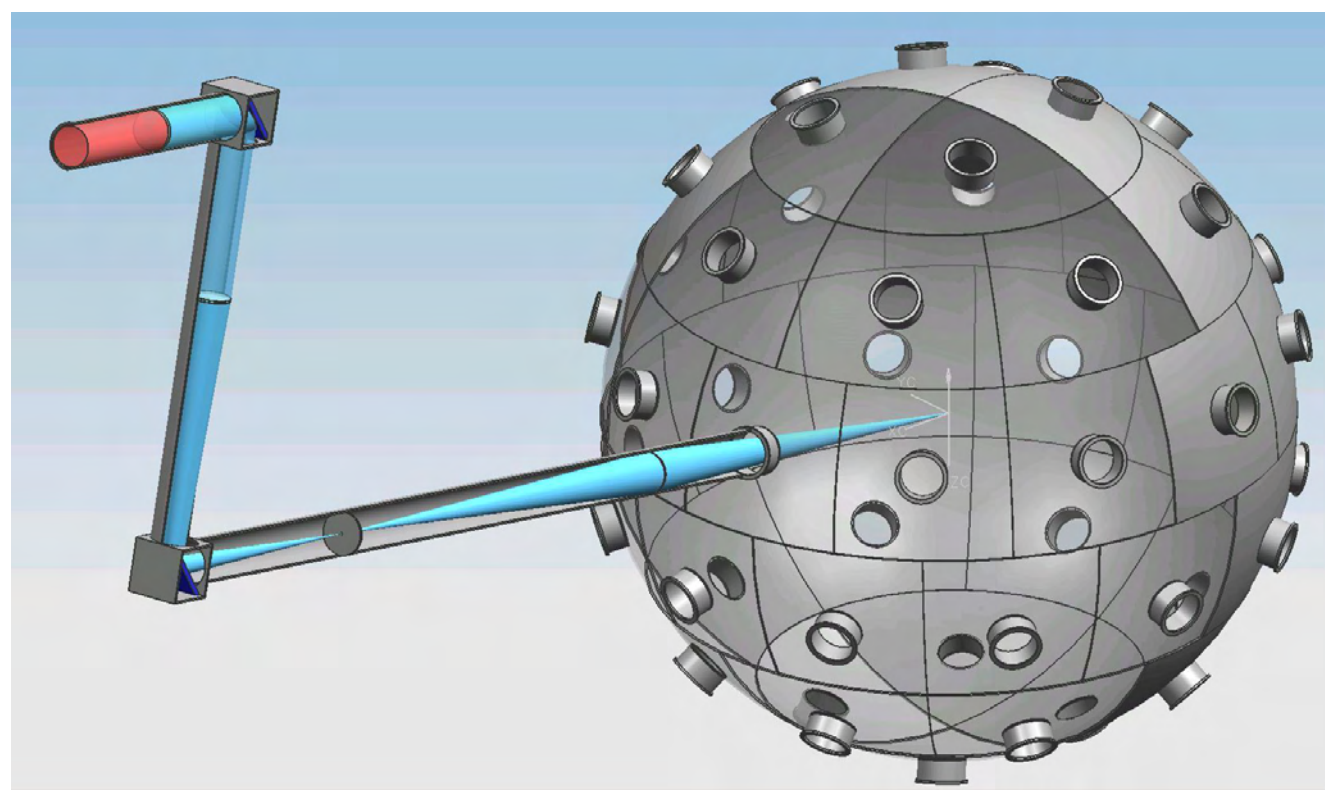
$$\tilde{I}(\theta) = \bar{I} \left( 1 + \sum_{k=1}^{\infty} a_k P_k(\cos \theta) \right)$$

where  $k$  is the legendre mode and  $a_k$  is calculated using

$$a_k = \frac{2k+1}{2} \int_{-1}^1 \frac{I(\theta)}{\bar{I}} P_k(\cos(\theta)) d(\cos(\theta))$$

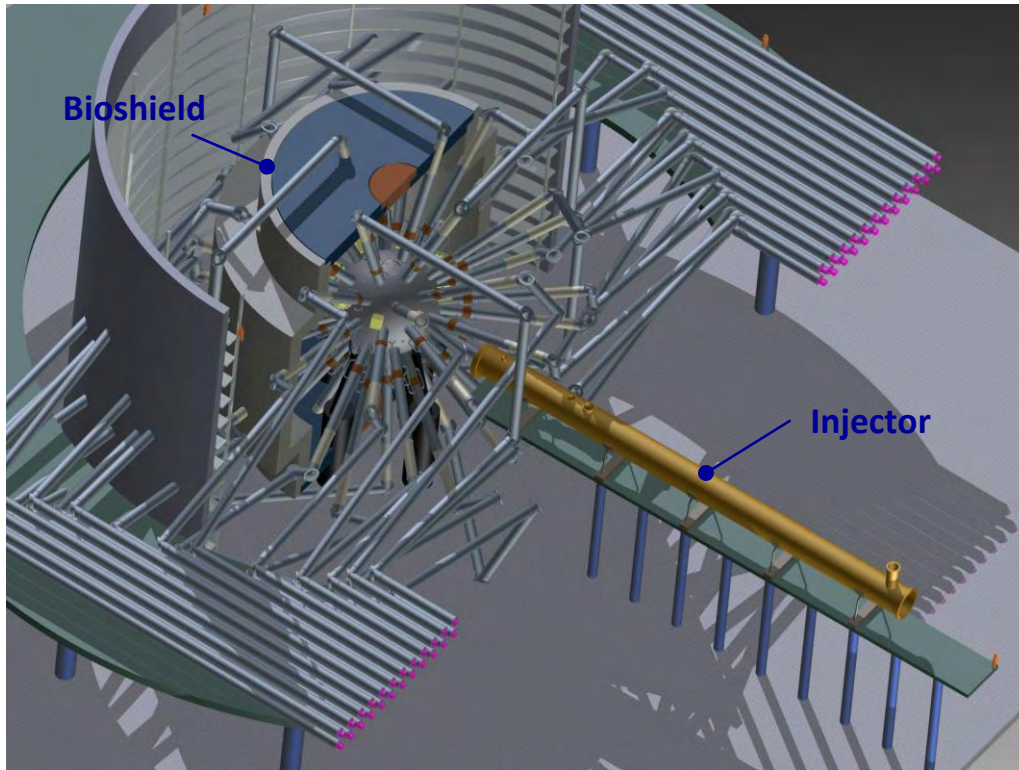
$a_k$  is here the normalized legendre mode coefficient.

## Geometry: 48 beams for spherically symmetric illumination

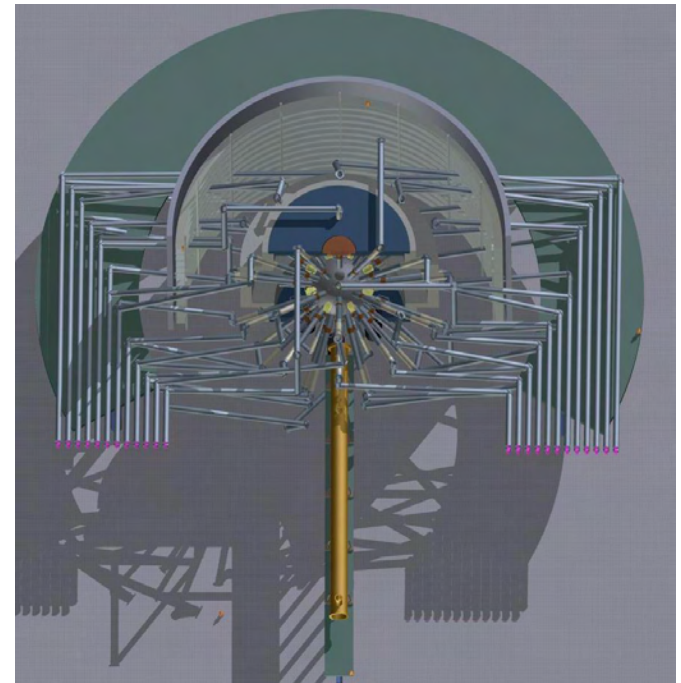


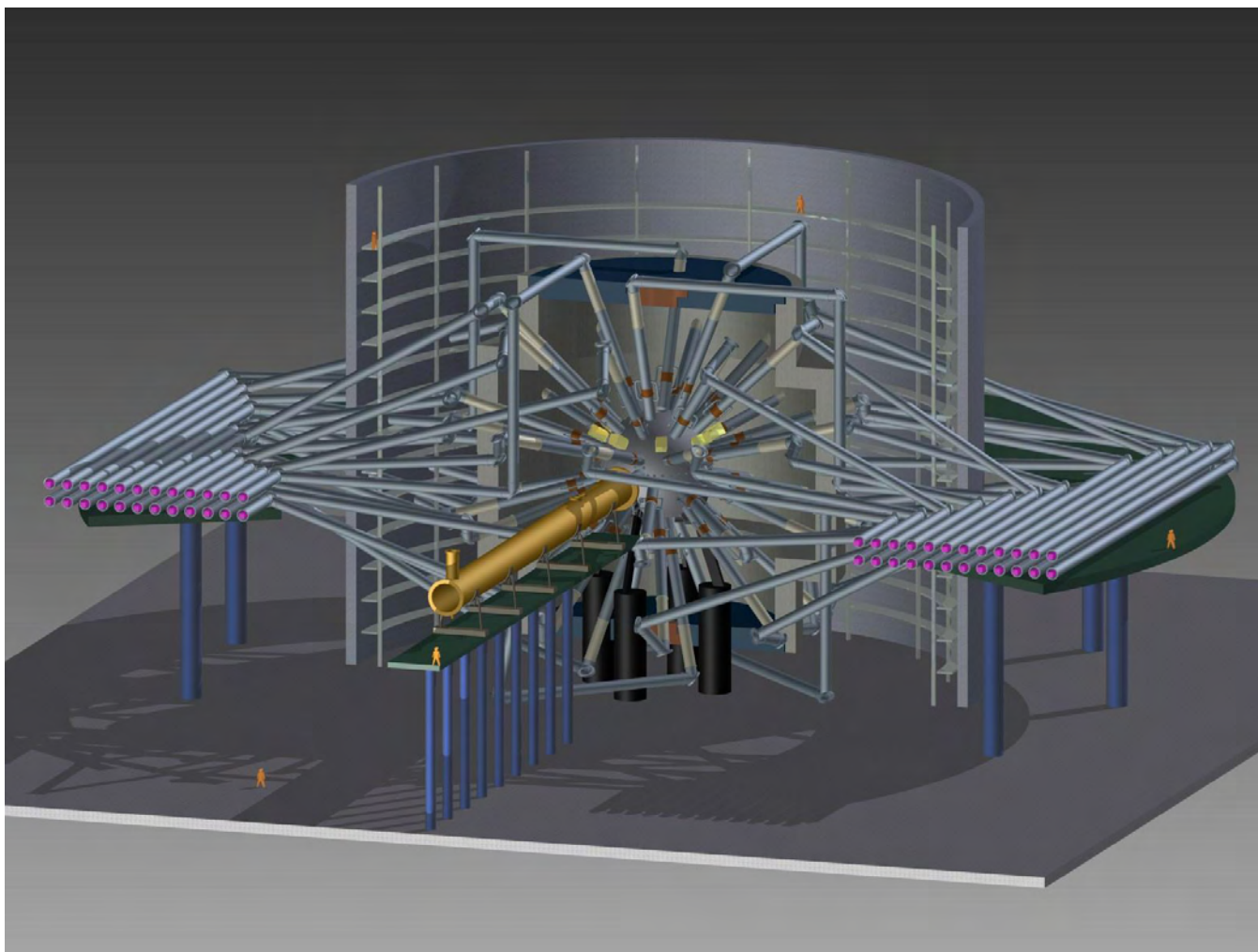
$N_b$	L	$N_i$	$\theta_i$ (deg)	$\phi_i$ (deg)	$M$	$\sigma_{rms}$
42	5	5 10 12	25.14 57.33 90.		2	$2.46 \cdot 10^{-2} \%$
46	4	8 15	30.55 70.12		3	$1.5 \cdot 10^{-4} \%$
48	12	4	21.23	0.	3	$1.77 \cdot 10^{-5} \%$
		8(4+4)	47.03	$\pm 23.36$		
		12(4+4+4)	74.95	0. $\pm 29.83$		
60	12	5	21.44	0.	3	$2.88 \cdot 10^{-5} \%$
		5	41.98	0.		
		10(5+5)	58.84	$\pm 23.97$		
		10(5+5)	81.27	$\pm 12.55$		

1. Arrival of beams compatible with polar illumination scheme (for HiPER Demo)
2. All mirrors are located outside the bioshield
3. Injector in the horizontal plane, 50 m length, exit plane 10m from the chamber center



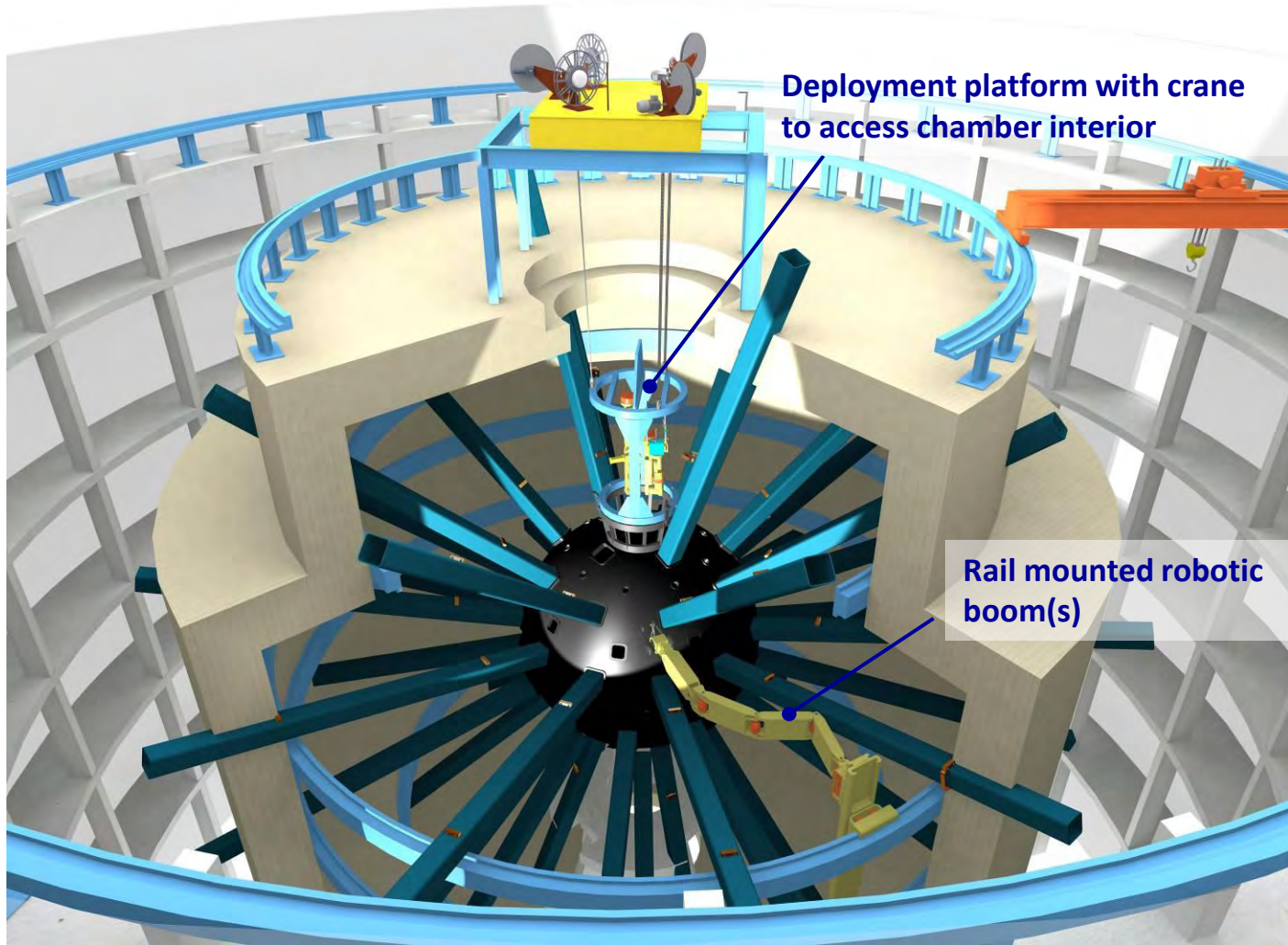
**Top view**

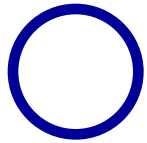






Equatorial plane where the injector is placed is unobstructed



**Challenge: acceleration trajectory** $v = 500 \text{ to } 1000 \text{ m/s}$  $a < 1000 \text{ g}$ 

$$s \geq \frac{v^2}{2a} \quad \textit{whatever injector design}$$

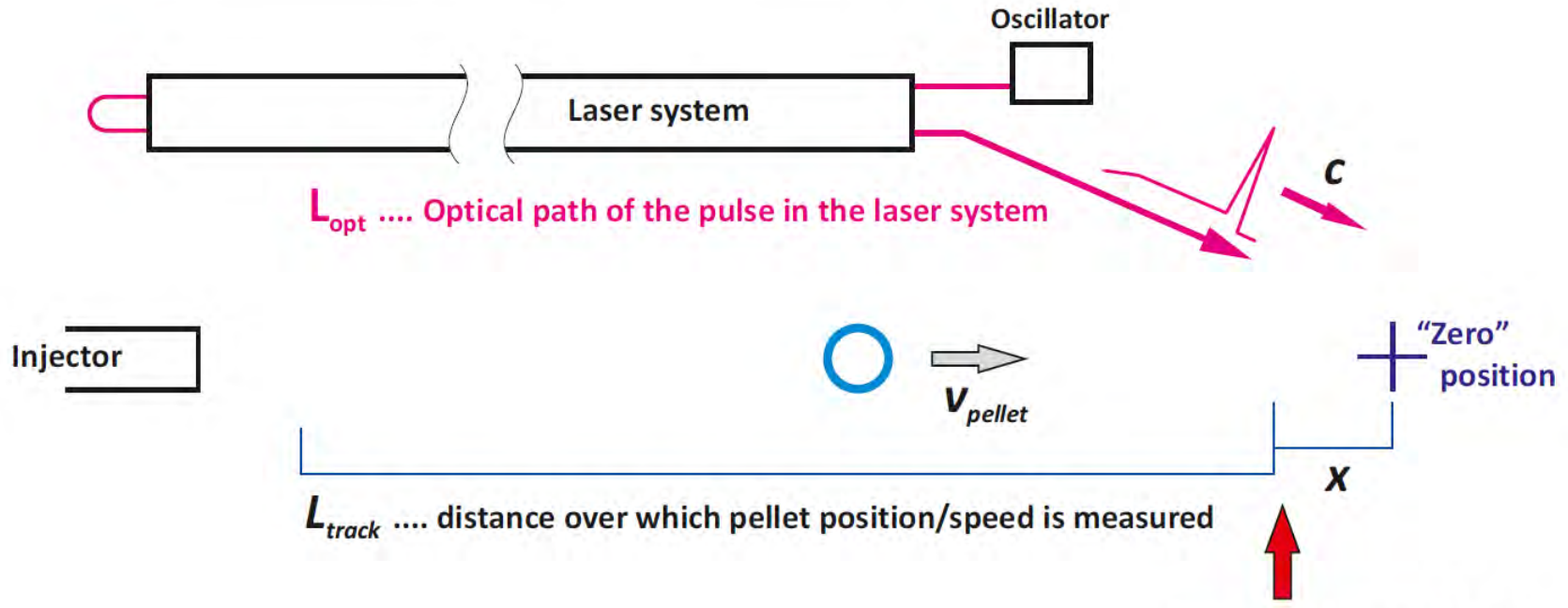
For  $v = 1000 \text{ m/s}$ :  $s \geq 50 \text{ m}$

For  $v = 500 \text{ m/s}$ :  $s \geq 12.5 \text{ m}$

For  $v = 300 \text{ m/s}$ :  $s \geq 4.5 \text{ m}$

*Lower injection velocities preferable !*

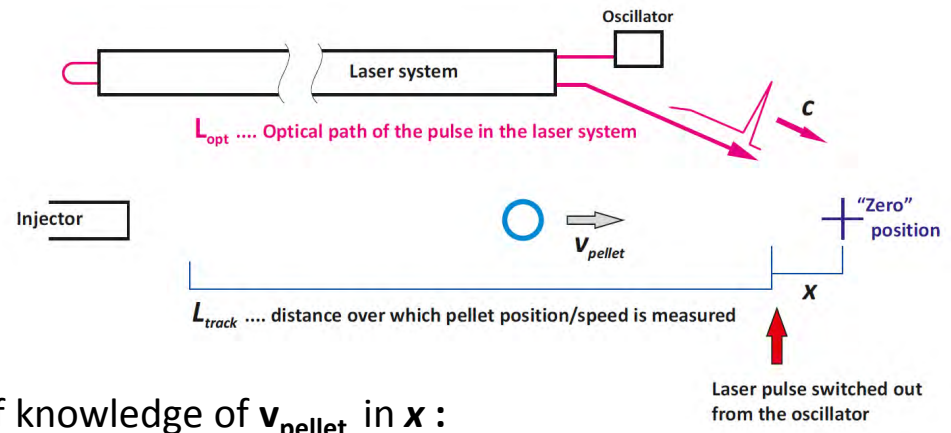
Laser pulse must meet in time with the injected pellet



Condition: 
$$\frac{x}{v_{pellet}} = \frac{L_{opt}}{c}$$

For  $v_{pellet} = 1000 \text{ m/s}$  and  $L_{opt} = 300 \text{ m}$ :  $x = 1 \text{ mm}$

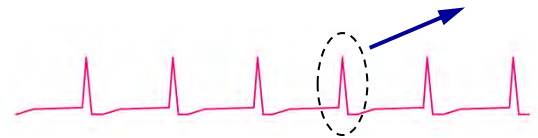
However, accuracy of the knowledge of  $v_{pellet}$  in point  $x$  is critical!



Accuracy of knowledge of  $v_{pellet}$  in  $x$  :

- ➡ Accuracy of knowledge of its arrival time to "0"
- ➡ Last chance to switch out the laser pulse from the oscillator and to set its arrival to "0"

Target tracking triggers pulse switch-out from the oscillator:



Target arrival prediction accuracy:

$$\Delta t \cong \left( \frac{\Delta v_{pellet}}{v_{0\ pellet}} \right) \frac{x}{v_{0\ pellet}}$$

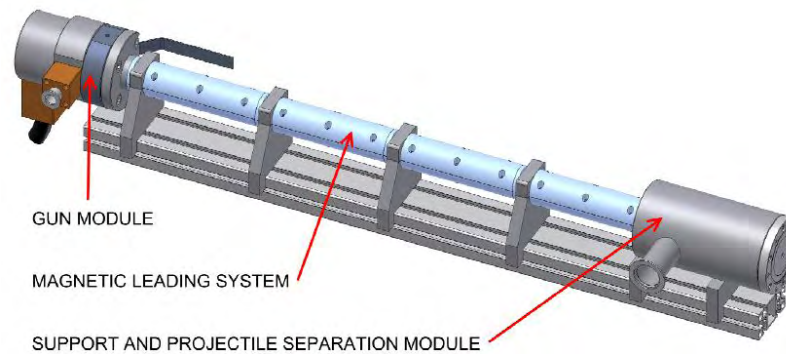
Sampling/tracking the target trajectory every mm (=1MHz at 1000 m/s) with 10  $\mu$ m accuracy:

$\Delta v/v = 10^{-2}$ :       $\Delta t = 10\text{ ns}$ ,    $\Delta x = 10\ \mu\text{m}$

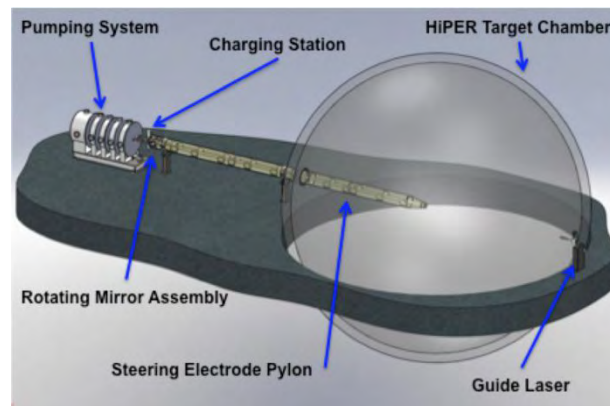
**10 ns uncertainty of target arrival can still be accommodated with pulse-to-pulse distance in the oscillator running at 100 MHz, though better accuracy of tracking would be favourable**

Search for innovative industry-supplied solutions: 200 kEuro development

## 1. Injector development & small-scale testbed: Delong Instruments (Czech Rep)



## 1. Target deflection and steering systems : General Atomics (USA)

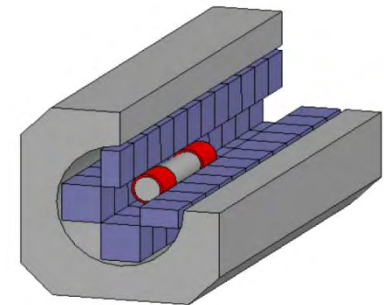
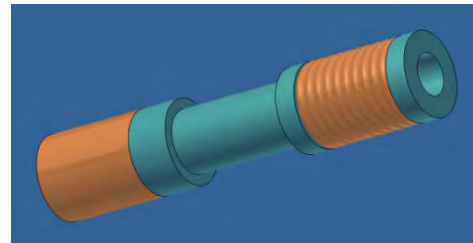
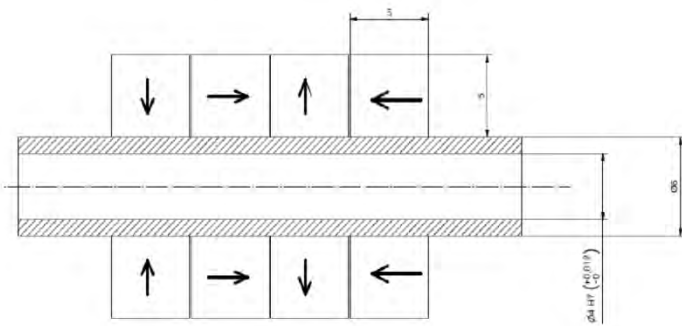


## Injector problem separated into two sub-problems

- a) Ultra-precise linear guiding + accelerator
- b) Sabot-pellet separator, sabot steering

## Principle selected for development: MG linear Halbach-type guideway

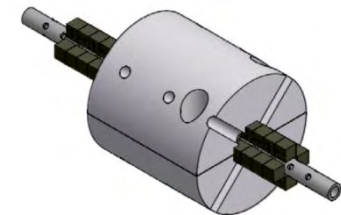
The guiding is dynamic: induction coils at both end of the sabot

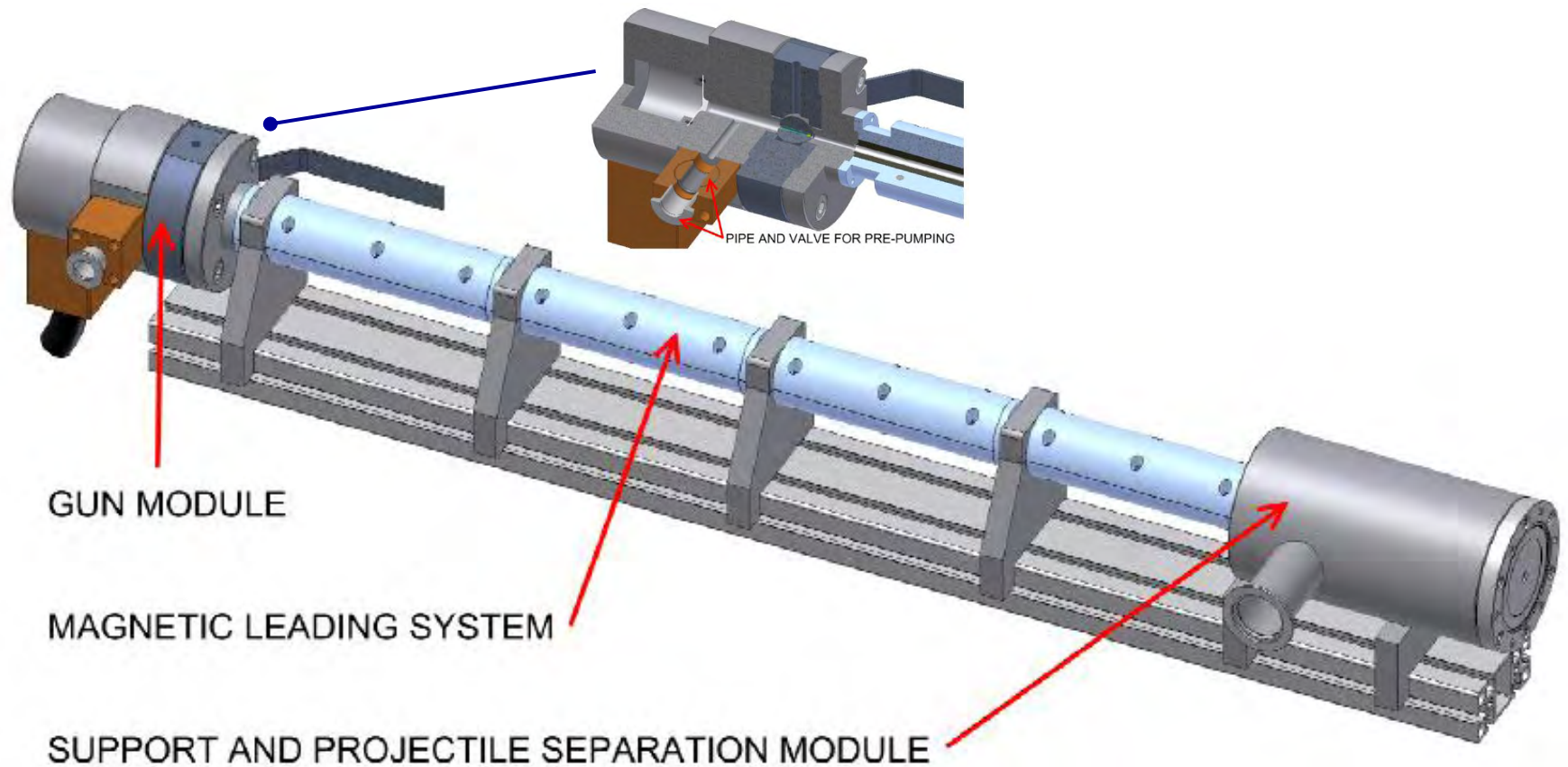


## Separated guiding and acceleration

Acceleration at “low speed” (500 m/s) by gas gun

Acceleration at speeds >500 m/s by laser ablation





## Construction of a prototype of 1m long module

Gas gun section and precision of a dummy target delivery will be tested



## Injector demonstrator assembling

1 meter long segment of the gas-acceleration section of the injector assembled (January 2011)

Diagnostic package to measure precision of the velocity (high-speed camera) and of lateral guiding (interferometer) being installed (February 2011)

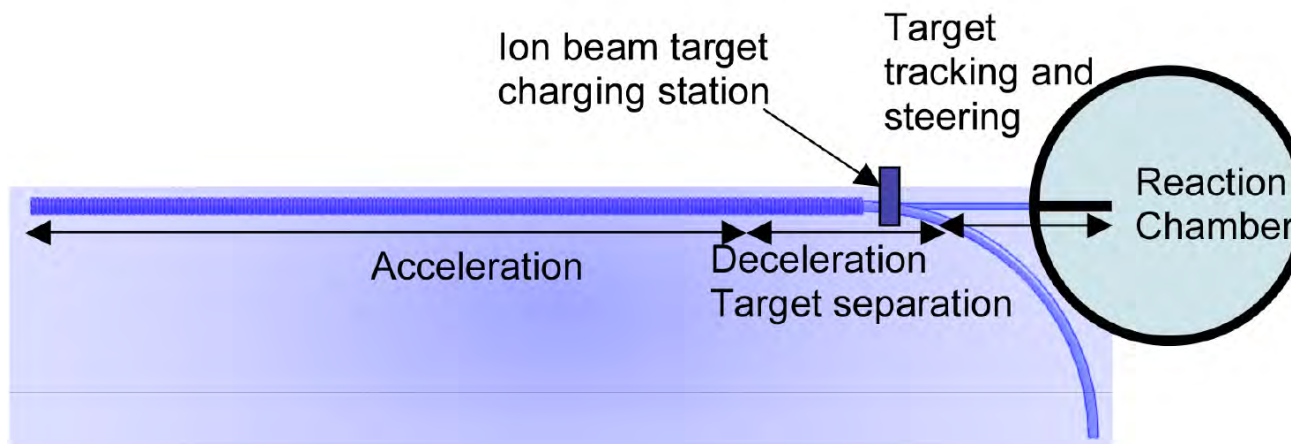
Tests to start in March 2011



## Steering and target-sabot separation:

Four plausible options suggested (General Atomics):

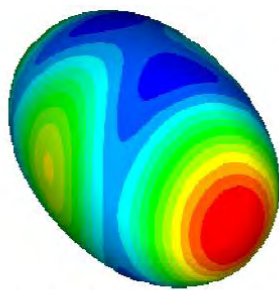
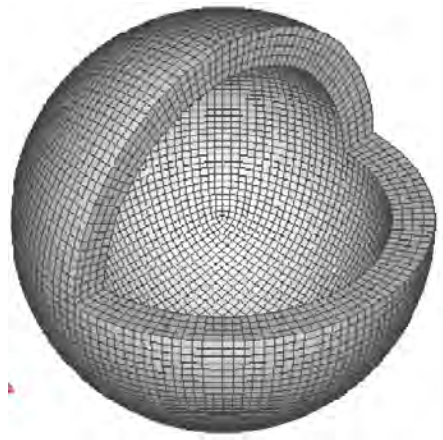
1. Electrostatic
2. Magnetic lens with superconductor layer (Pb) on the target
3. Active magnetic steering
4. Laser ablation



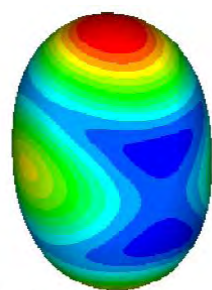
**Study of target shape during acceleration: finite element analysis**  
**2-mm diameter pellet studied (shell+cryogenic D-T)**  
**0.2mm DT fuel layer thickness, 0.74mg mass**

### Lowest modes of oscillations:

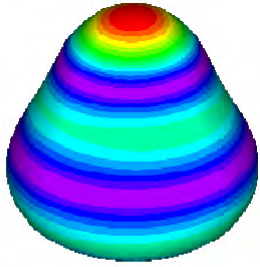
Pellet FEM



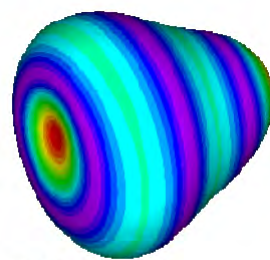
Output Set: Mode 1, 1352.496 Hz  
Deformed(1.081): Total Translation  
Contour: Total Translation



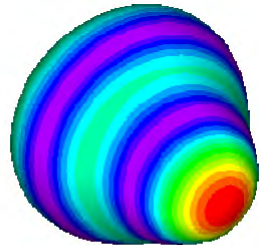
Output Set: Mode 2, 1352.504 Hz  
Deformed(1.083): Total Translation  
Contour: Total Translation



Output Set: Mode 6, 1827.544 Hz  
Deformed(1.088): Total Translation  
Contour: Total Translation



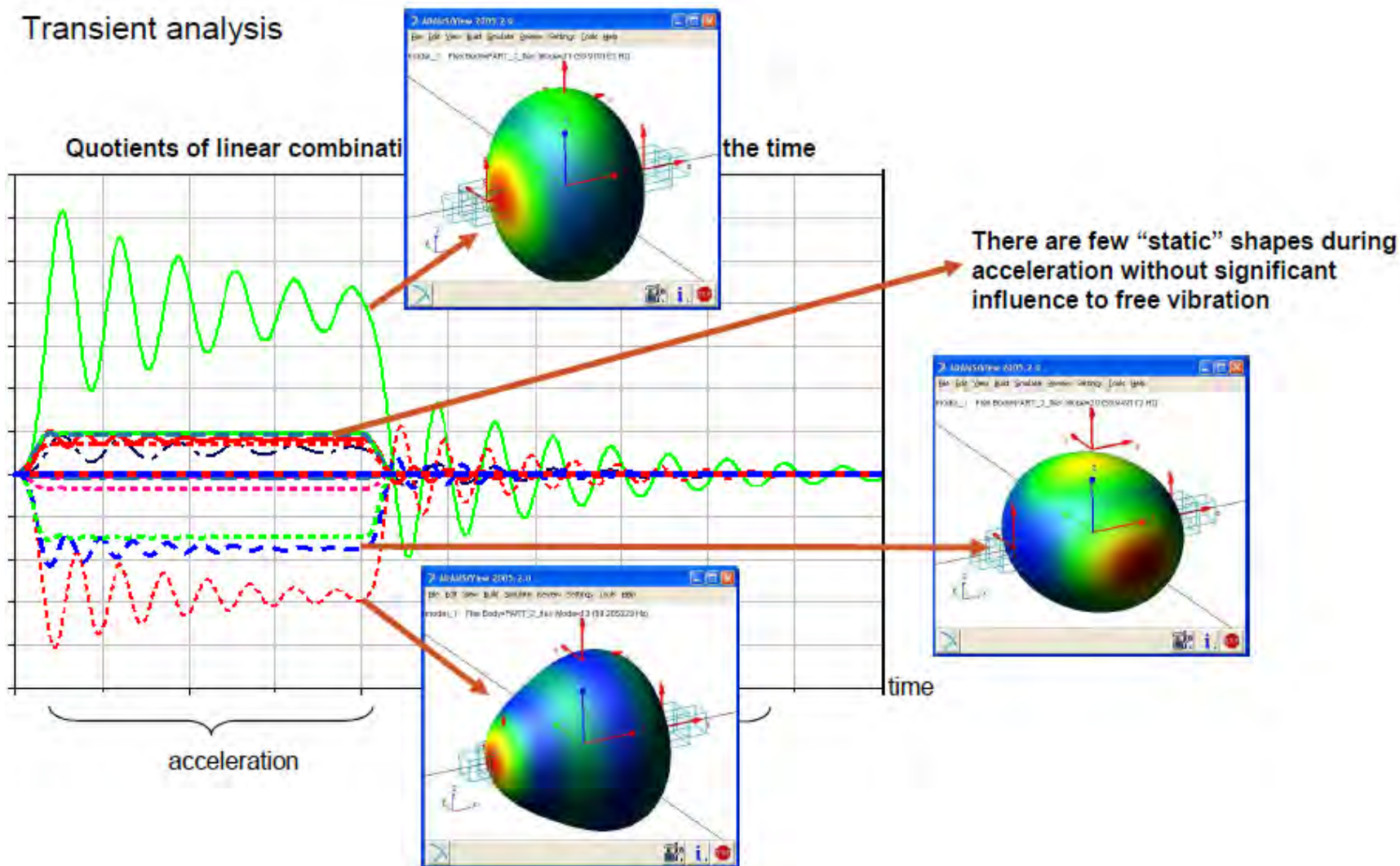
Output Set: Mode 7, 1827.555 Hz  
Deformed(1.061): Total Translation  
Contour: Total Translation

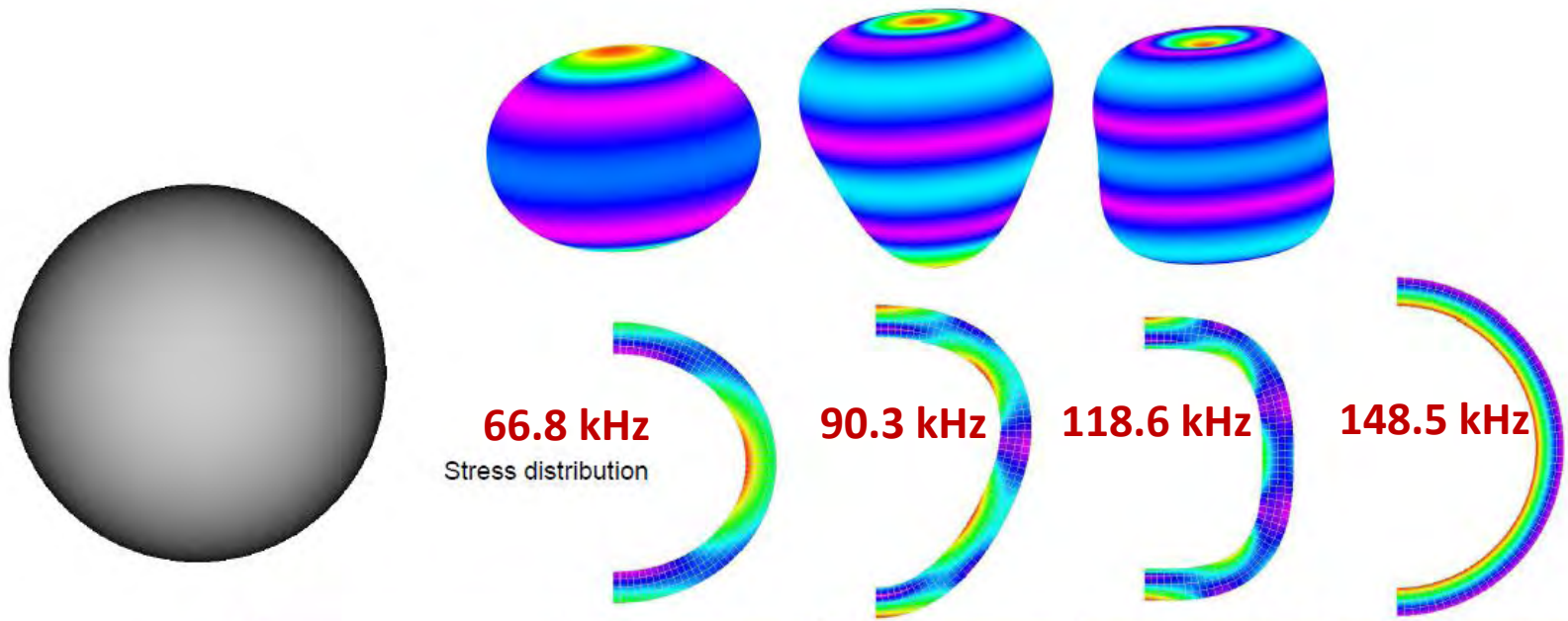


Output Set: Mode 8, 1827.585 Hz  
Deformed(1.391): Total Translation  
Contour: Total Translation

## Acceleration 1000 g over 50 m to the speed 1 km/s

Transient analysis





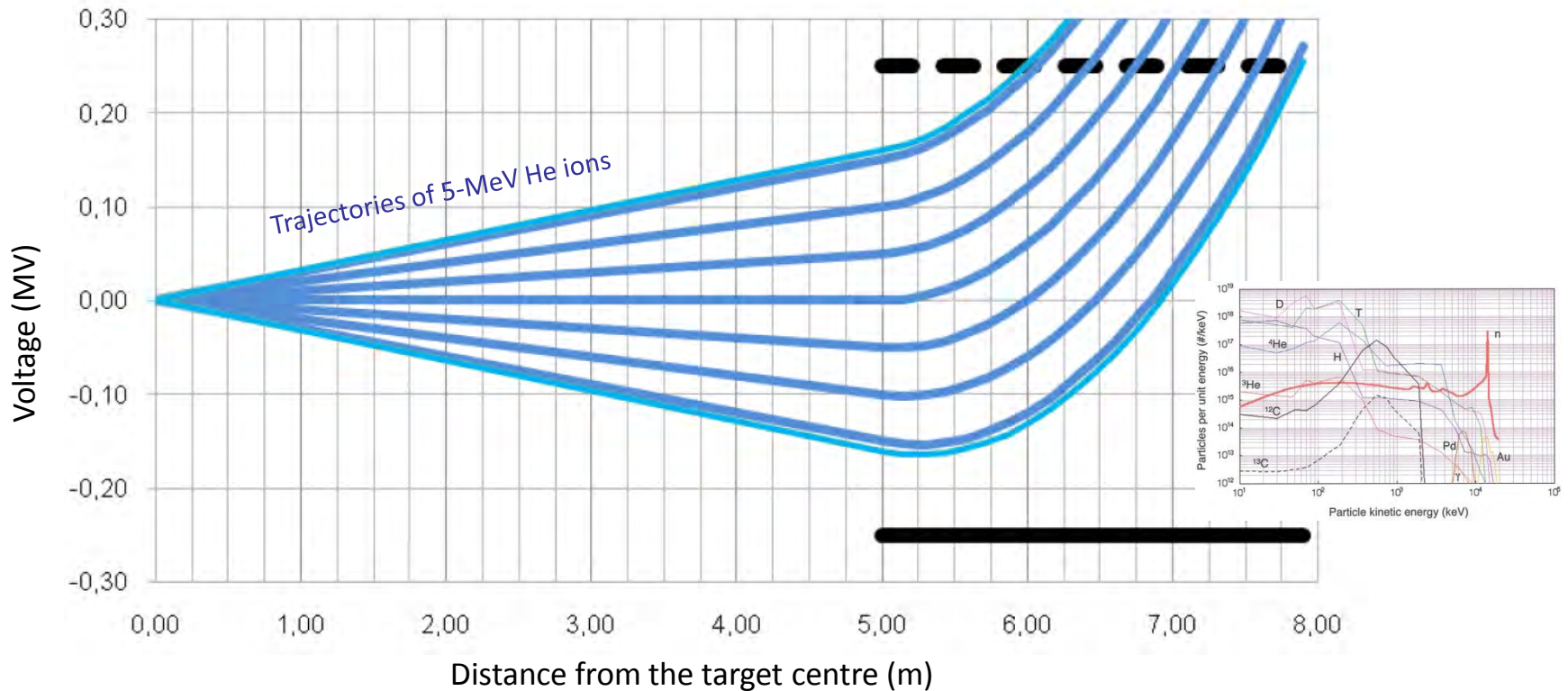
	Eigen shape No.1 „cigar-lentil“	Eigen shape No.2 „pear“	Eigen shape No.3 „cylinder“	Eigen shape No.4 „breathing“
Frequency	66858 Hz	90329 Hz	118629 Hz	148512 Hz
At maximal stress $\sigma_{HMH} = 90$ kPa will be maximal displacement	$u = 1.17 \mu\text{m}$	$u = 0.98 \mu\text{m}$	$u = 0.67 \mu\text{m}$	$u = 0.57 \mu\text{m}$

Deformations of the pellet accelerated at 1000g upon its arrival to the chamber center are  $<1 \mu\text{m}$

**Simulations of FI and indirect-drive targets underway**

Electrostatic deflector: preferred over magnetic solution due to field magnitude

2.9 m long electrodes located between the final lens and the chamber perimeter



**Potential of collection of unburned T on the negative electrode!**

**Potential solutions addressing critical issues of repetition rate target injection identified**

**There seems to be no conceptional show-stopper for target injection at repetition rate of 10 Hz**

**Prototyping of the injector, of the steering systems and achieving target tracking accuracy 10 microns or better critical for demonstrating viability of the suggested solutions**



L.A. Borisenko<sup>1,2</sup>, I.V. Akimova<sup>1</sup>, A.A. Akunets<sup>1</sup>,  
N.G. Borisenko<sup>1</sup>, A.I. Gromov<sup>1</sup>, Yu.A. Merkuliev<sup>1</sup>, A.S. Orekhov<sup>1</sup>

<sup>1</sup>*P.N.Lebedev Physical Institute, Moscow, Russia*

<sup>2</sup>*Lomonosov Moscow State University, Moscow, Russia*

# METALS PRODUCED AS NANO-SNOW LAYERS AND AS NANOPARTICLES SUSPENDED IN POLYMER FOAM FOR CONVERTERS OF LASER LIGHT INTO X-RAY FOR INDIRECT TARGETS AND FOR INTENSIVE EUV SOURCES.



P. N. Lebedev

Physical Institute



MSU  
Faculty of Physics

# OUTLINE

- ✘ Low-density nano-snow metal layers down to 1% of solid material density are considered. Specification of such structures and their parameters is required for pre-experimental non-destructive target characterization. The intrinsic structures have nano-sized average cells.
- ✘ Such low-density structures can be used inside indirect laser targets and as a cover of inner walls of advanced hohlraum to increase radiation temperature and x-ray emission.
- ✘ Searching for better x-ray emitters in plasma polymer aerogels with metal nanoparticles are discussed.





# NANO-SNOW LAYERS FABRICATION

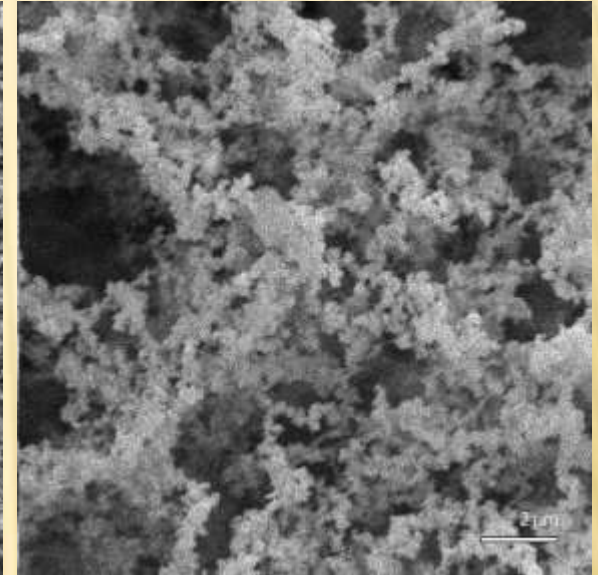
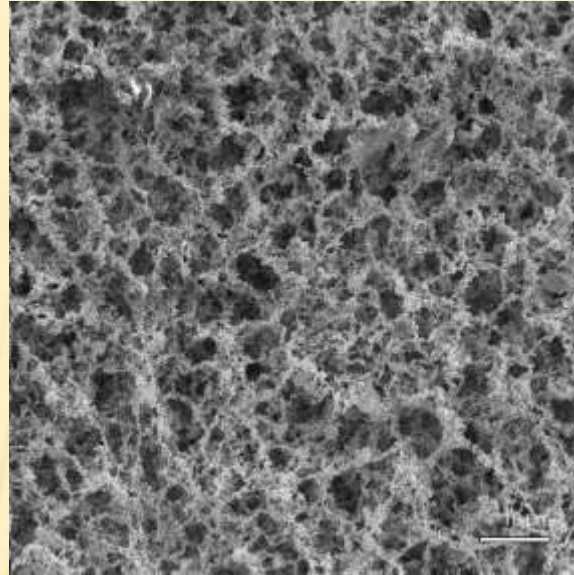
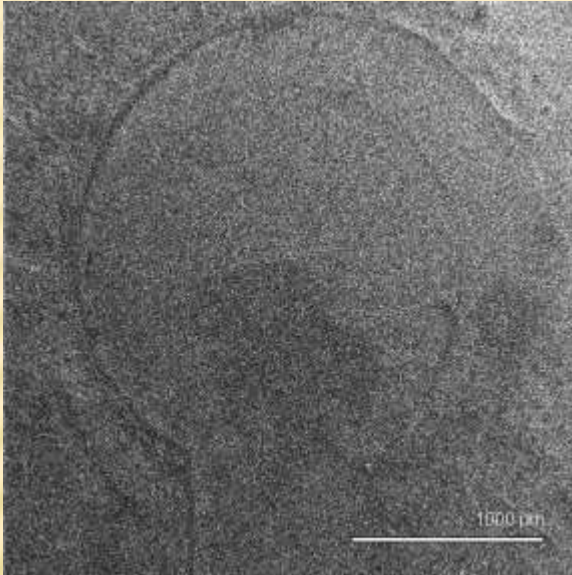


Dr. Gromov with the metal foam production facility (upper)



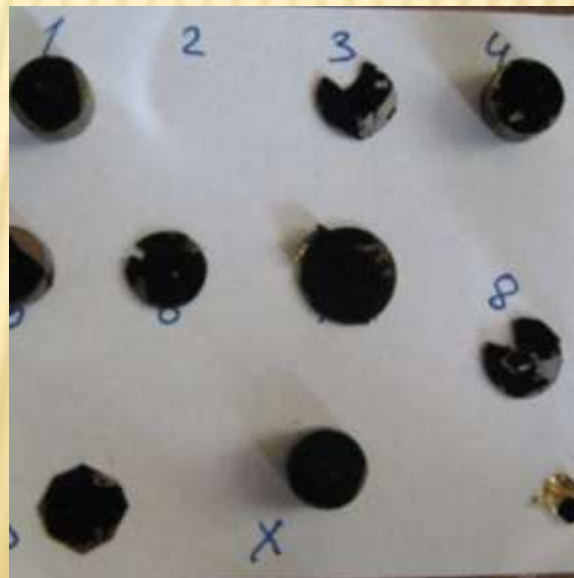
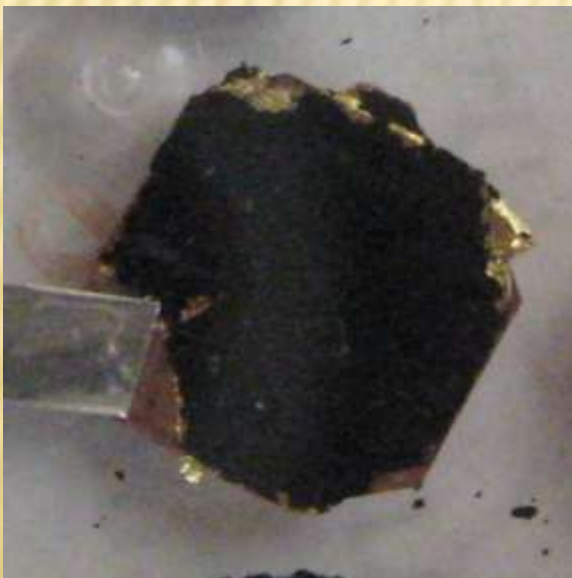
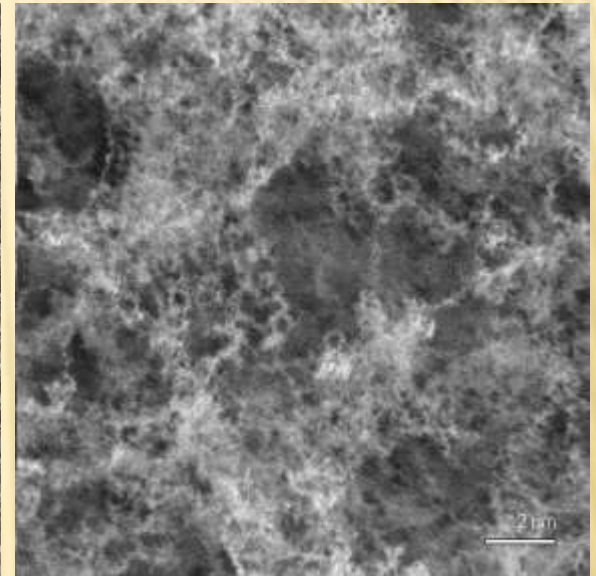
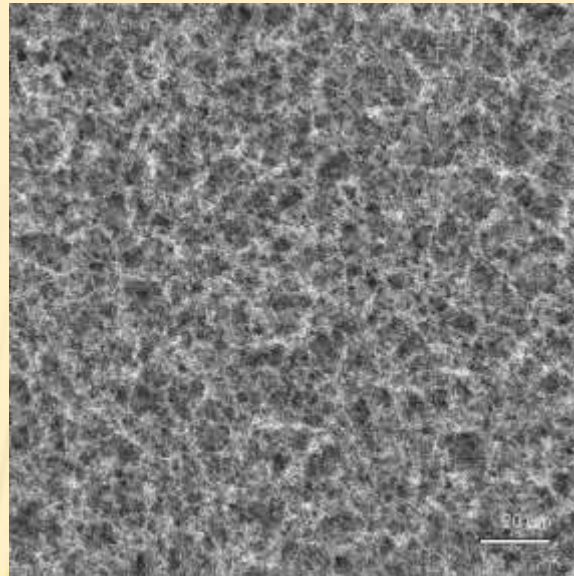
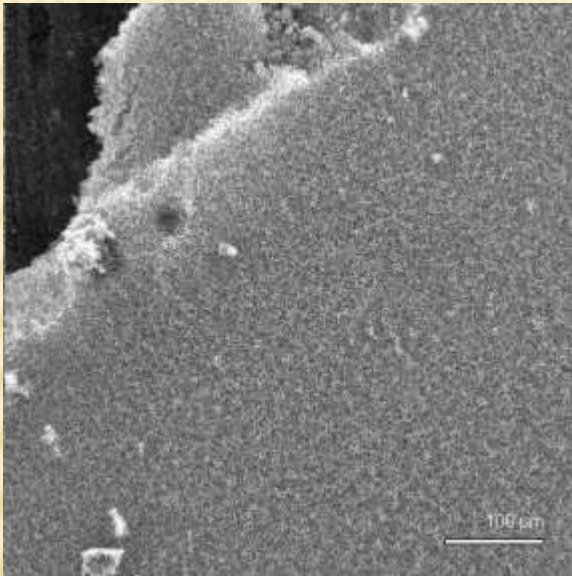
- × Set-up scheme:
- × 1 - vacuum vessel,
- × 2 - bottom,
- × 3 - vacuum and gas pumps,
- × 4 - vessel with heated metal,
- × 5 - heat shield,
- × 6 - targets, 7 - "witness".

# BISMUTH TARGETS



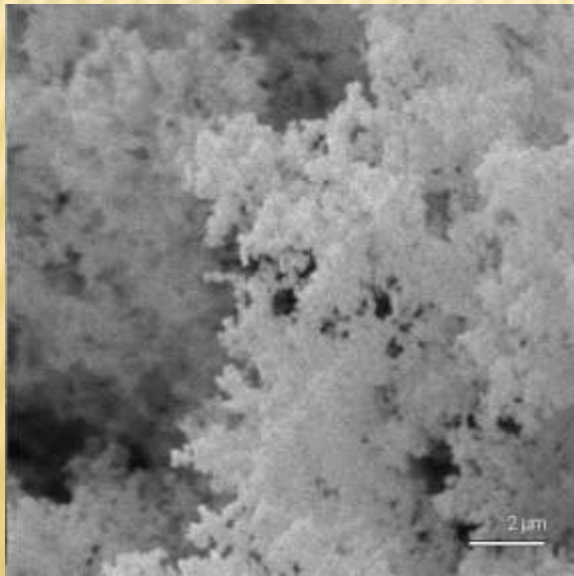
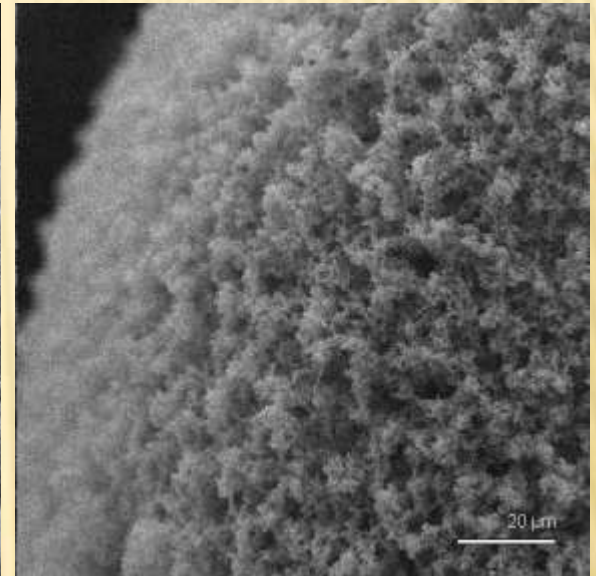
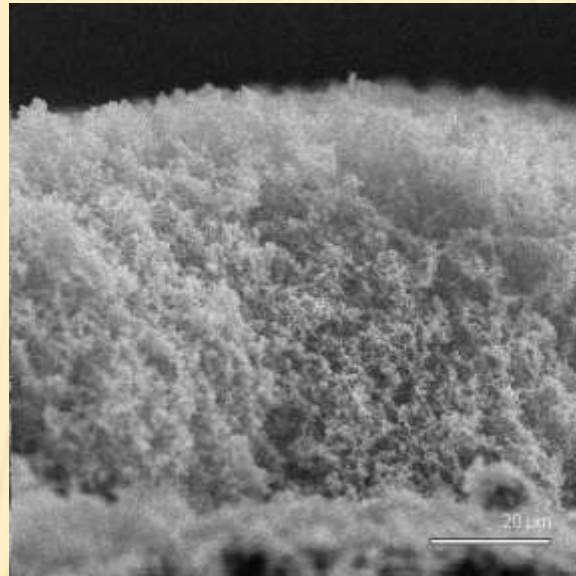
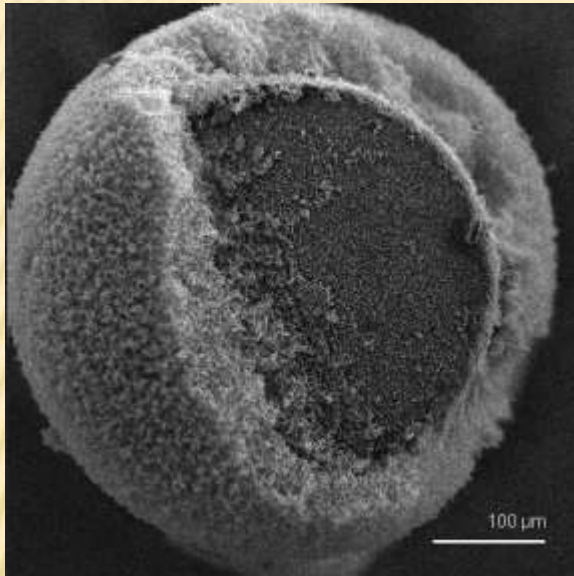
- ✘ SEM images of the Bi target. Homogeneity and similarity of the sample structure is visible on different scales. (upper)
- ✘ Bi targets 80 and 135 μm thick. (left)

# GOLD TARGETS



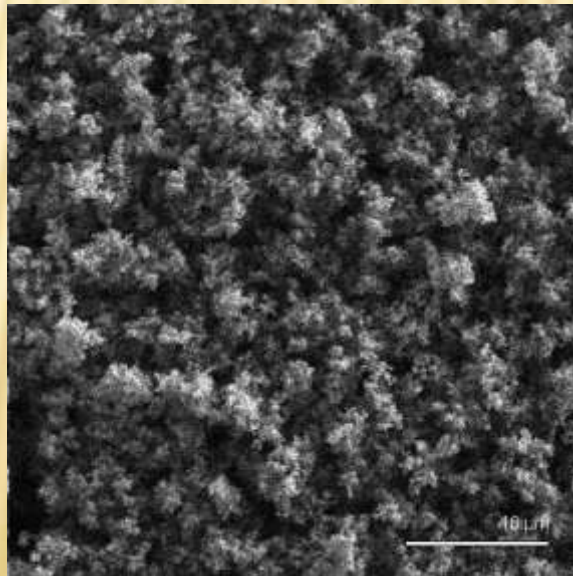
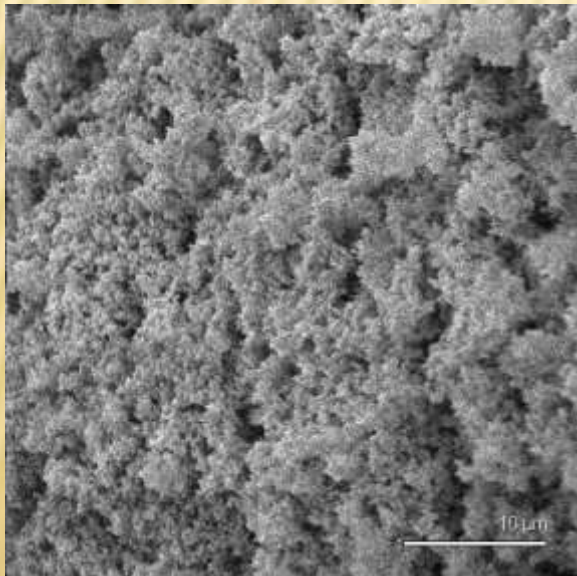
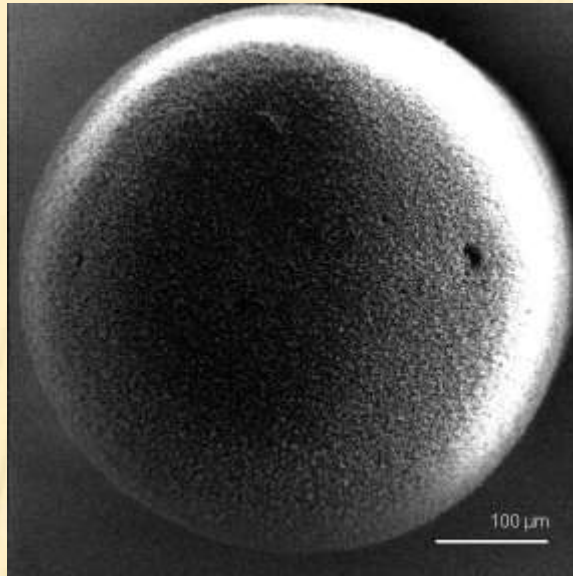
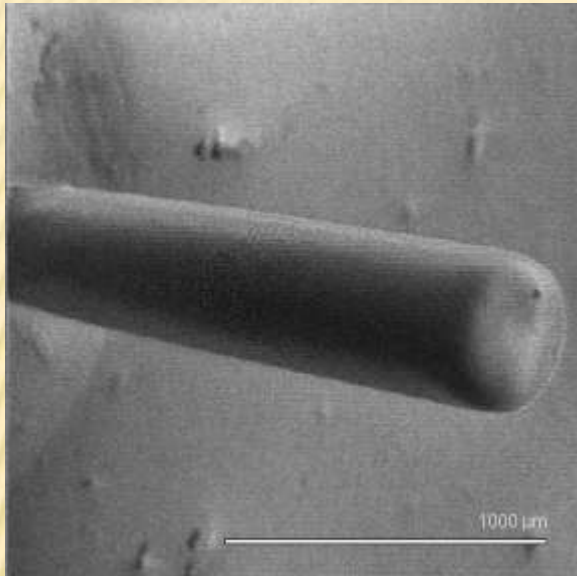
- ✘ SEM images of the Au target. The intrinsic structure on different scales resembles Bi one which is due to similar Z number. (upper)
- ✘ Au targets of various properties. (left)

# SEM IMAGES OF THE “WITNESS”



- × Velocity  $V$  of nanoparticle precipitation in the low-pressure
- × Camera can be estimated with the Stokes law by the weight their interaction. During precipitation leads to formation of fibers of nanoparticles and clews of fibers. However the distance,  $\rho$  – between nanoparticles (camera  $0.05 \text{ m}^3$ , 5 g of metal  $\Rightarrow 17 \text{ m/km}$ ) is considered unpleasant for any significant aerodynamical forces during similar spheres' fall.
- × where  $g$  – free fall acceleration,  $\eta$  – viscosity coefficient.
- × The structure of nano-snow layer on the graphite cylinder is the same as on the target.
- × Velocity of 100 nm solid bismuth nanoparticle in  $\sim 500 \text{ Pa}$  Ar atmosphere is approximately 2 cmph. So collection of all the particles of the metal “fog” down to 10 nm in diameter would take more than a month.

# SEM IMAGES OF THE “WITNESS”



- ✘ Diameter of nanoparticles in the nano-snow layer and the layer density depend on the gas pressure in the camera and the gas itself.
- ✘ Low-density Bi layers are rather fragile and can sinter at the temperatures around 50-70 C.

# SKYSCAN 1074 MICROTOMOGRAPH

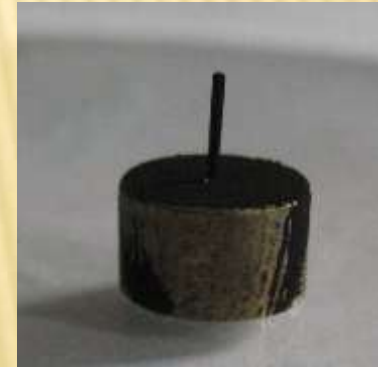
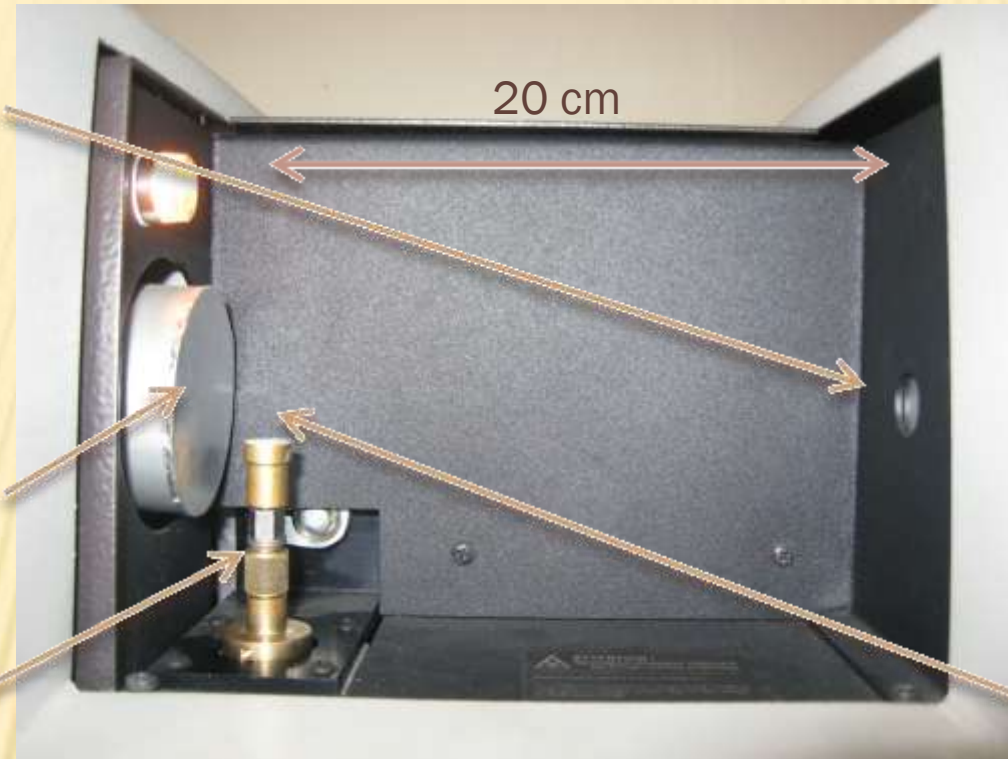
X-ray tube window

- $U=20-40$  kV
- $A_{\max}=1000$   $\mu$ A
- $\varnothing = 100$   $\mu$ m

CCD-camera

looking at  
phosphor screen  
under thin Al filter

- Pixel size  $21$   $\mu$ m
- 12 bit depth

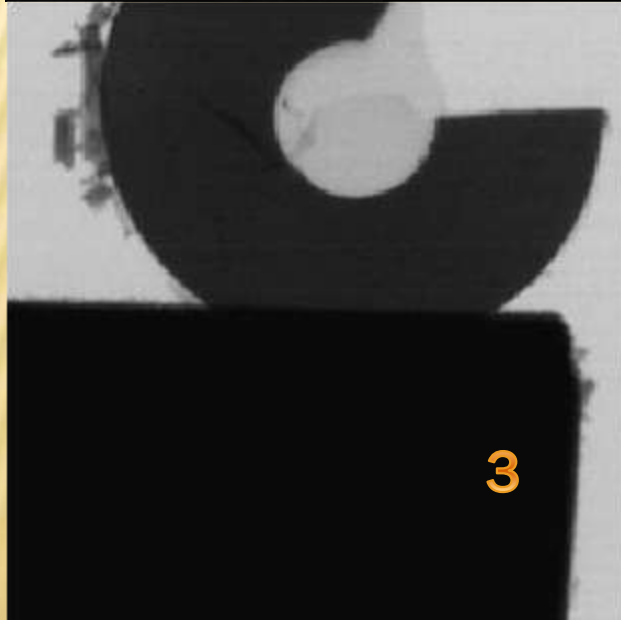
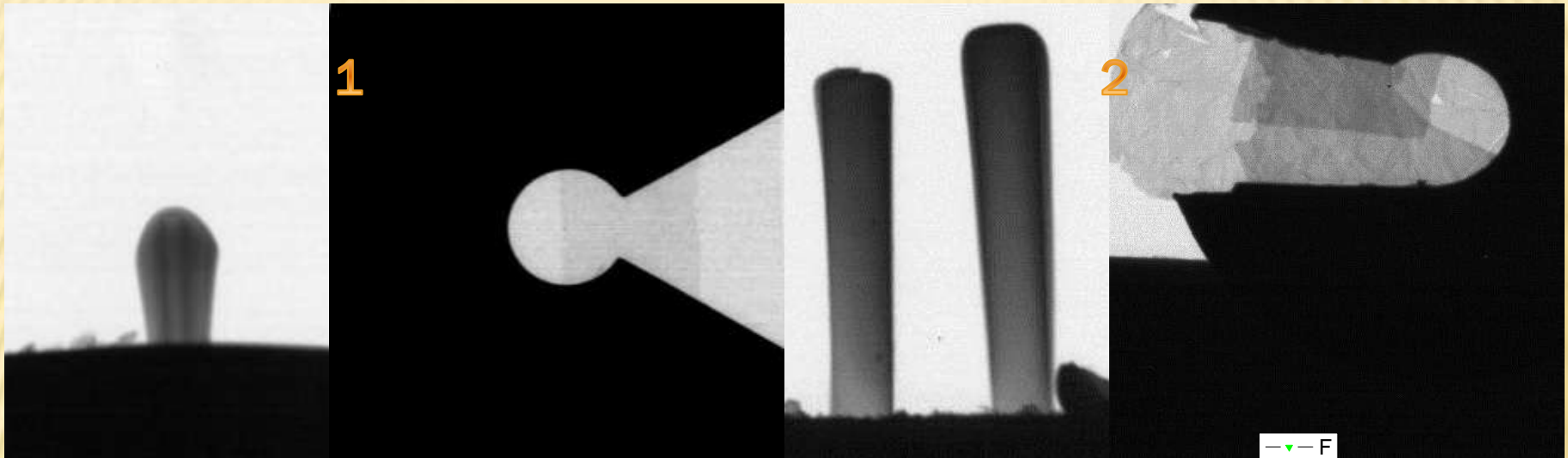


Au "witness" on  
the holder.

Rotating table for  
the samples.  
Minimum rotating  
angle -  $0.9^\circ$  (400  
steps per 1 full  
turn)

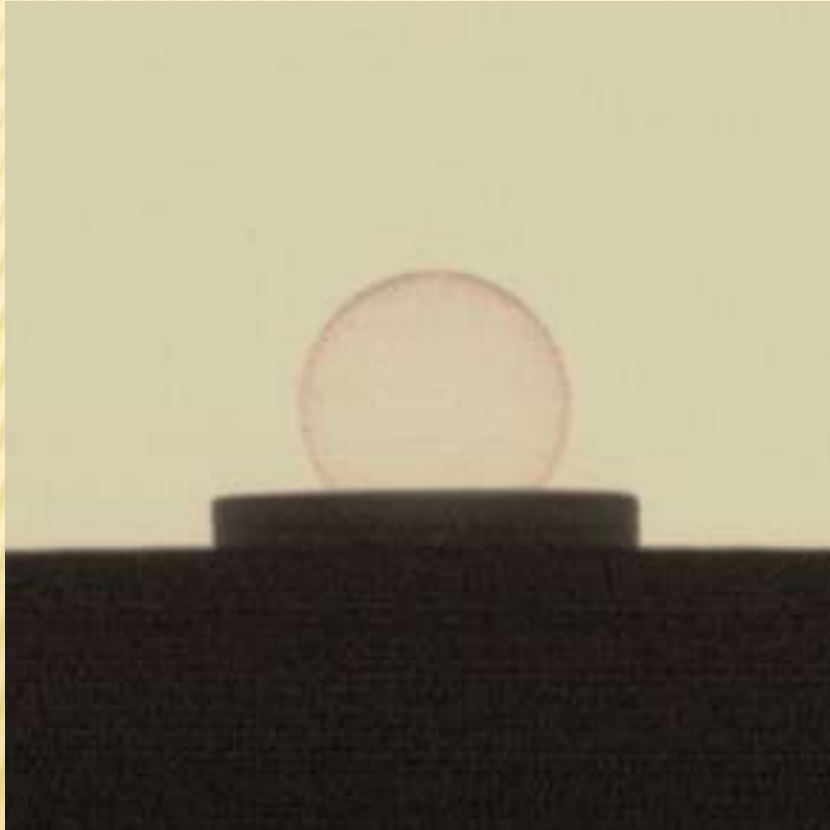


# TARGET CHARACTERIZATION

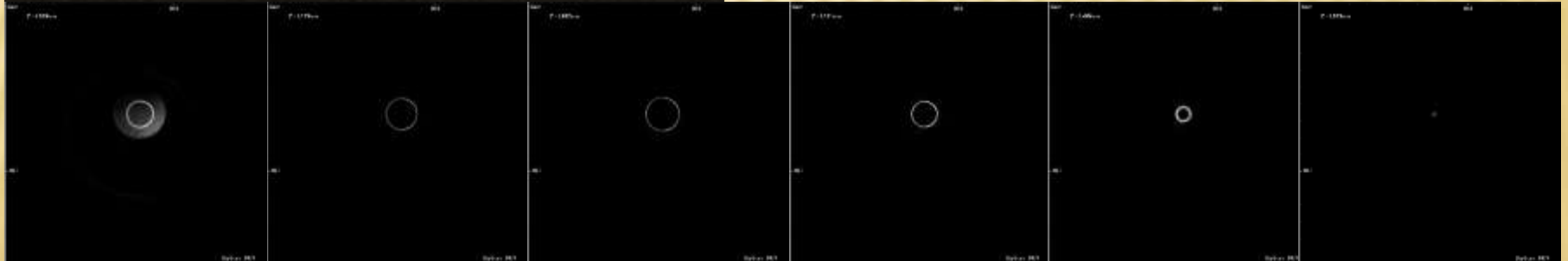


Material	Thickness	Absorption ratio, $\text{cm}^{-1}$
Bismuth	0.25	1428
	0.50	1418
	1.0	1442
	2.0	1452
	3.0	1453
Gold	0.14	3094
	0.28	3176

# PRECISION INCREASE



- ✘ Additional information about the target can be used for precision increase. However, an ill-defined problem is solved only for a flat picture. With given devices additional manipulations introduce errors of the same or even lower order of accuracy as the achieved refinement if solving the problem for 3D.





# TARGETS WERE USED IN LASER-PLASMA EXPERIMENTS

---

- ✘ **Experimental study of conversion of laser radiation ( $\lambda=1.05$  mkm,  $10^{14}$  W/cm<sup>2</sup>, pulse duration 0.5 ns, energy 15 J) into x-rays in solid and in low-density bismuth indicated 10% increase of conversion ratio in nano-snow layers in comparison with solid metal layers. The spectrum becomes softer. [ref]**

[ref] N.G. Borisenko, A.I. Gromov, Yu.A. Merkuliev, A.S. Orekhov, S. Chaurasia, S. Tripathi, D.S. Munda, N.K. Gupta, L. Dhareshwar. Comparison of laser light conversion efficiency into x-rays in solid bismuth and in low-density bismuth.// Preprint of the P.N. Lebedev Physics Institute, 2011, N29.

# TAC AEROGEL FABRICATION

1 Solution

! Ultrasonic agitation with M-nanoparticles

2 Gelation initiated

3 Solvent exchange

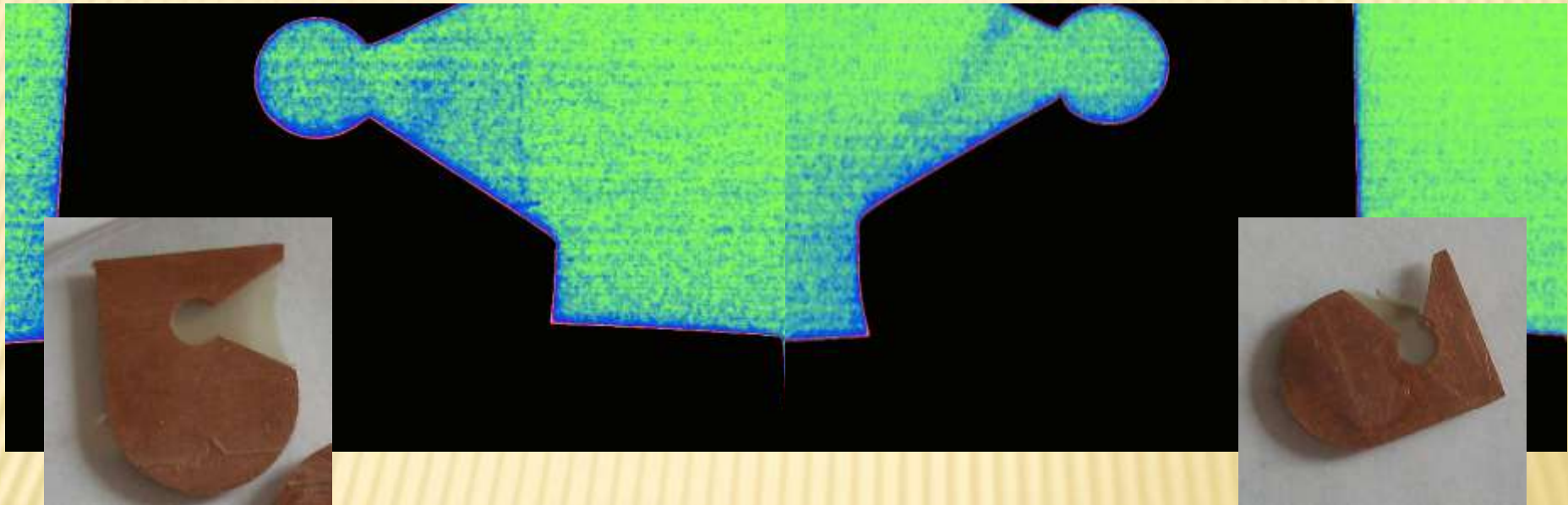
4 Critical point drying

Polymer aerogel in the washer [ref]

[ref] Borisenko N.G., Khalenkov A.M., Kmetik V., Limpouch I., Merkuliev Yu.A., Pimenov V.G. (2007). Plastic aerogel targets and optical transparency of undercritical microheterogeneous plasma.// FuSci and Tech. 51, 655-664



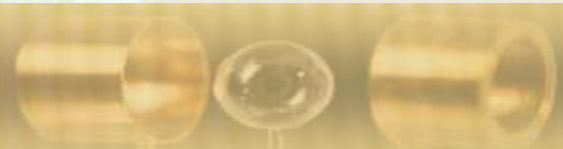
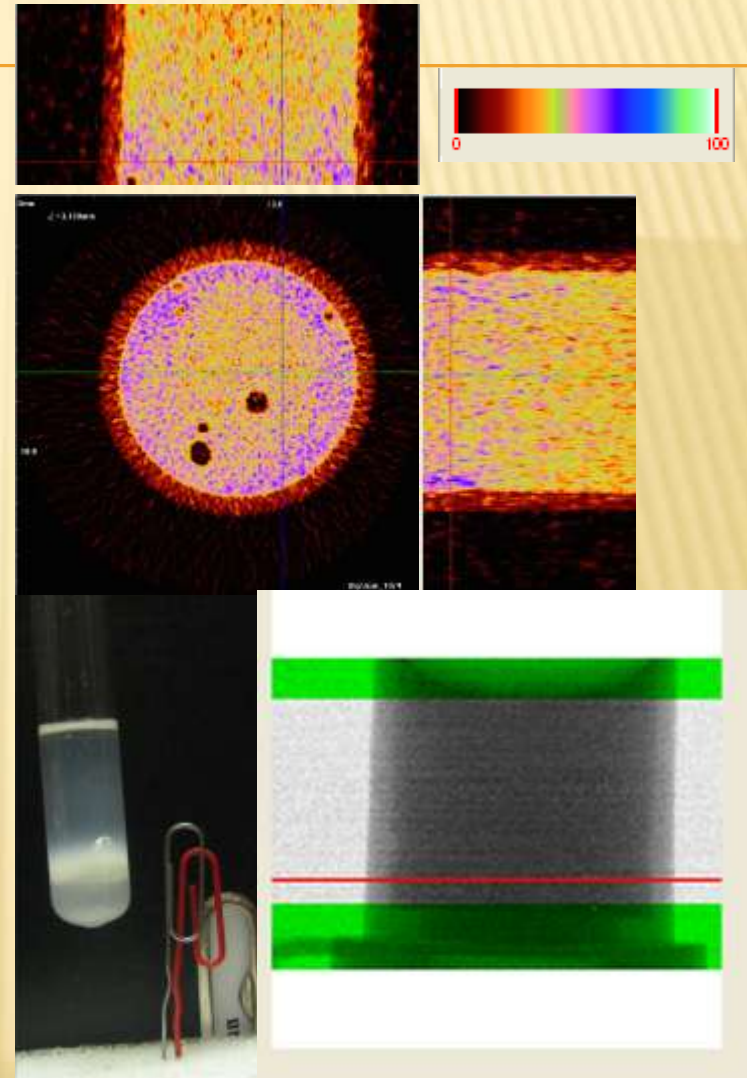
# CU-DOPED (10%) TAC AEROGEL



500  $\mu\text{m}$  thick Cu-doped (10%) TAC foams, 6 mg/cc, are visible on the microradiogram. Defect of density non-homogeneity on the edge of the foam is visible on the right picture. Method of tomograph calibration and final target characterization is to be developed.

# CONCLUSION

- ✘ An additional method of target characterization has been added to earlier existing ones in Thermonuclear Target Laboratory, LPI, and is now being developed. The data on x-ray optical density of the material is provided by the microtomograph SkyScan 1074 then calibration and mathematical processing are used to achieve such target characteristics as density and layer thickness.
- ✘ For nearly transparent targets defects of structure are visible. Optical density and density gradient can be observed on the scale of  $\sim 20$  mkm. With mathematical methods boundaries may be characterized more precise than 1 pixel value (precision  $\sim 6$  mkm).
- ✘ Earlier the commercial tomograph was proposed and used for samples of the scale of 1 cm. At present submillimeter foam and aerogel samples are characterized successfully. (See also the presentation of A. Orekhov et al on this workshop)



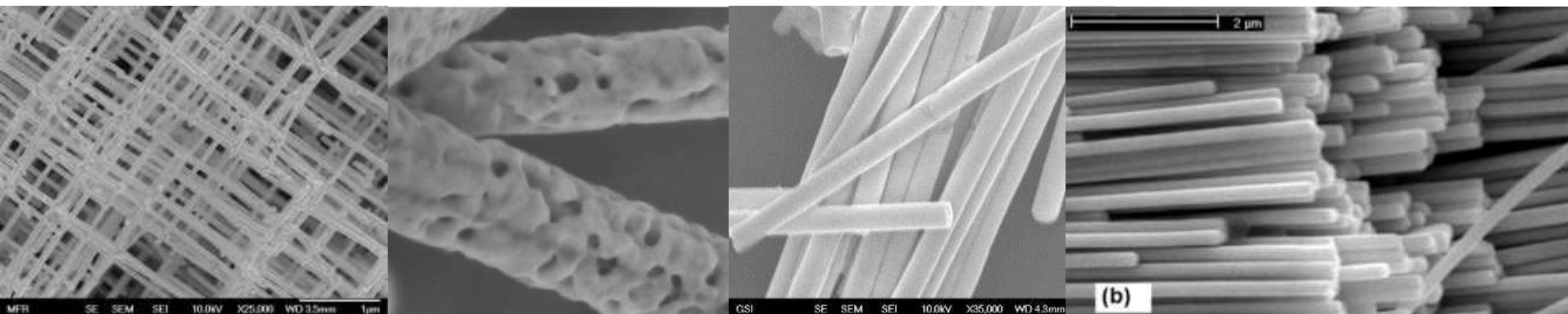
**THANK YOU FOR YOUR ATTENTION**



# Micro- and Nanowire Arrays by Heavy-Ion Irradiation and Electrodeposition

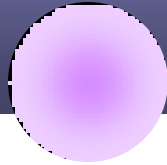
**M.E. Toimil-Molares**

Materials Research Department  
GSI Helmholtz Center for Heavy Ion Research  
Darmstadt (Germany)

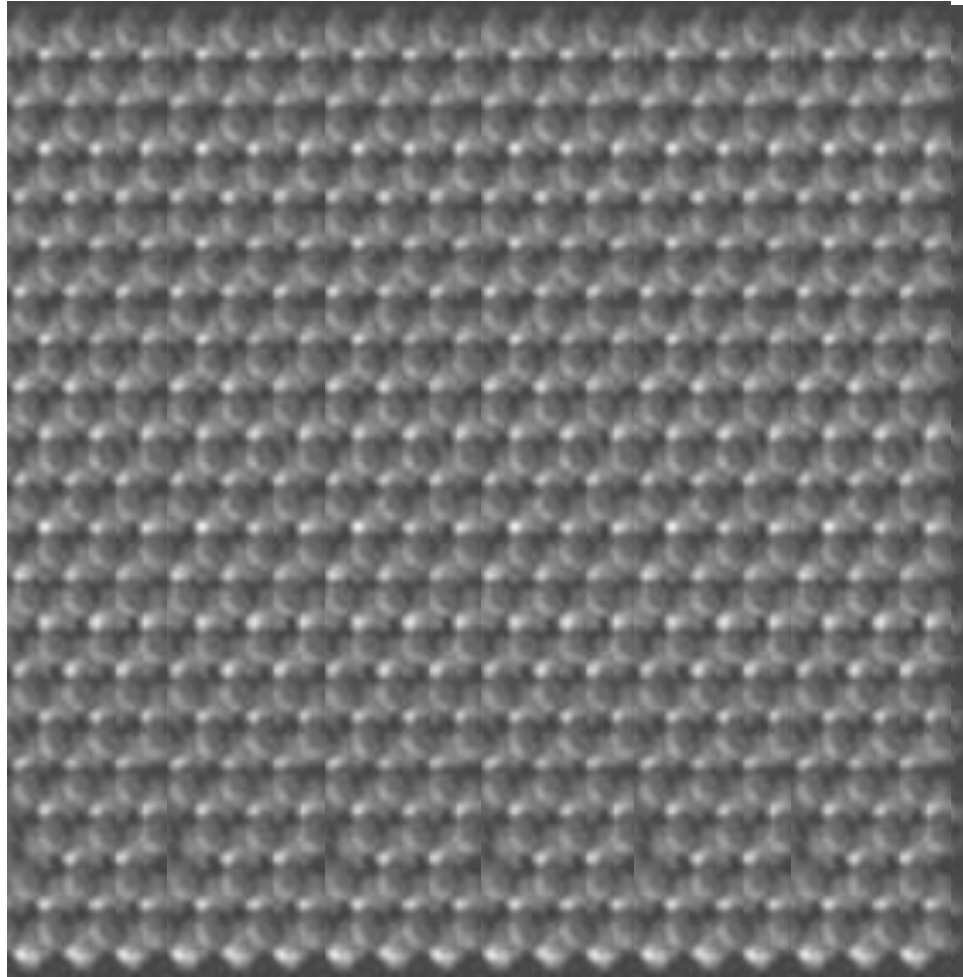


# Outline

- What is the template method?
- Which kind of structures can we fabricate?
- Which parameters can we control and to which extent? e.g. material, geometry, size, crystallinity
- Examples of micro- and nanostructures currently developed at GSI

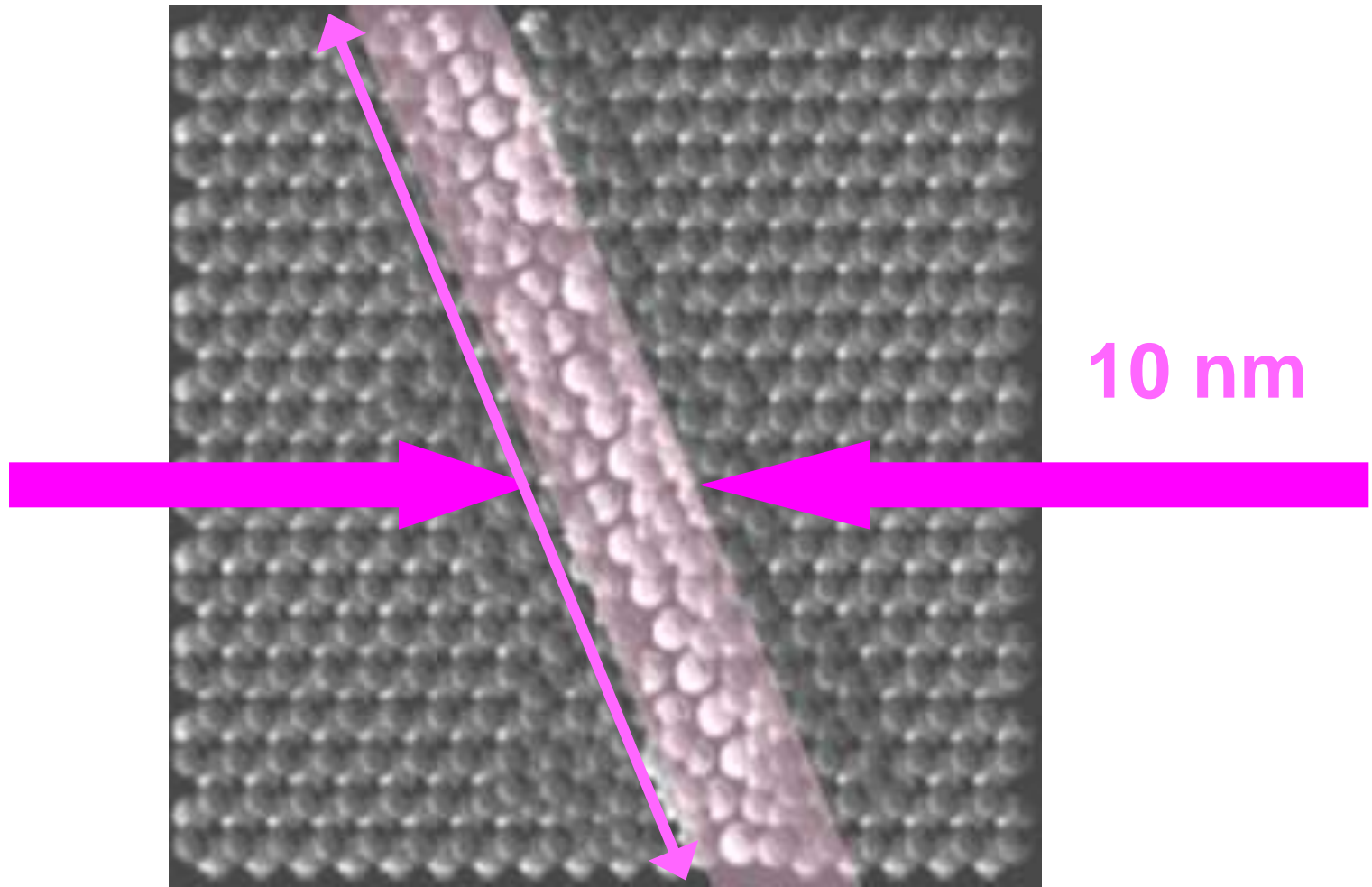


**ion beams**  
kinetic energy: MeV- GeV  
10% of velocity of light





# ion track = nanostructure

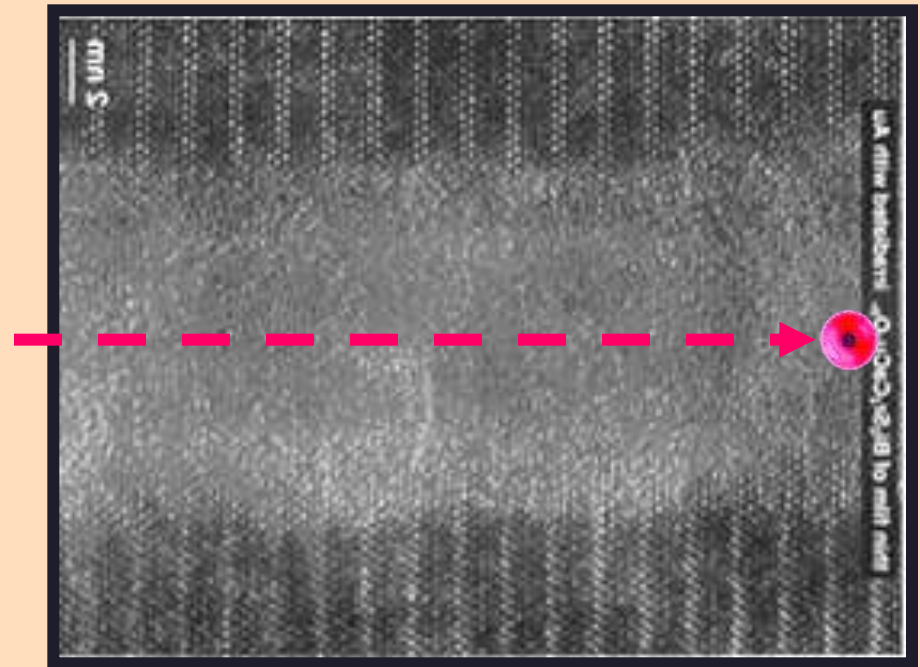
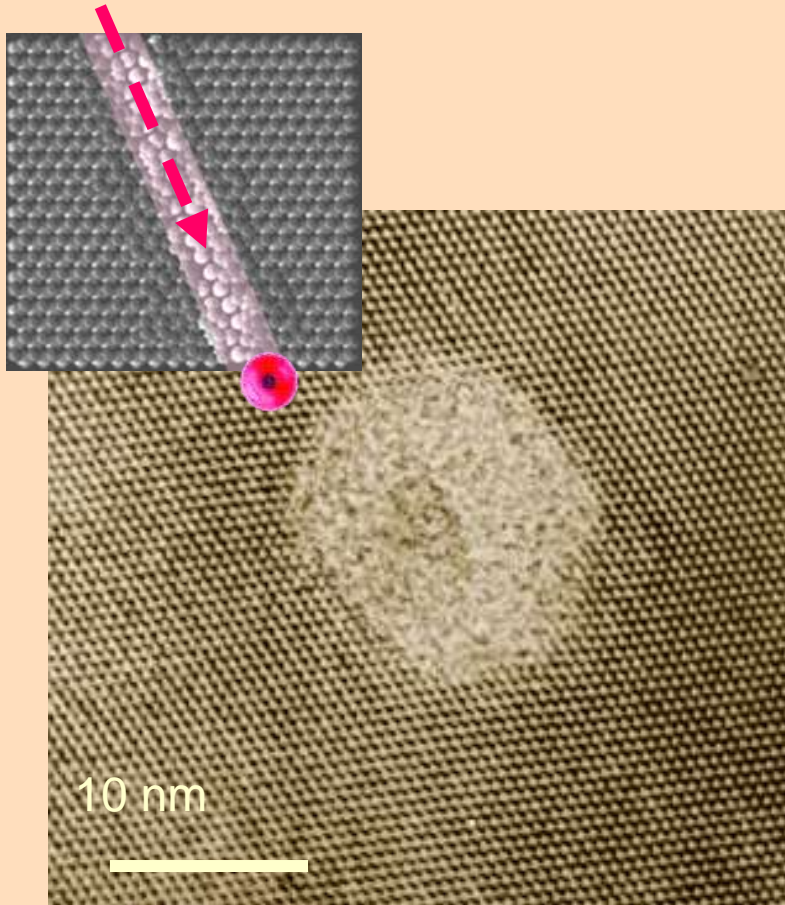
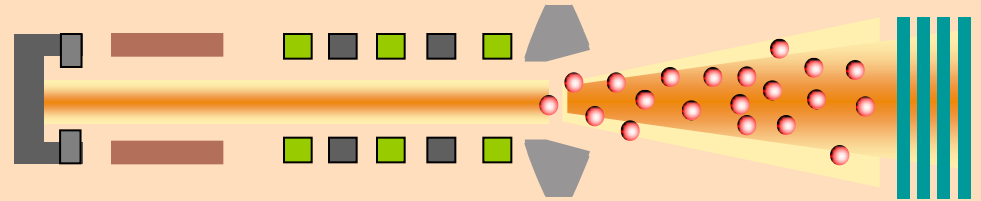


10 nm

10-100  $\mu\text{m}$

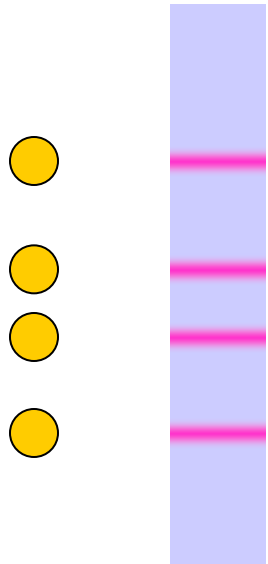
# Nanostructures by Heavy Ion Lithography

- Energy (max.) ~ 2 GeV
- Range: ~ 100  $\mu\text{m}$
- Fluence: 1 -  $10^{10}$  ions/ $\text{cm}^2$



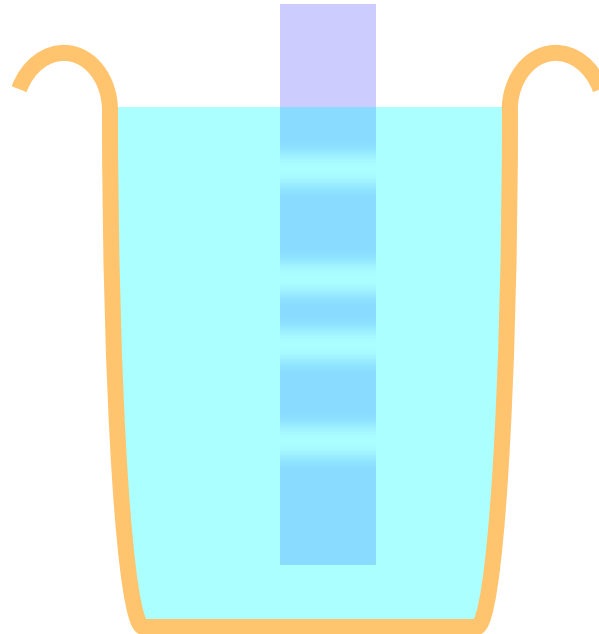
Latent ion tracks

# Fabrication of micro- and nanopores



**irradiation**

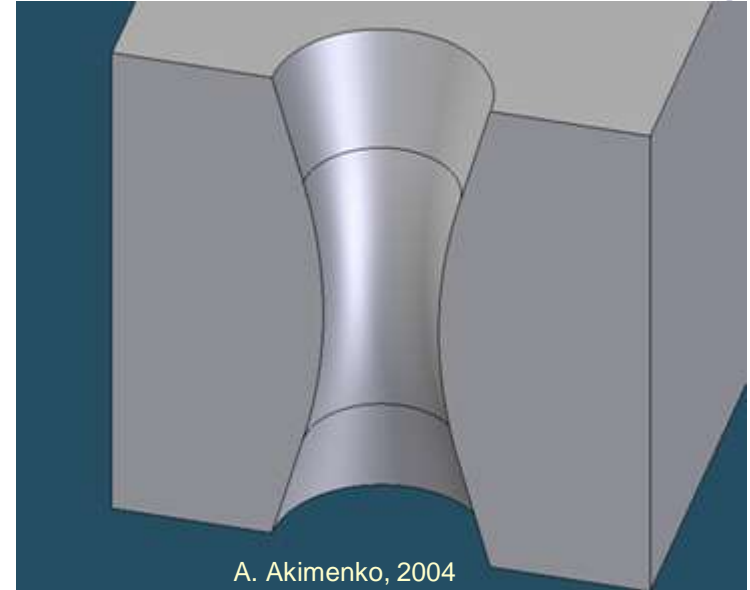
Polymers  
Mica  
SiN thin films



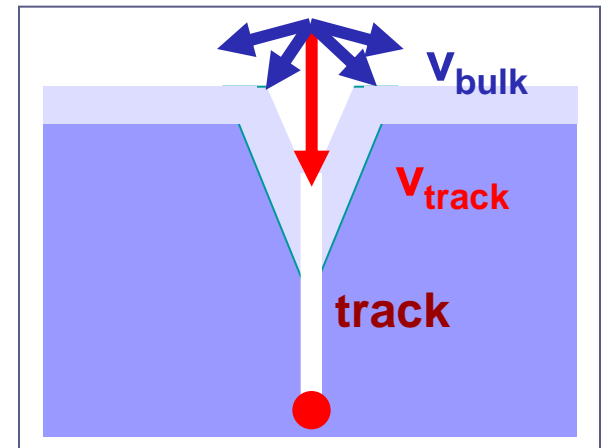
**chemical etching**

(NaOH, NaOCl, HF)

selective ion-track etching

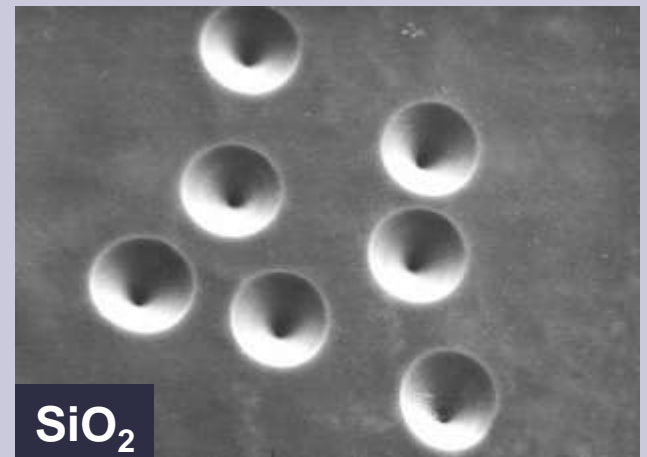
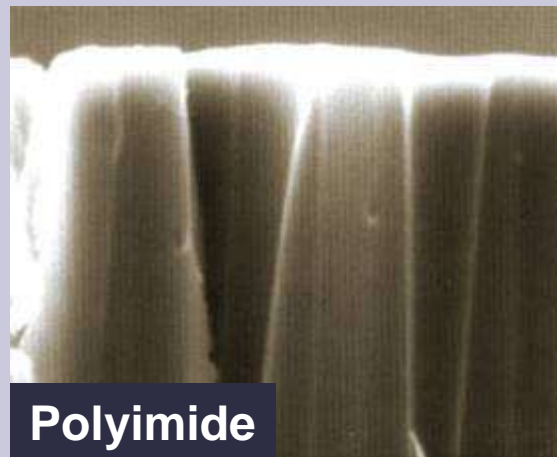
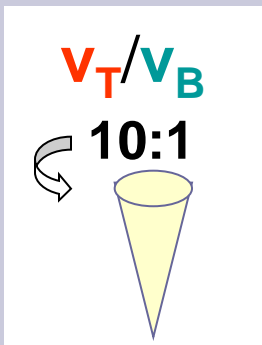
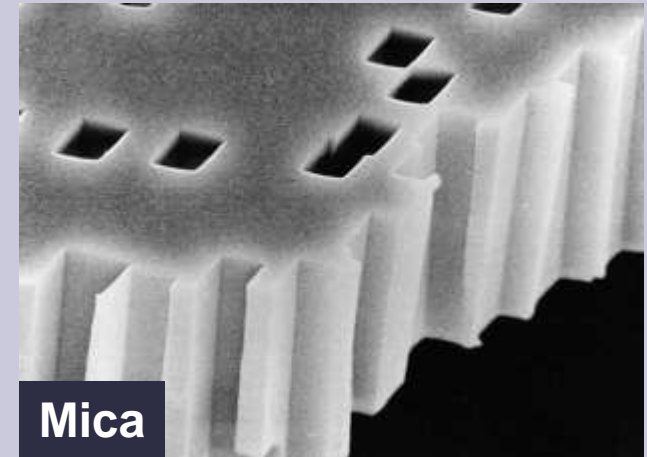
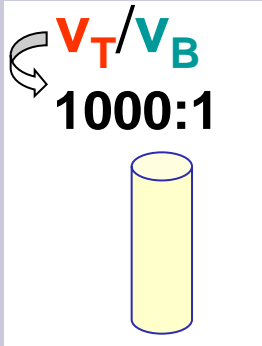


A. Akimenko, 2004

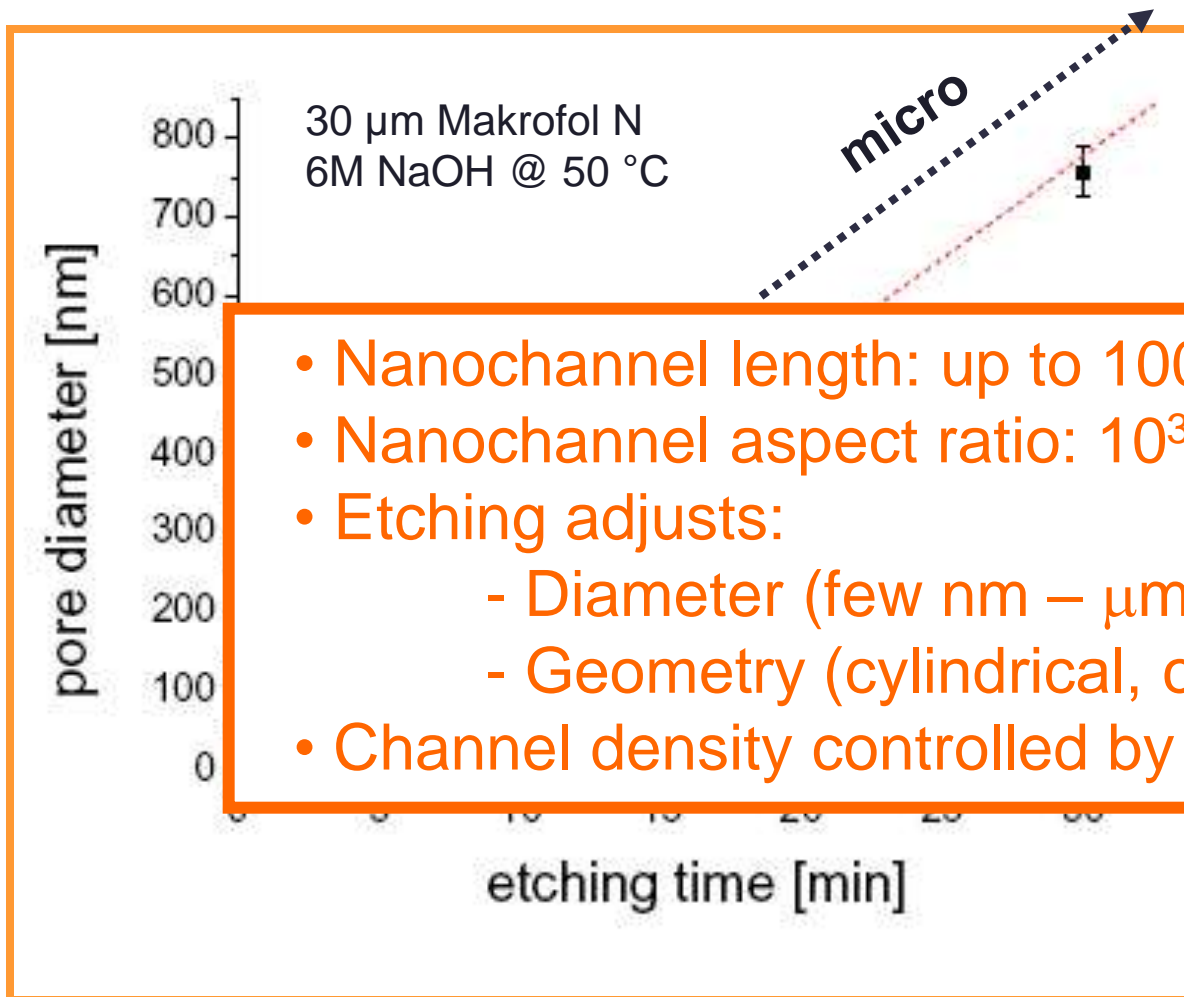


# Pore Geometry

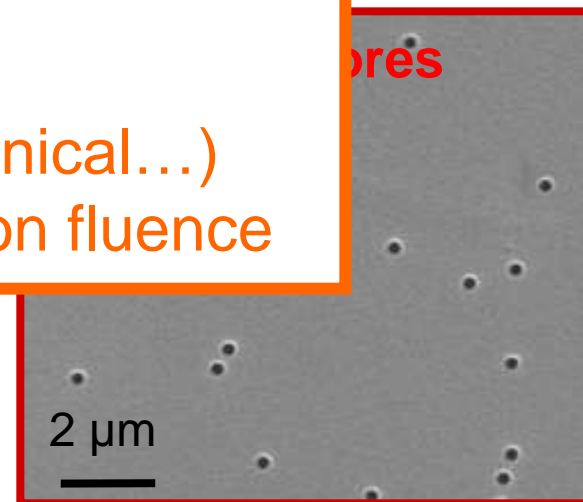
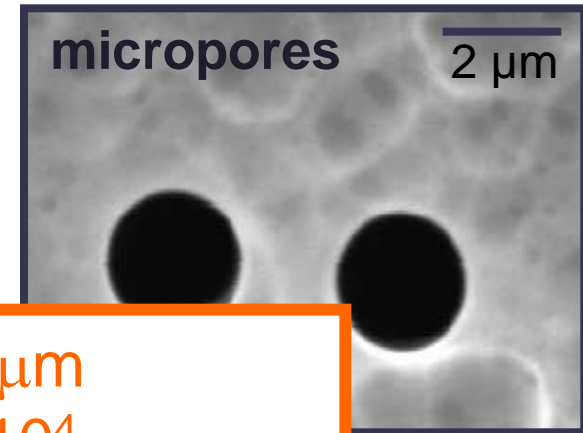
$V_{\text{Track}} / V_{\text{Bulk}}$  = determines opening angle



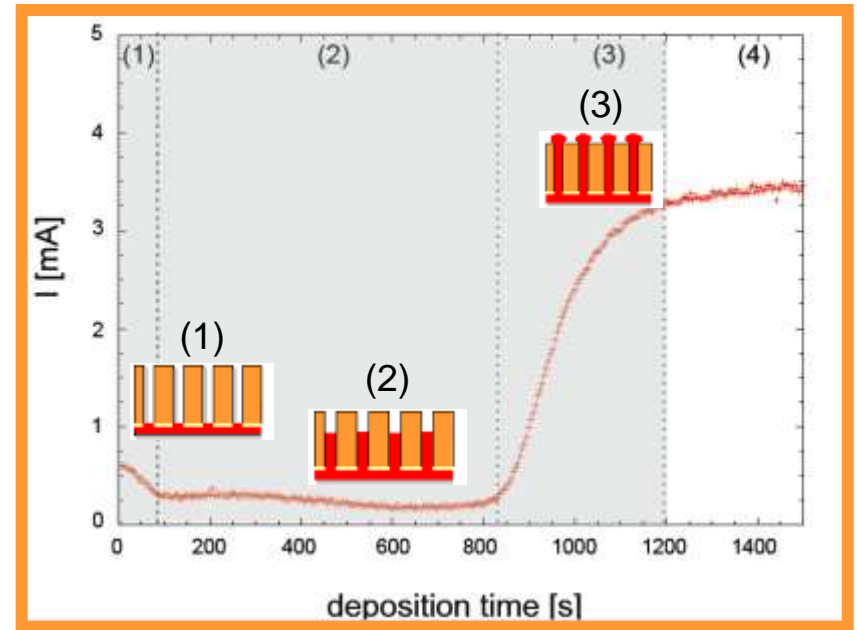
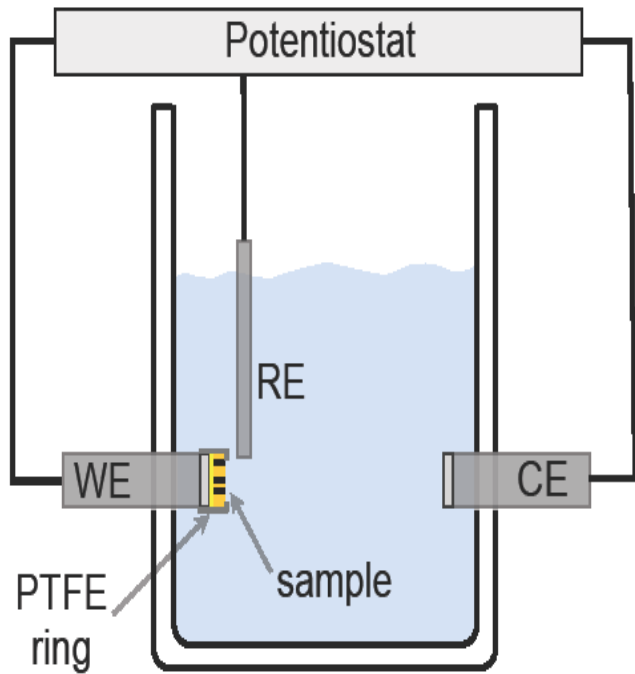
# Pore Diameter vs. Etching Time



- Nanochannel length: up to 100 µm
- Nanochannel aspect ratio:  $10^3$ - $10^4$
- Etching adjusts:
  - Diameter (few nm – µm)
  - Geometry (cylindrical, conical...)
- Channel density controlled by ion fluence



# Electrodeposition of Micro- and Nanowires



## Parameters:

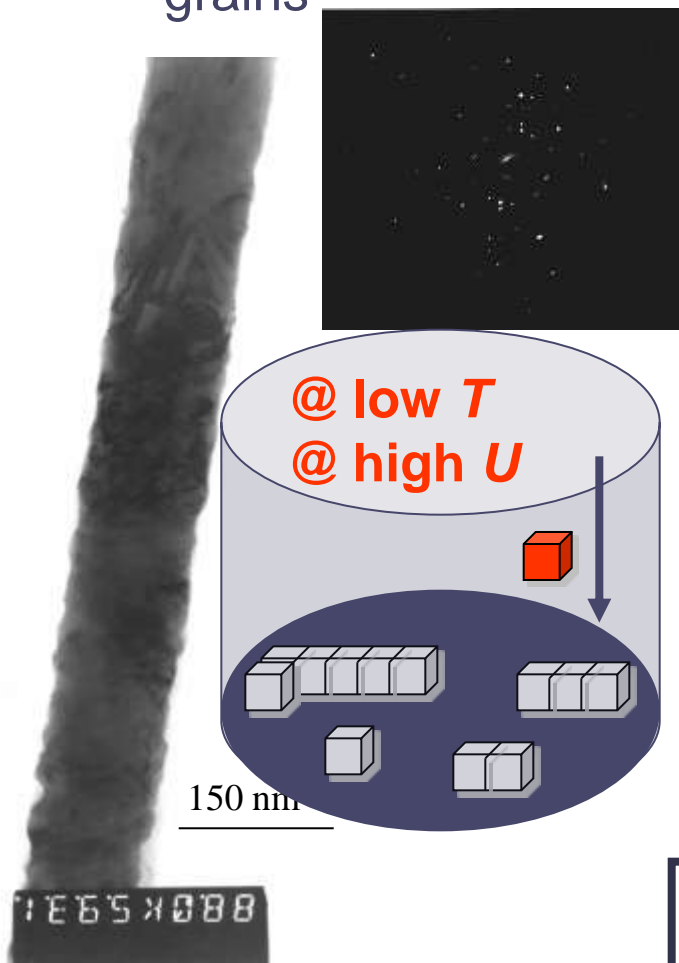
- Electrolyte
- Temperature
- Voltage
- Cell geometry
- Convection  
(stirring, ultrasound)
- Electrodes

## Control:

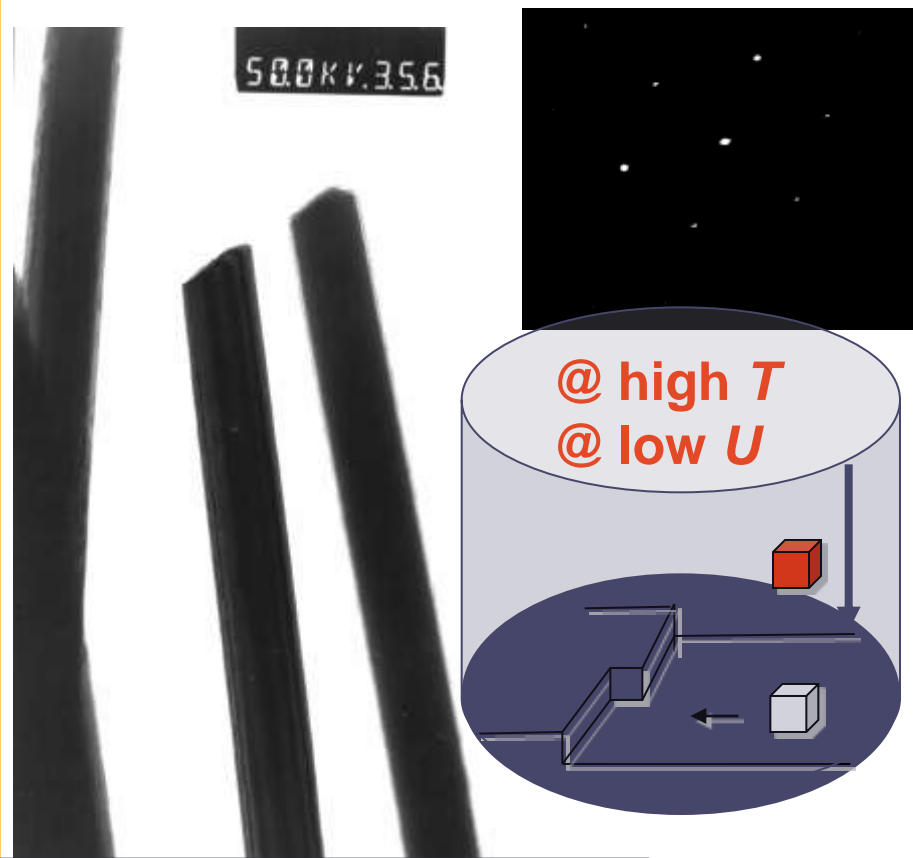
- Composition
- Crystallinity
- Roughness

# Control over Crystallinity

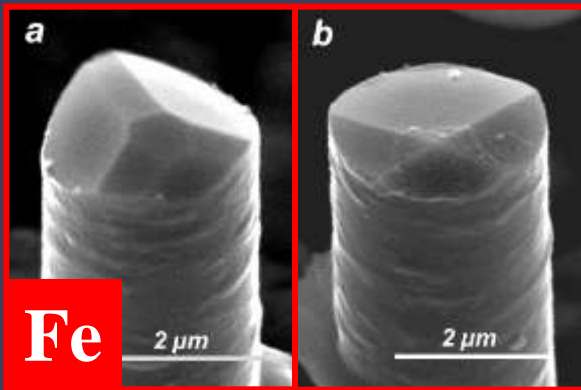
Nucleation and formation of new grains



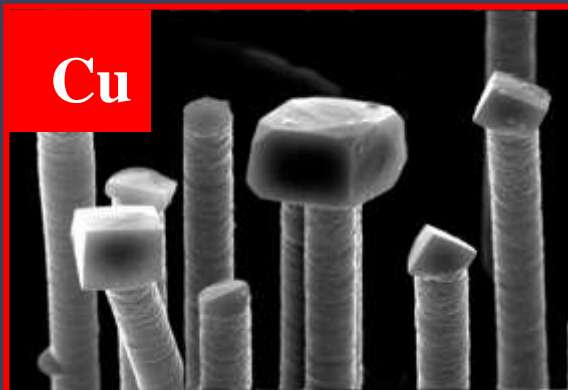
Build up of existing crystals



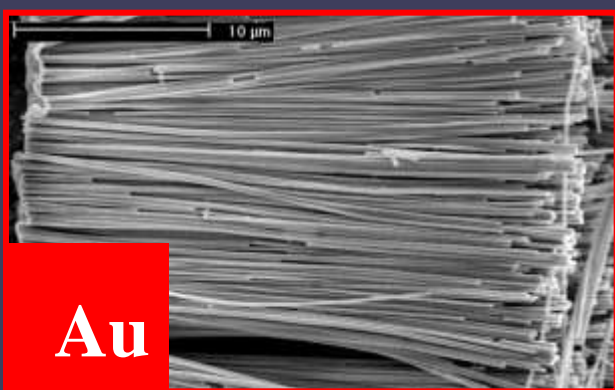
- Copper nanowires
- $\text{Cu}_2\text{SO}_4$  based electrolyte
- 23 – 50 °C
- Potentiostatic



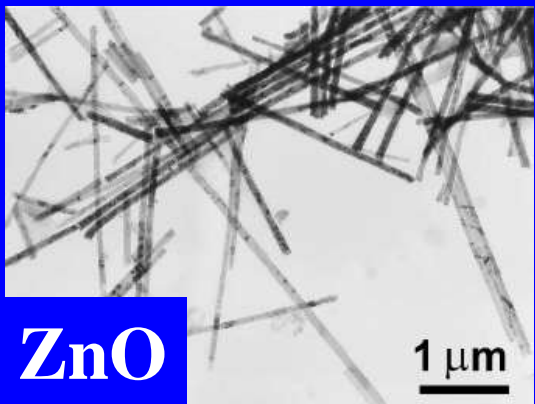
**Fe**



**Cu**



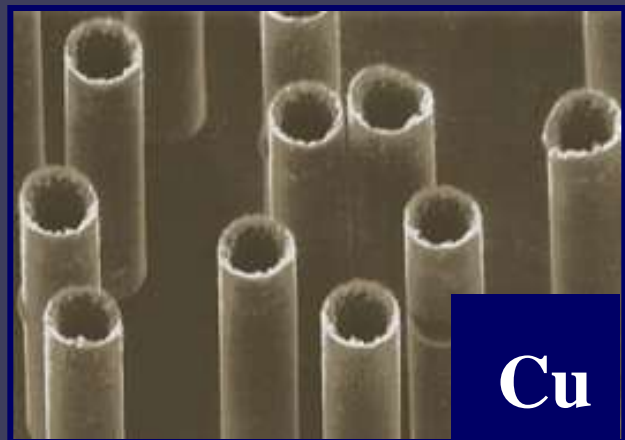
**Au**



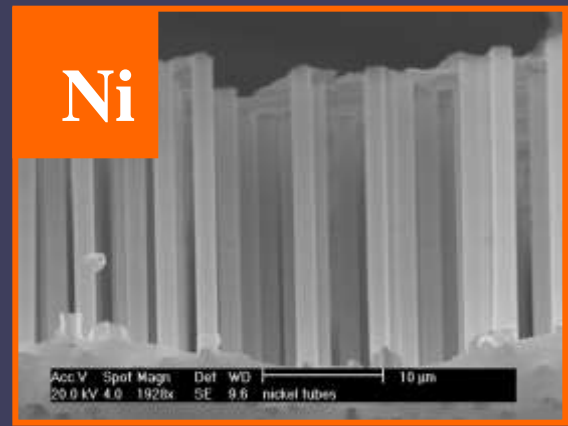
**ZnO**

**Metals:** Cu, Au, Ni, Fe, Pt  
**Semimetals:** Bi  
**Semiconductors:** ZnO  
**Multilayers:** Cu/Co

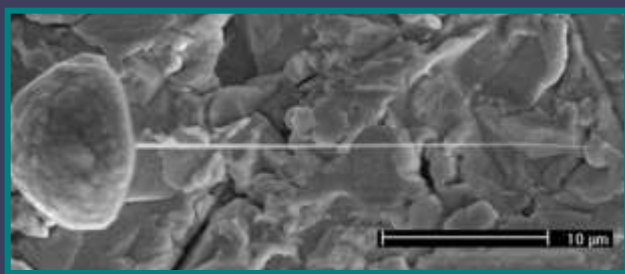
Choice of electrodeposition conditions → poly- and single-crystalline nanowires:  
 Cu, Au, Bi, Sb, Fe, Ni, Ag,...



**Cu**



**Ni**

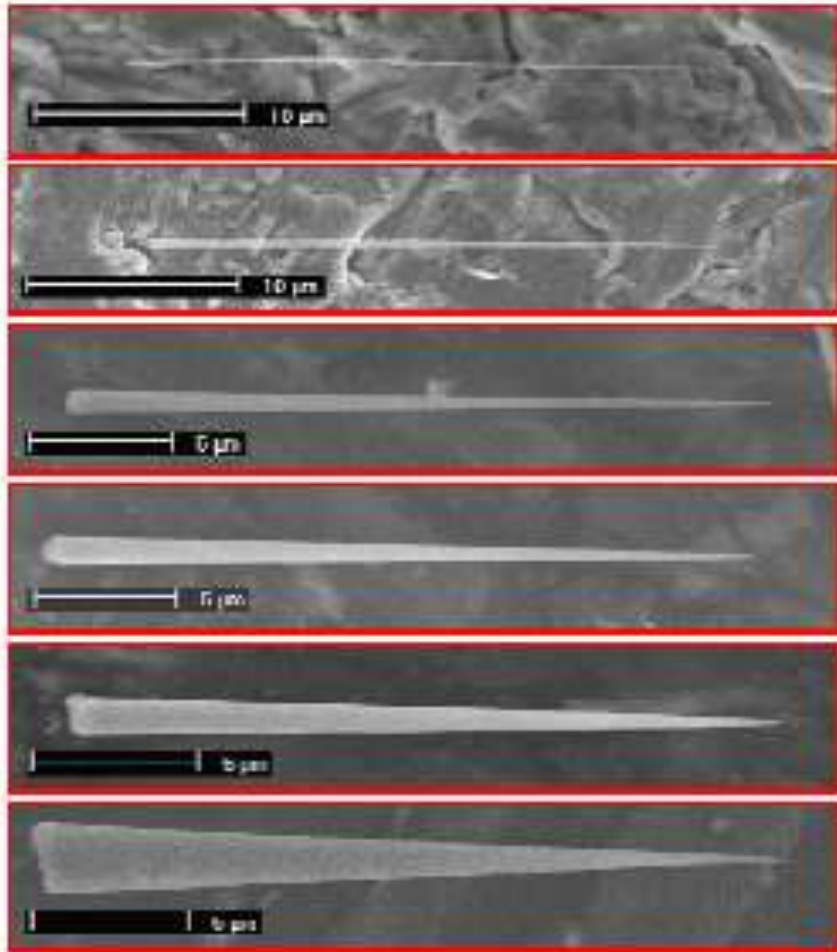


**Conical Cu/Co**



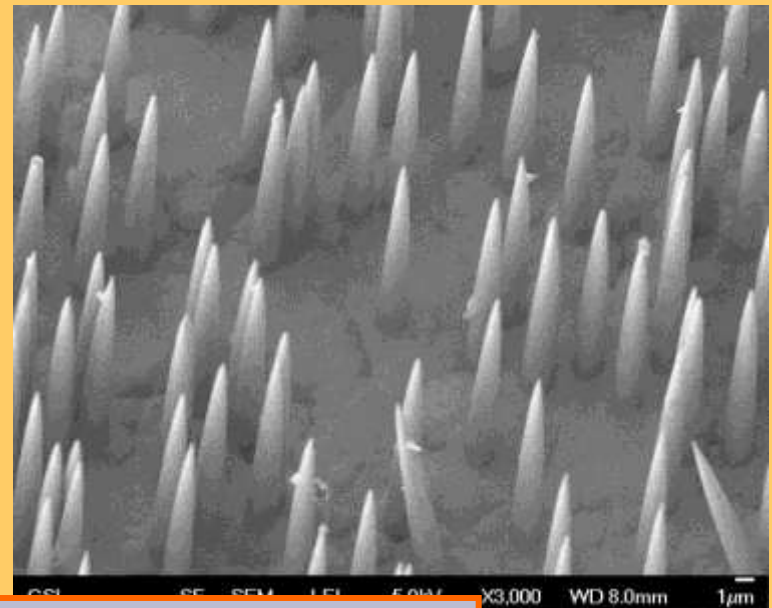
# Control over Geometry

Nanowire geometry controlled by etching conditions



Increasing methanol concentration increases the apex angle of the nanostructures

Freestanding conical wires

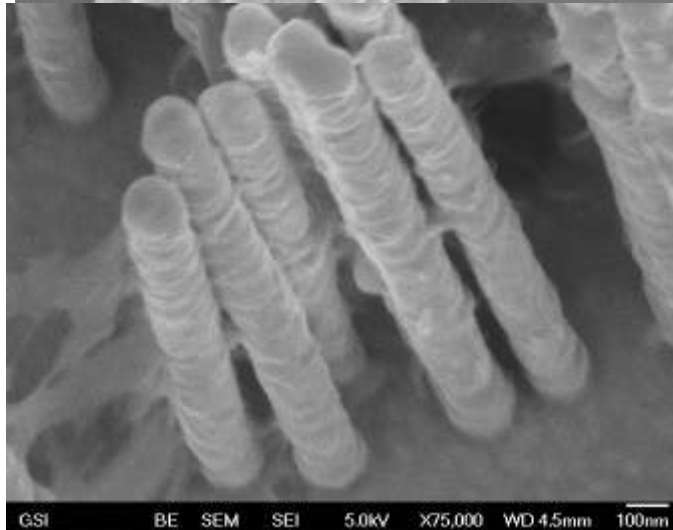
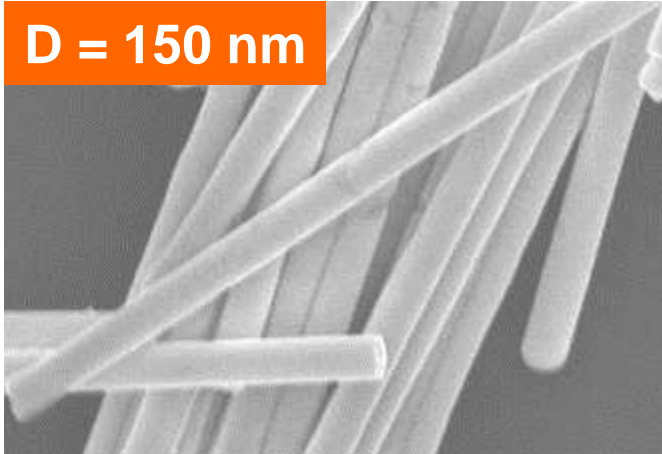


Smooth contour

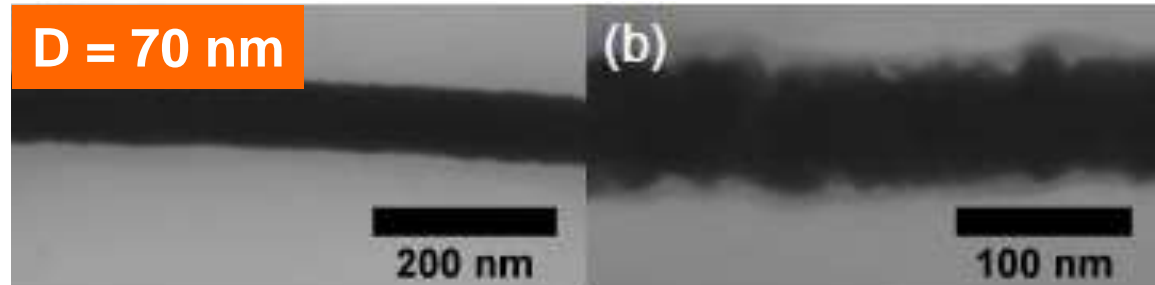
# Nanowires with various surface roughness

Nanowire morphology controlled by the inner surface of the nanopores in the template

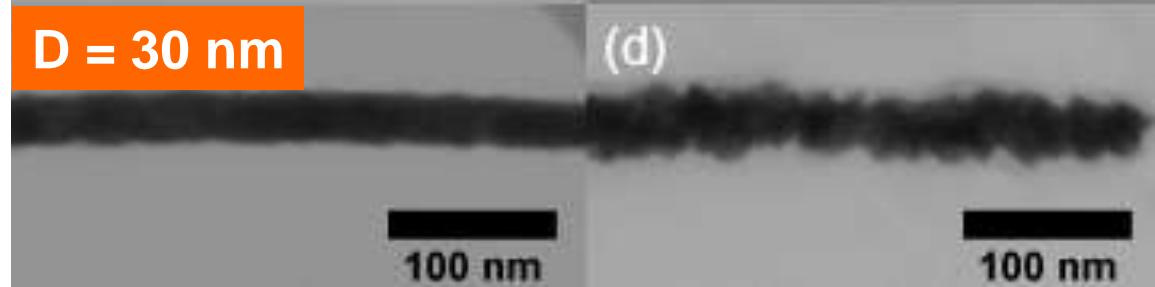
D = 150 nm



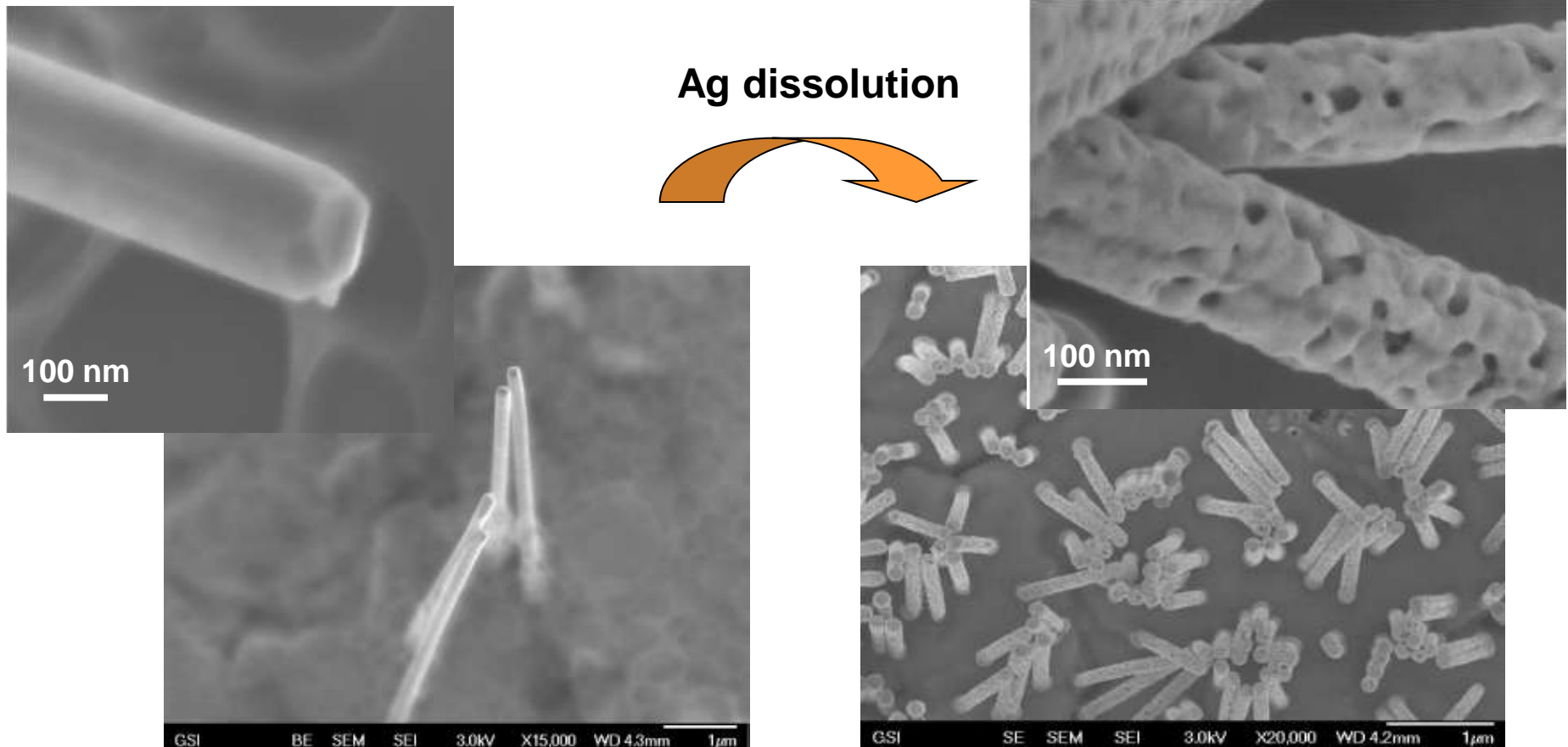
D = 70 nm



D = 30 nm



# AuAg alloy and porous Au nanowires

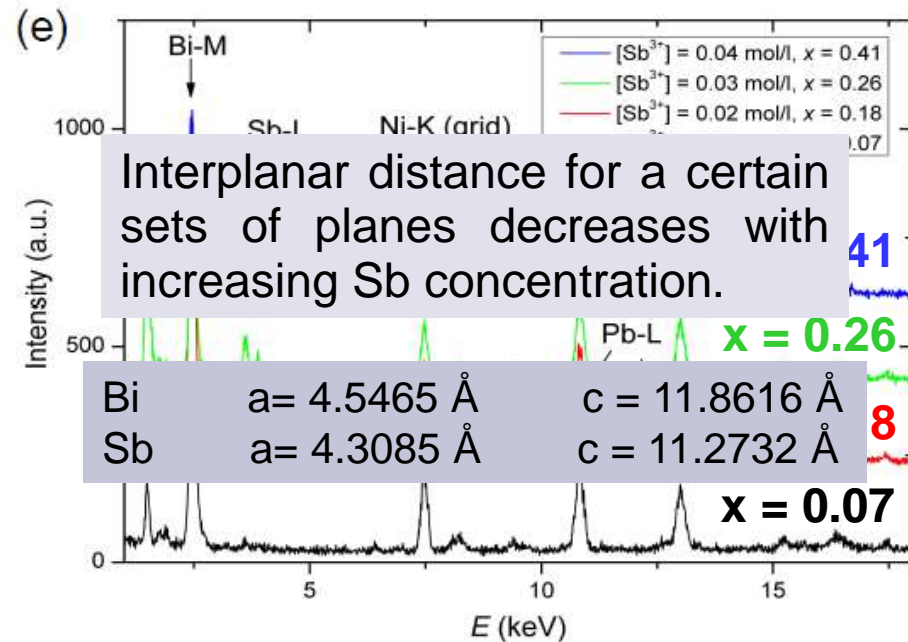


→ Constant  $U$   
→ Faceted silver gold nanowires  
indicating large crystals

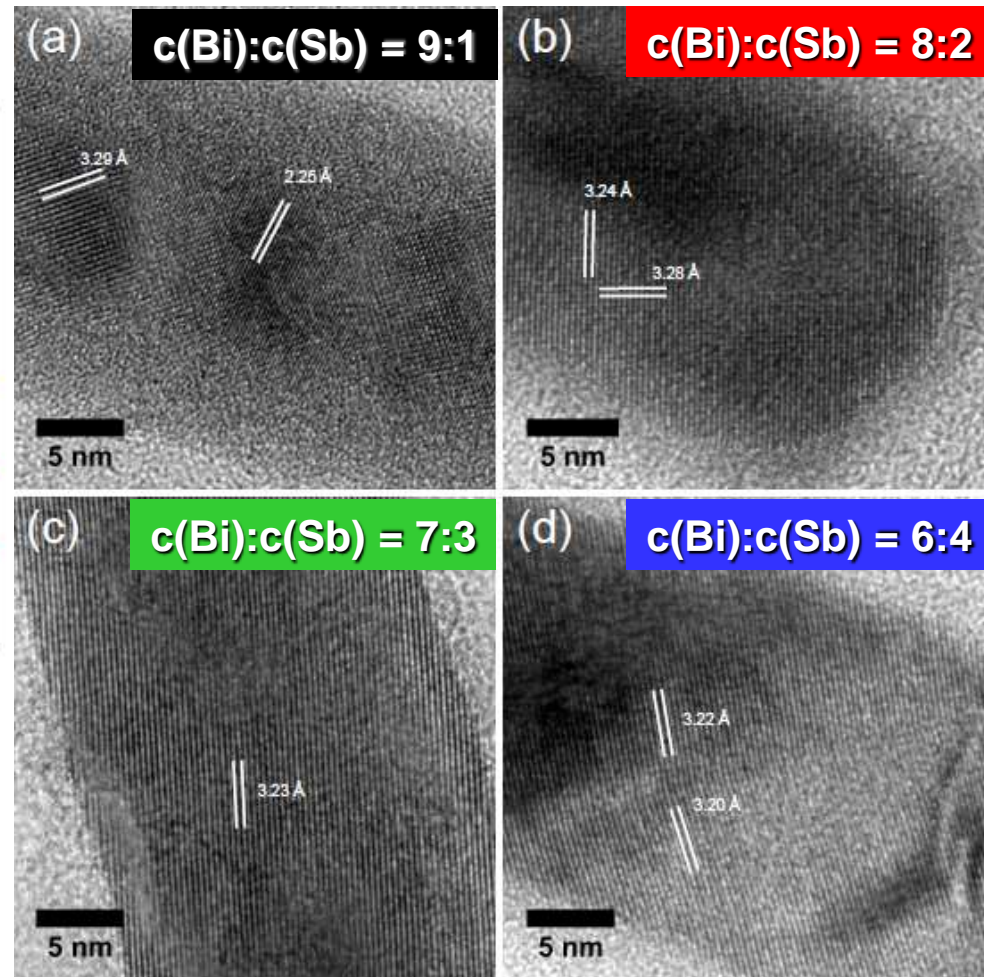
→ Porous Au wires with 10-30 nm pores  
→ Reduced diameter after Ag etching

# Composition of $\text{Bi}_{1-x}\text{Sb}_x$ nanowires

## HRTEM-EDS



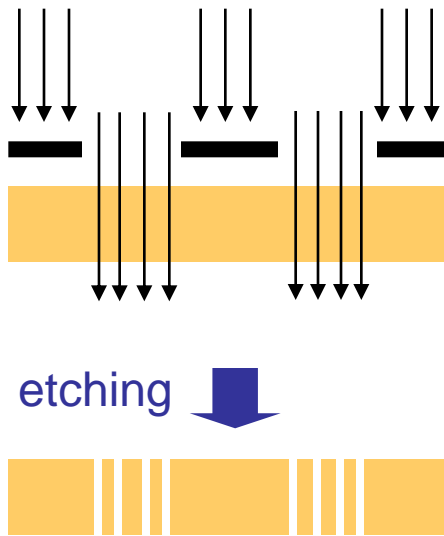
An increase in the concentration of Sb ions in the electrolyte results in an increase in Sb concentration in the alloy wires.



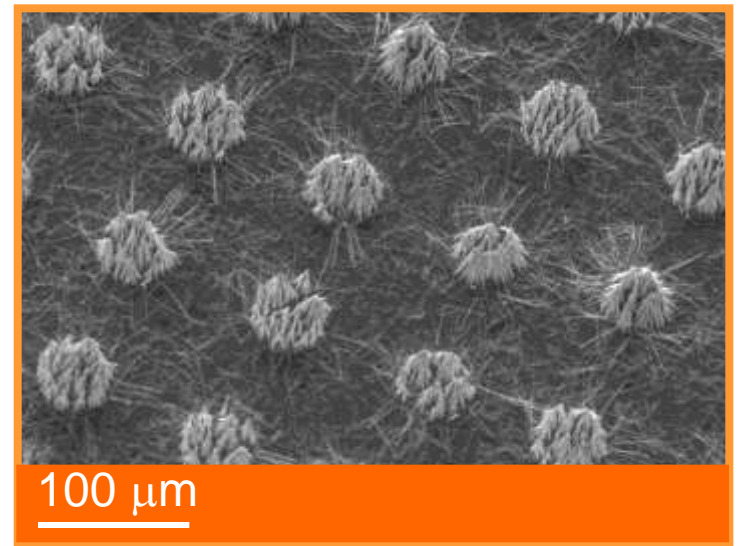
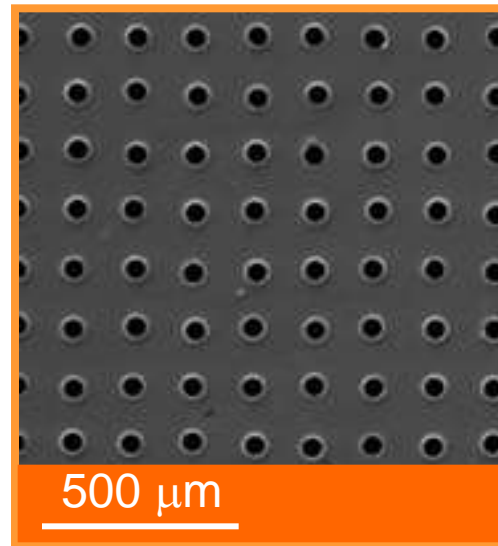
# Ion Track Technology: to close the nano-micro gap

1. Irradiation through mask to microstructure etched ion track membranes →

mask

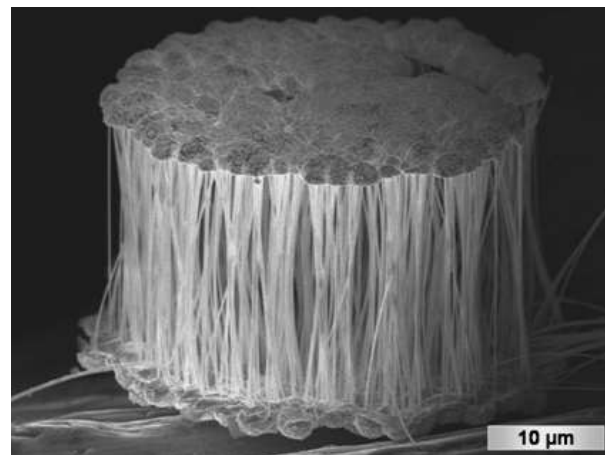
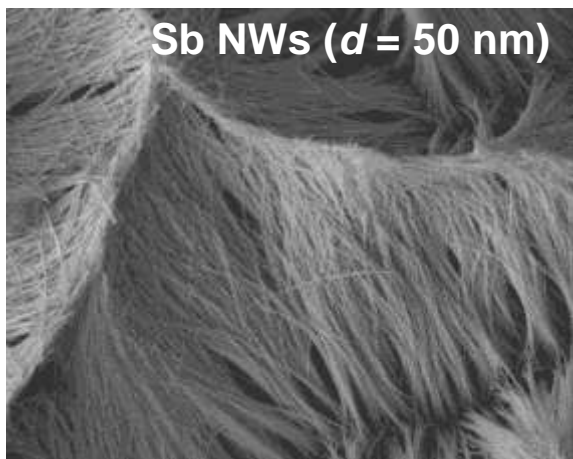


50  $\mu\text{m}$  diameter NW arrays

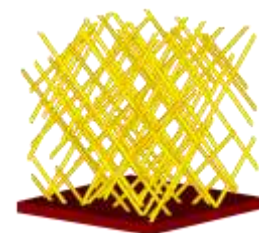
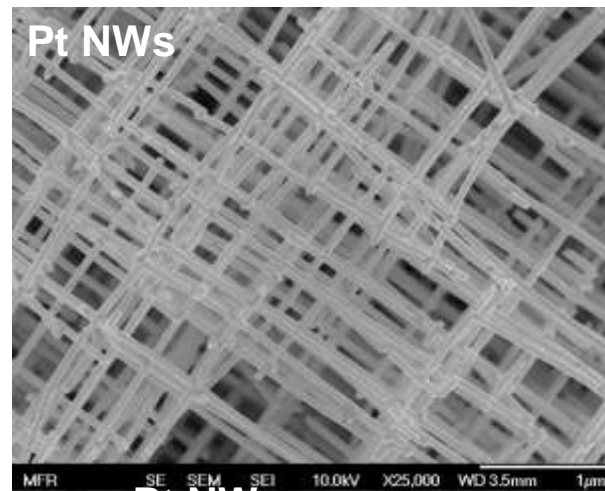


# Ion Track Technology to close the nano-micro gap

2. To remove membrane maintaining mechanical stability of the NWs.



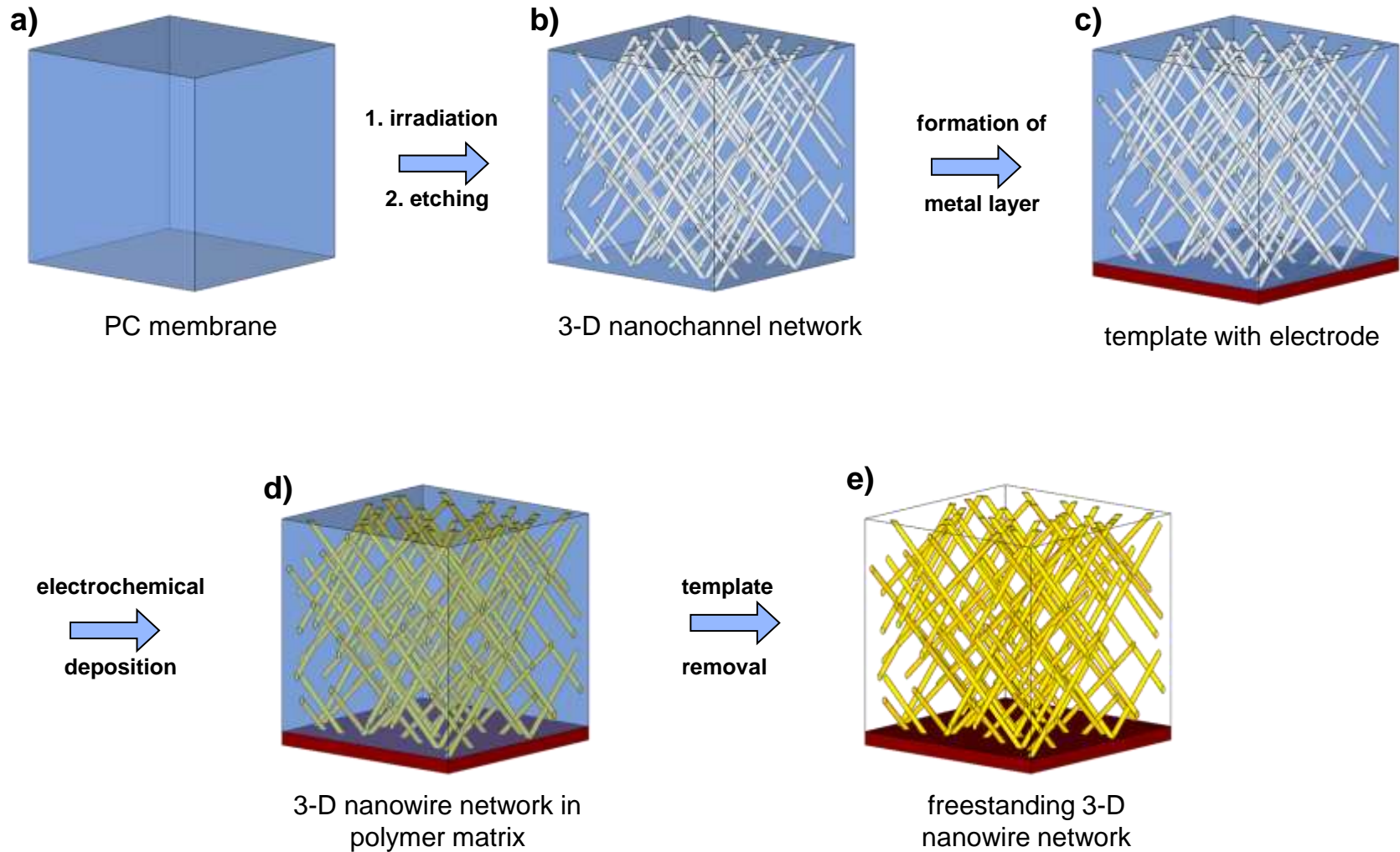
NW  
„microreactor“



NW  
Network

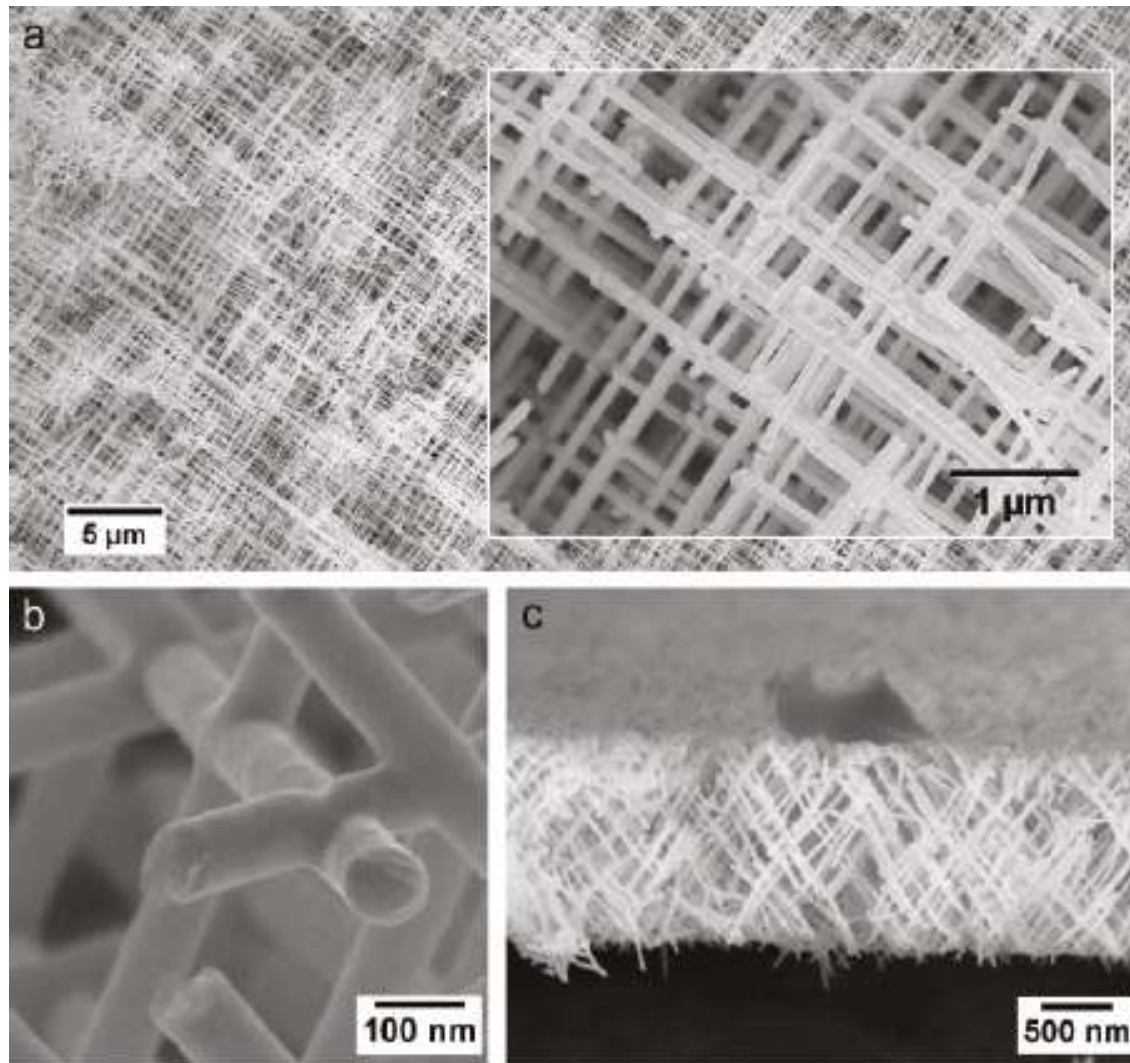
Typical nanowire "spaghetti" after template dissolution

# Ion Track Technology to close the nano-micro gap



# Ion Track Technology to close the nano-micro gap

Pt

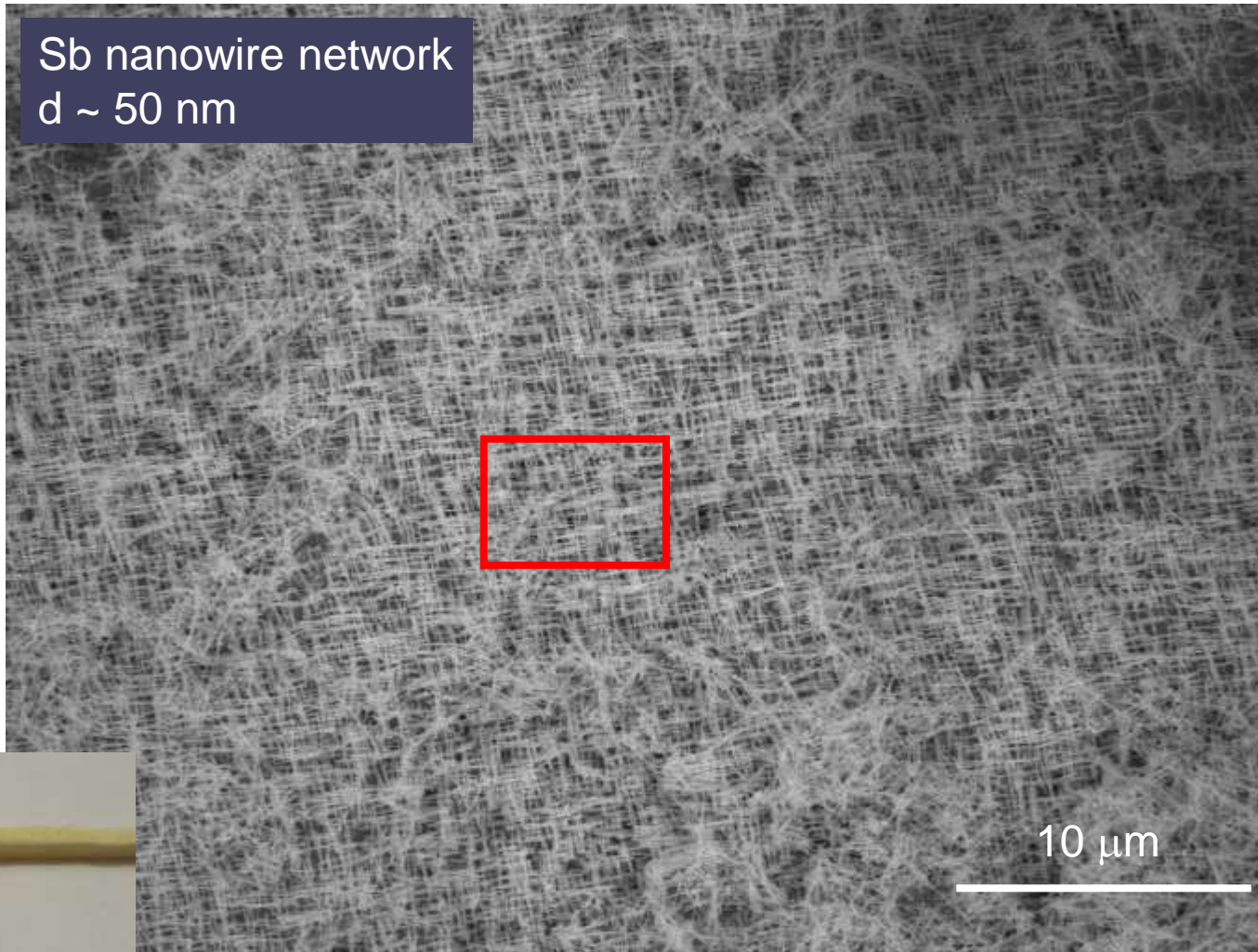




# 3D Nanowire Networks

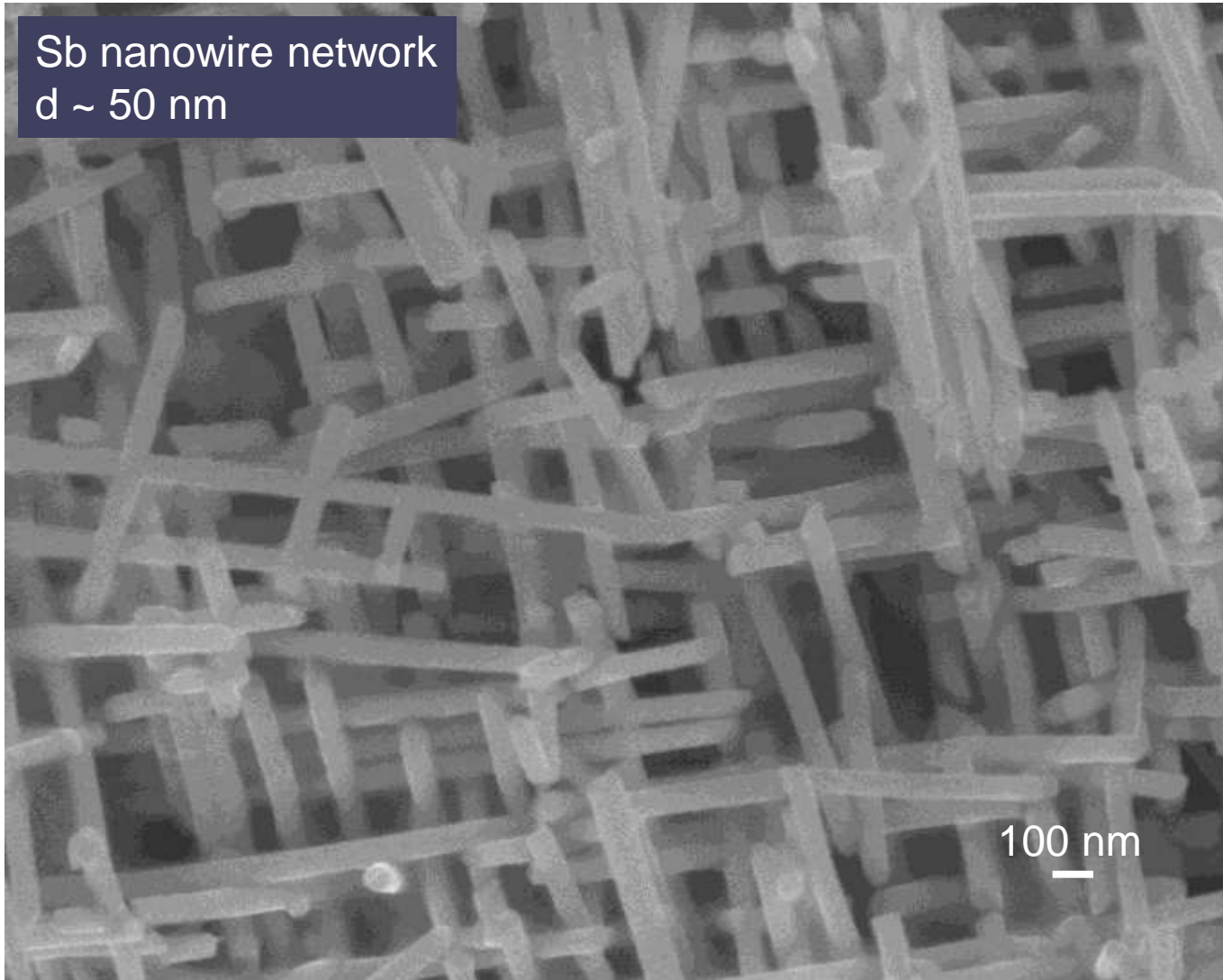
**Sb**

Sb nanowire network  
d ~ 50 nm

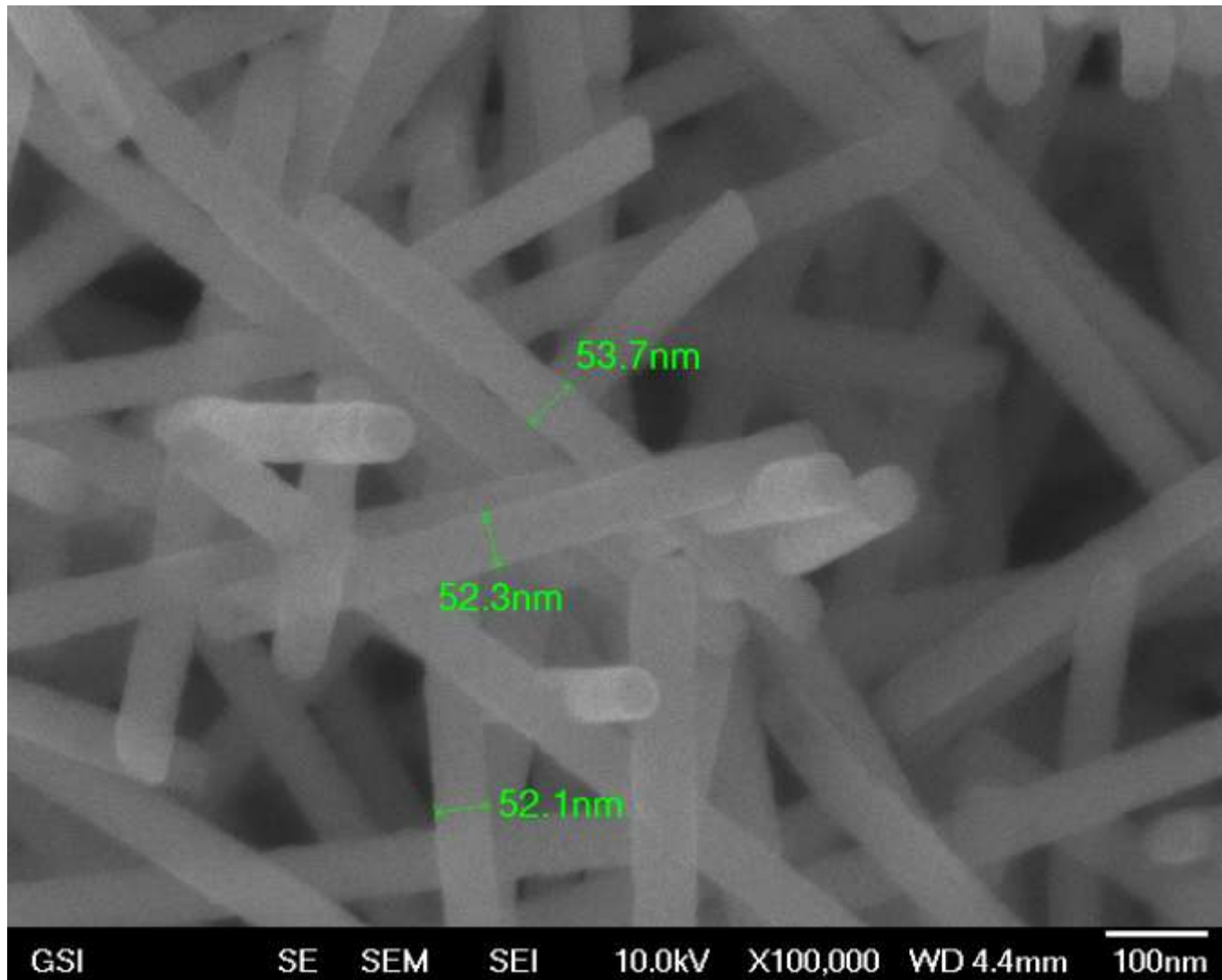


# 3D Nanowire Networks

Sb nanowire network  
d ~ 50 nm

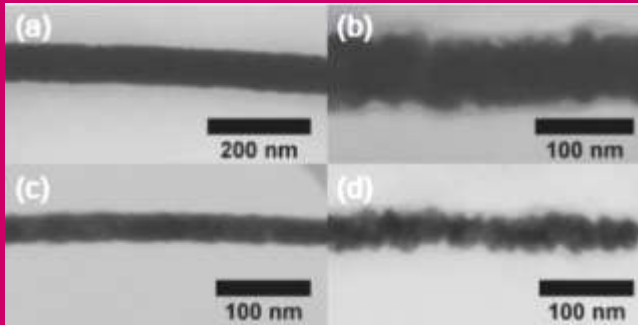


# 3D Nanowire Networks

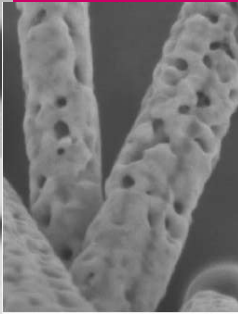


# Micro- and Nanostructures *Palette*

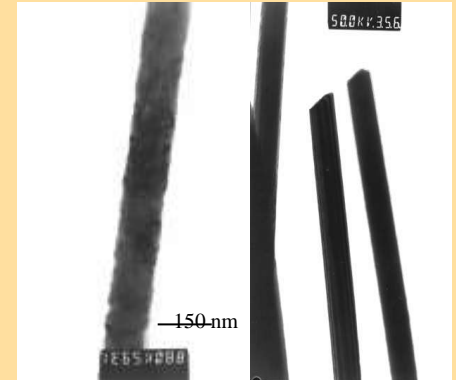
## Smooth vs rough



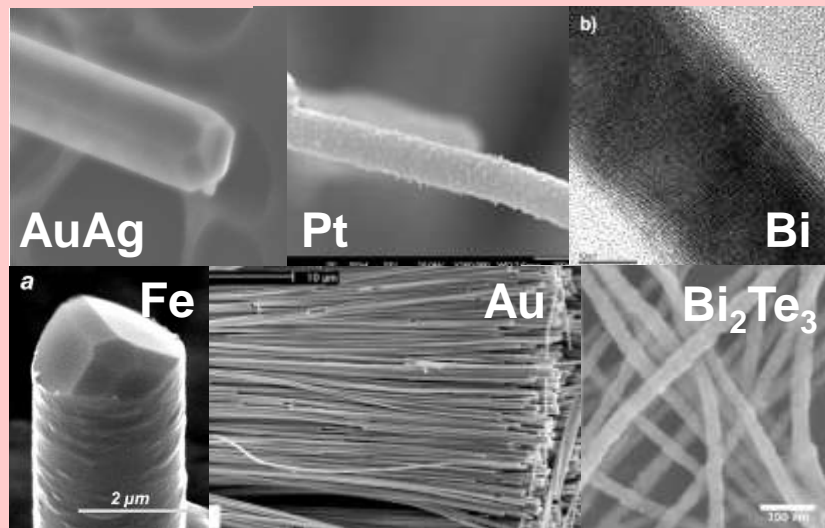
## Porous



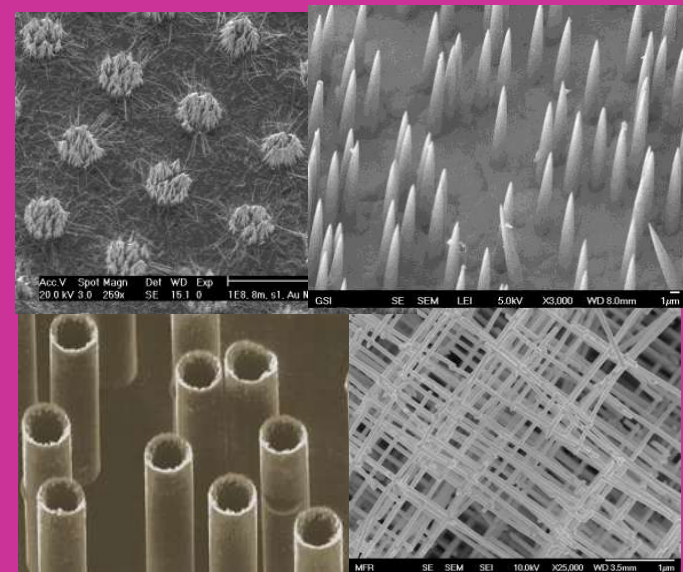
## Polycrystalline and single-crystalline



## Materials



## Tubes, cones, networks...



# Conclusions

- A large variety of micro- and nanowire structures can be fabricated by electrodeposition in etched ion track membranes.
- Excellent control over material, geometry, size, crystallographic properties, and surface characteristics, achieved by proper selection of fabrication parameters.
- Interesting objects include:
  - Nanowires with controlled length, radius and aspect ratio
  - Smooth, rough and porous nanowires
  - Nanowires with controlled roughness
  - Micro-structured nanowire arrays
  - Nanowire networks
- Investigation of their properties is underway:
  - Optical properties (IR-spectroscopy, EELS-STEM)
  - Electrical properties
  - Thermoelectrical properties
  - Thermal stability

# THANKS!!

## GSI Nanowire Students :

Ina Alber, Sven Mueller, Oliver Picht,  
Michael Wagner, Markus Rauber,  
Janina Krieg, Christian Schoetz,  
Christian Mueller



**Materials Research Group at GSI**



**GSI Nanowire Group**



MAX-PLANCK-GESELLSCHAFT

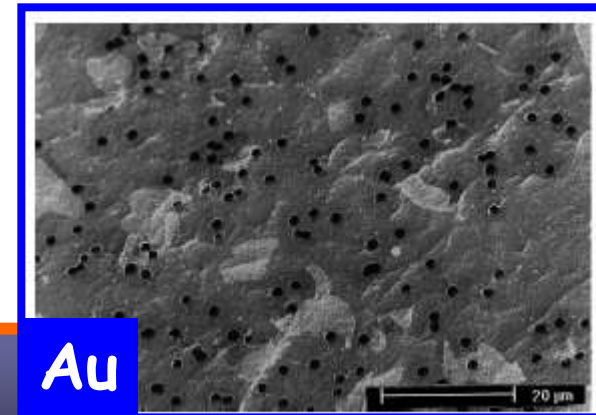
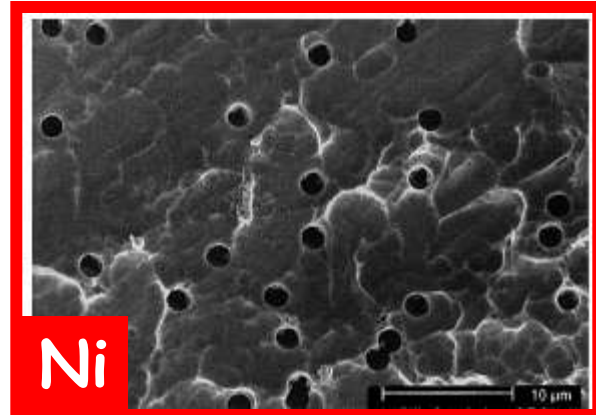
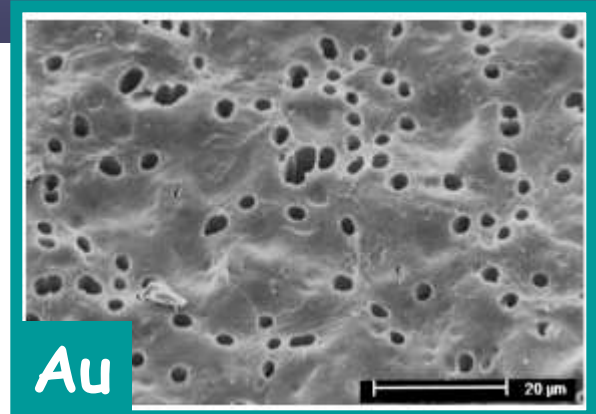
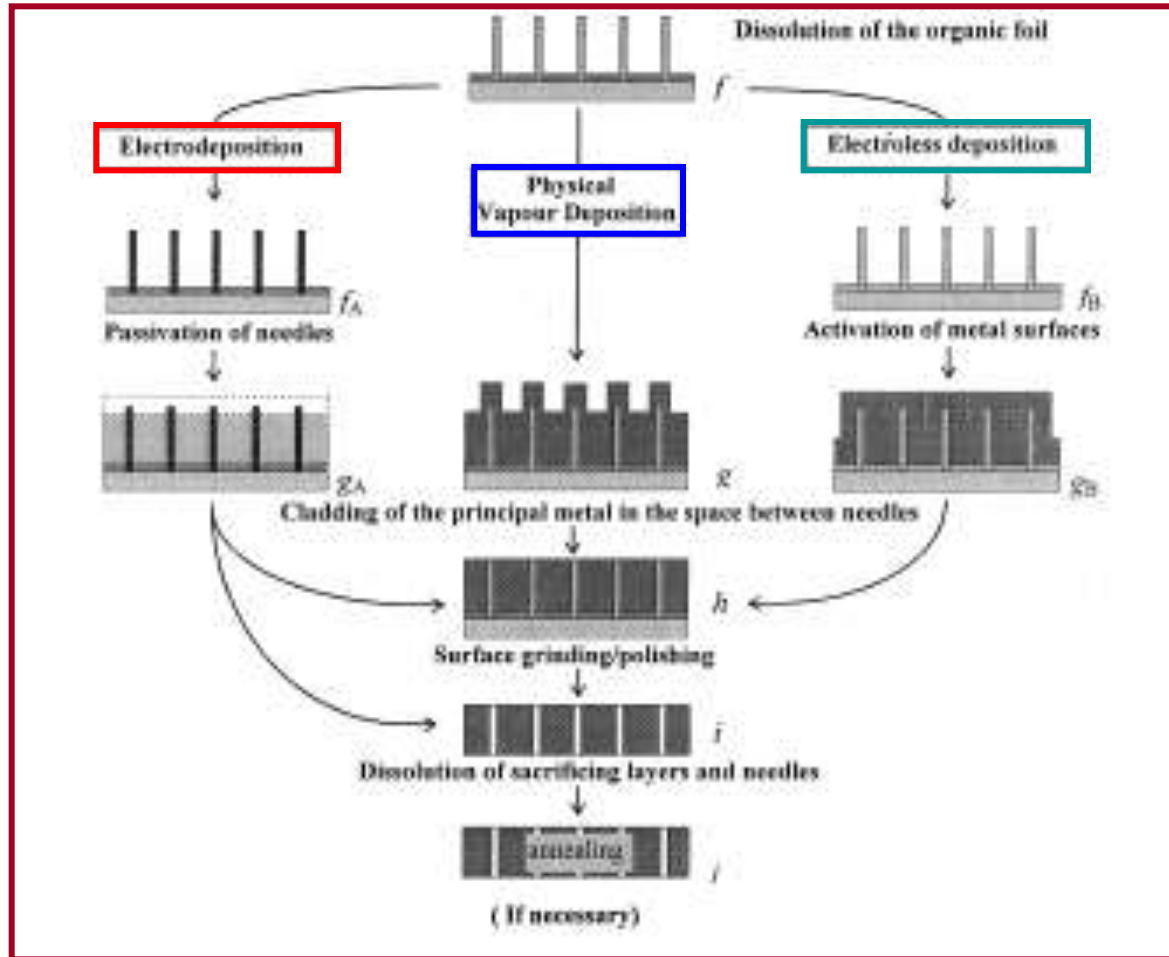
## Collaborators:

Prof. G. Mueller (Field Emission, Uni Wuppertal),  
Prof. A.M. Pucci (IR spectroscopy, Uni Heidelberg),  
Dr. W. Sigle (TEM, MPI, Stuttgart)  
Prof. F. Voelklein (Thermoelectrics, Uni Wiesbaden)  
Dr. Doug L. Medlin (TEM, Sandia National Labs)





# Metal membranes by double replication





# Synthesis and Characterisation of Low Density Porous Polymers Made by Reversible Addition Fragmentation Chain Transfer (RAFT)

Wigen Nazarov<sup>1</sup>, Christopher Musgrave<sup>1</sup>, Kimberley L. Anderson<sup>2</sup>,  
Nick Bazin<sup>3</sup>, Douglas Faith<sup>3</sup>

<sup>1</sup> *University of St Andrews, Unit 4, High Energy Laser Materials Laboratory, North Haugh, St Andrews, Fife, KY16 9ST, UK.*

<sup>2</sup> *Department of Pure & Applied Chemistry, University of Strathclyde Thomas Graham Building, 295 Cathedral Street, Glasgow, G1 1XL, UK.*

<sup>3</sup> *Atomic Weapons Establishment, Reading, RG7 6DP, UK.*

## Aims and objectives

- To synthesise a polymeric foam with high degree of polydispersity index using RAFT reagent.

$$\text{PDI} = \frac{\overline{M_w}}{\overline{M_n}} \geq 1$$

- To use RAFT synthetic method and investigate the effect of RAFT reagents for the production of polymeric foams, specifically poly-HIPE foams
- To investigate the differences between HIPE foam synthesised using RAFT reagents and HIPE foams synthesised by free radical polymerisation – FRP

# Foams made from High Internal Phase Emulsions HIPE

## General:

- HIPEs have high strength at low density in comparison to other foams
- They have an open pore cellular structure and have been used in laser targets for many years
- All PolyHIPE used in laser targets have been synthesised from Styrene, Chlorostyrene and Divinyl Benzene monomers,

## Styrene Methyl methacrylate polyHIPE investigated in this Project:

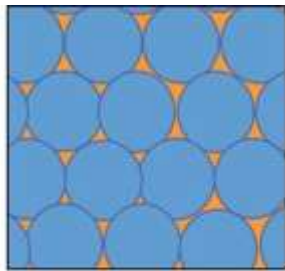
- Reasons for using Styrene Methyl Methacrylate co-polymers:
  - 1) It is a well characterised co-polymer system,
  - 2) Because measurements of polydispersity was important, Styrene-co-methyl methacrylate is soluble in many solvents, but styrene-co-DVB not as soluble

## High Internal Phase Emulsions HIPE

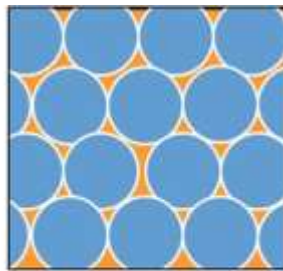
HIPE is an emulsion which consists of a dispersed (internal) and continuous phase stabilised by an appropriate surfactant.

For an emulsion system to qualify as a HIPE the dispersed (internal) phase must occupy more than 75% by volume. Typically most HIPEs are about 90% internal phase.

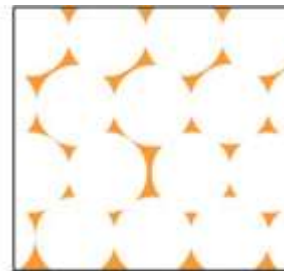
In the production of foams using HIPEs the internal phase is the pore former and the continuous phase is the polymerisable monomer (or monomers), stabilised by a surfactant and an initiator.



HIPE emulsion



polymerising  
HIPE emulsion

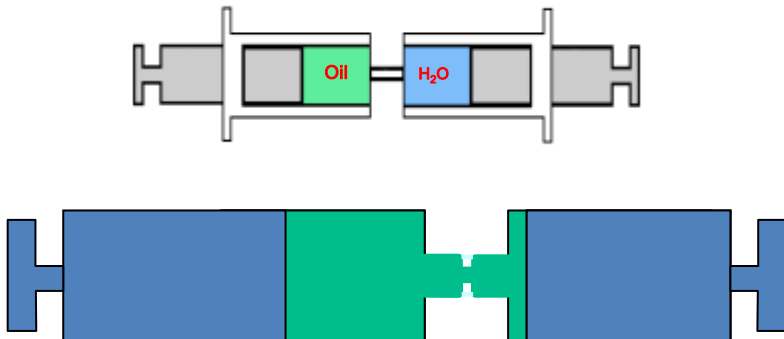


porous PolyHIPE

# Emulsification

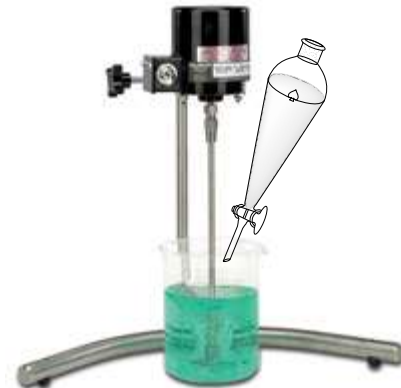
## 1. Syringe Method

The emulsion is produced by the shear force created when the liquids squeeze through the small orifice of the gas tight syringes, which are connected by a luer lock.

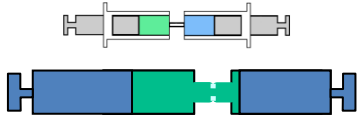


## 2. Mechanical Stirrer Method

The emulsion is produced by slow addition of the aqueous phase to the continuous oil phase, whilst stirring at moderate shear.



# Steps in Foam Production



emulsify



Place in airtight  
containers and  
Cure at 60 °C



Soxhlet  
Solvent  
extraction



Dry in moderate  
Oven or air

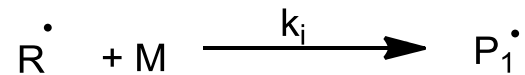


# Difference between FRP and RAFT polymerisation

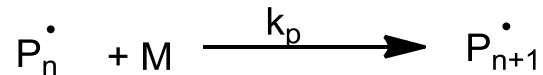
# Free Radical Polymerisation

ALL polyHIPE Foams made for Targets are made by Free Radical Polymerisation FRP

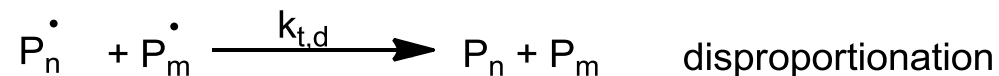
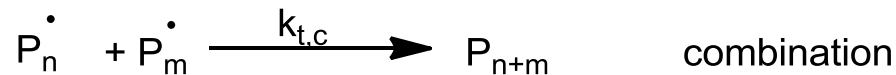
Initiation



Propagation



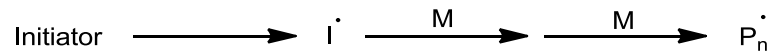
Termination



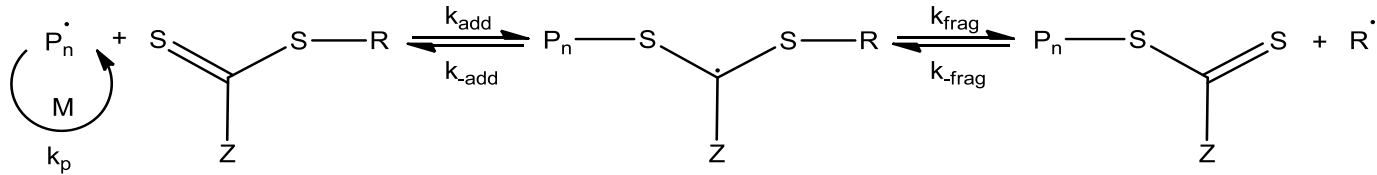


# Controlled Radical Polymerisation and the RAFT process

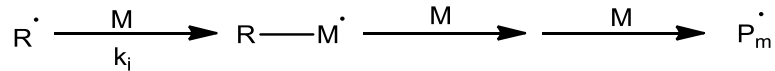
Initiation



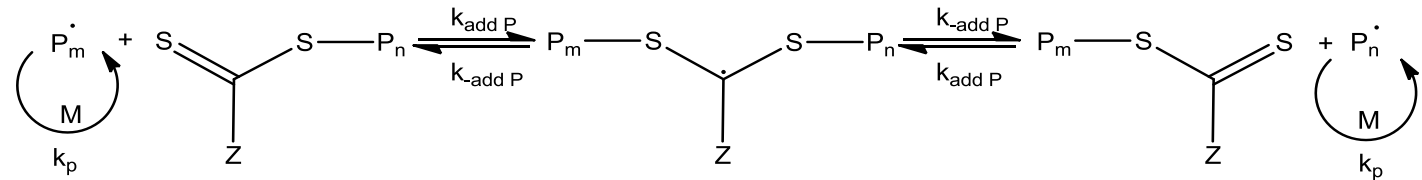
Reversible chain transfer/propagation



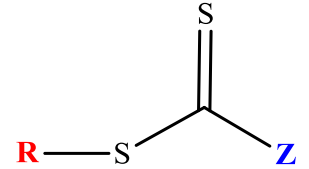
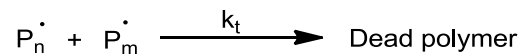
Reinitiation



Chain equilibrium/propagation

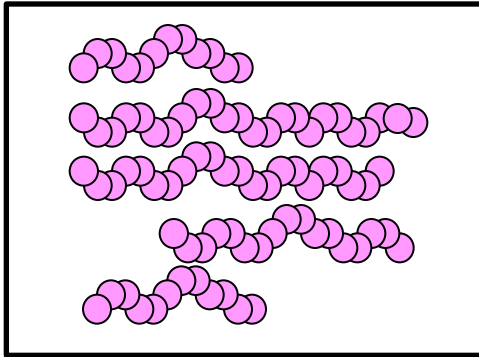


Termination



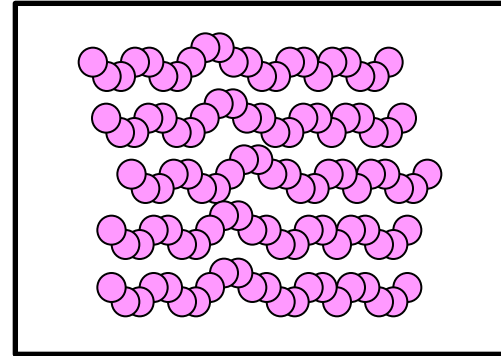
General Structure of RAFT reagent, **free radical leaving group R** and a **group Z which modifies the reactivity** of the C=S bond

## Comparisons between FRP and RAFT



### Free radical polymerisation

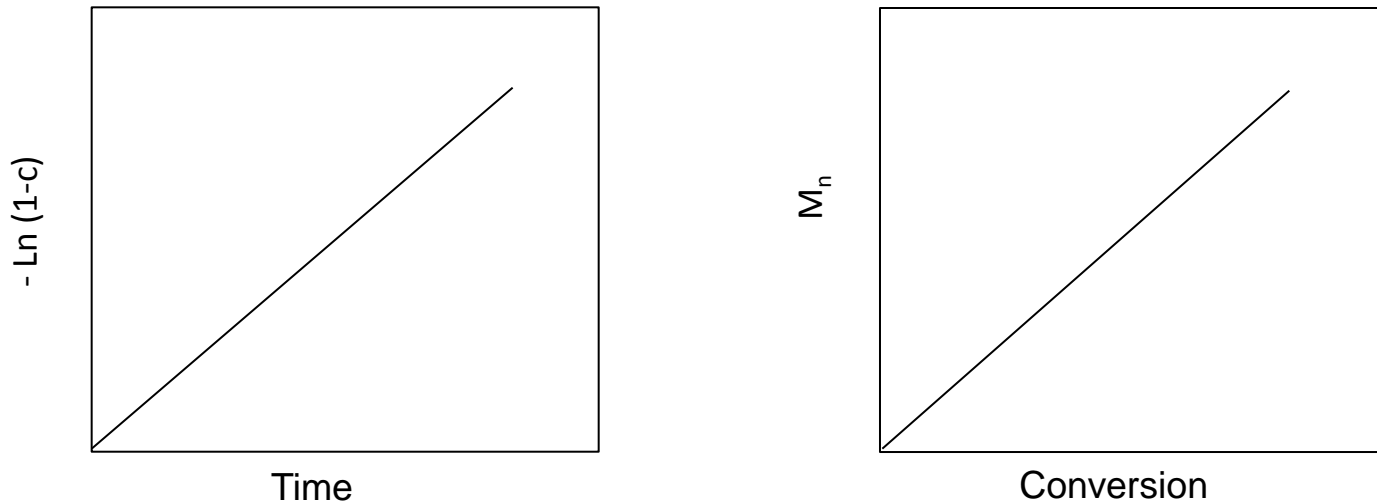
- Not a living process
- Cannot form architected polymers such as block copolymers
- Broad molecular weight distribution, high polydispersity index



### Controlled radical polymerisation

- Living process
- Able to produce architected polymers such as block copolymers
- Controlled molecular weights obtained, low polydispersity index

## Effect of RAFT reagent - Controlled polymerisation



- A plot of  $-\ln(1-\text{conversion})$  against time should show linear relationship
- The molecular weight ( $M_n$ ) should evolve linearly with conversion, close to theoretical prediction

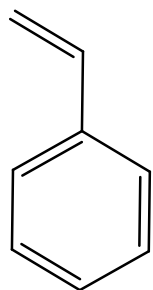
This trend is observed because the rate of polymer growth is constant and not dependant on monomer concentration but on

$$\frac{[\text{Monomer}]}{[\text{RAFT agent}]}$$

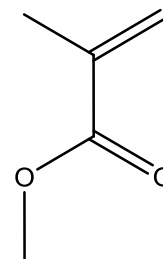
- Polydispersity index should decrease towards 1 as conversion increases, with final value  $<1.5$

## Polymer system prepared by RAFT polymerisation

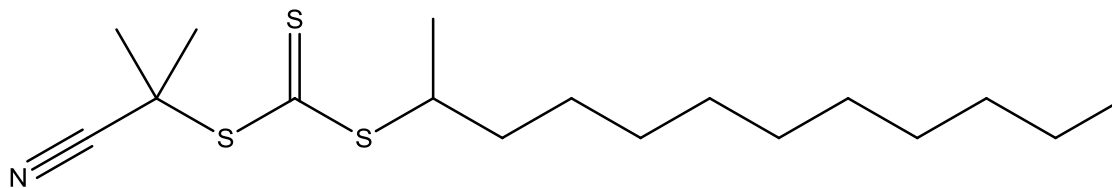
Monomers	Molar Ratio of Monomers	Polymer
styrene + methyl methacrylate	1:1, 2:1	PS- <i>co</i> -PMMA
styrene + methyl methacrylate (by RAFT polymerisation)	2:1	PS- <i>co</i> -PMMA



Styrene



Methyl Methacrylate (MMA)



S-(2-cyano-2-propyl)-S-dodecyltrithiocarbonate

## Choosing the reaction conditions for RAFT Polymerisation concentrations used

The ratio of RAFT agent to initiator must be kept high, to minimise the free radical interactions which results in termination

The ratio of [monomer] to [RAFT agent] pre determines the maximum number average molecular weight ( $M_n$ ) which will be reached.

$$\textit{Targetted degree of Polymerisation} = \frac{[\textit{monomer}]}{[\textit{RAFT agent}]}$$

$$M_{n(\textit{calc})} = (\textit{degree of polymerisation} \times M_{(\textit{monomer})}) + M_{(\textit{RAFT agent})}$$

For polymerisation of styrene and Methyl Methacrylate using RAFT reagents the following different concentrations of RAFT reagents used:

**Predicted  $M_{n \text{ calc}}$  = 30 365 g/mol - Small**

**Predicted  $M_{n \text{ calc}}$  = 141 119 g/mol - Medium**

**Predicted  $M_{n \text{ calc}}$  = 207 213 g/mol - Large**

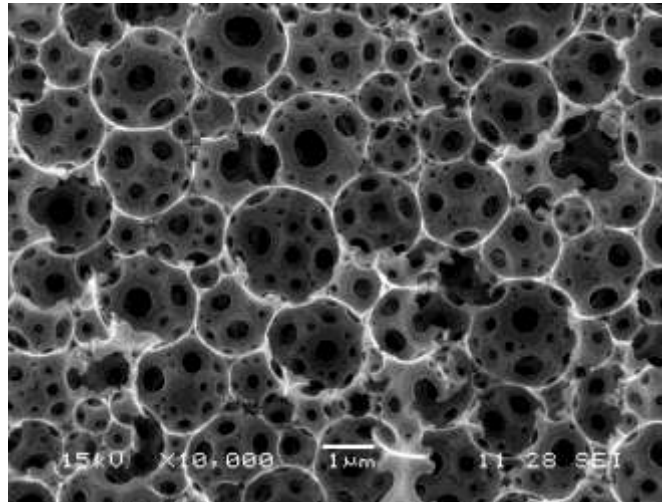
# Results and characterisation

## Results – GPC

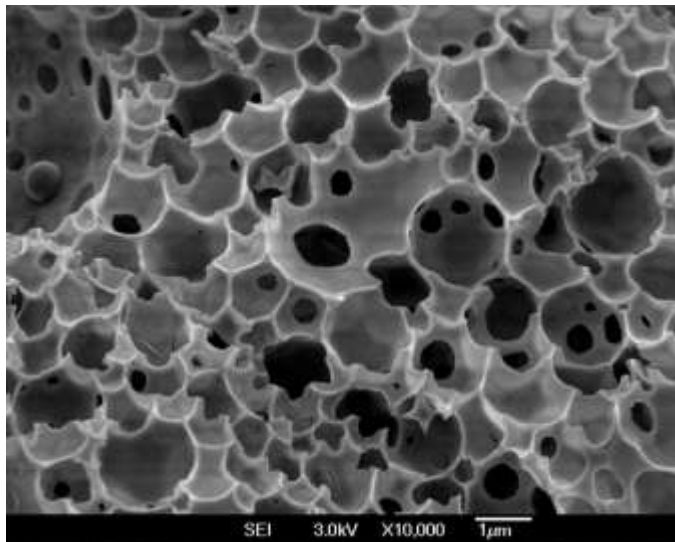
Sample	Molecular Weight Distribution (Polystyrene Equivalent) / Daltons				
	$M_n$	$M_w$	$M_z$	$M_p$	PDI
PS- <i>co</i> -PMMA <b>FRP</b>	113 900	533 000	1 892 300	178 700	4.68
PS- <i>co</i> -PMMA <b>RAFT Small</b> Peak 1	18 700	27 300	36 100	25 900	1.46
PS- <i>co</i> -PMMA RAFT Small Peak 2	Insufficient peak resolution			570 400	
PS- <i>co</i> -PMMA <b>RAFT Medium</b> Peak 1	81 150	159 230	268 760	130 000	1.96
PS- <i>co</i> -PMMA RAFT Medium Peak 2	Insufficient peak resolution				
PS- <i>co</i> -PMMA <b>RAFT Large</b> Peak 1	44 000	91 300	152 700	80 600	2.08
PS- <i>co</i> -PMMA RAFT Large Peak 2	Insufficient peak resolution				

# Results - SEM images

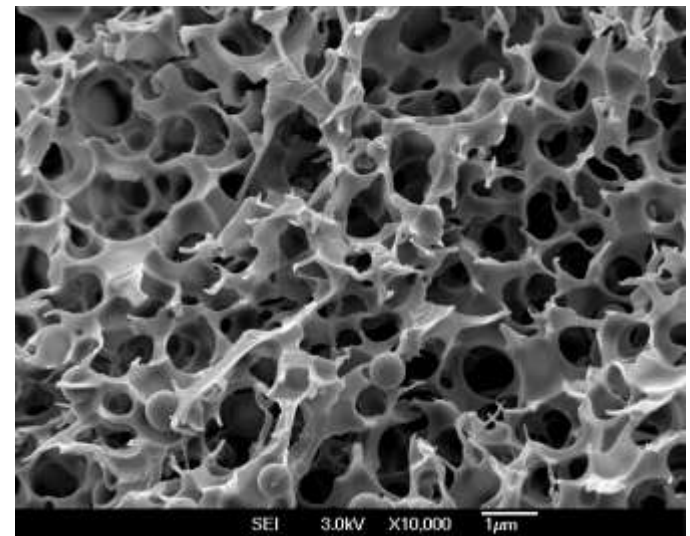
In all micrographs, Magnification = 10,000 Marker = 1  $\mu\text{m}$



PS-co-DVB HIPE



PS-co-PMMA RAFT Small



PS-co-PMMA HIPE Normal



# TDNMR results for Styrene-MMA polyHIPE foam

Material	Polymerisation method	T <sub>1</sub> relaxation time (ms)	T <sub>1ρ</sub> relaxation time (ms)	T <sub>2</sub> relaxation time (ms)
2:1 S:MMA	FRP	449 ± 3	0.7 ± 0.2	0.0083 ± 8 × 10 <sup>-5</sup>
			6.6 ± 0.2	
	RAFT small	320 ± 9	0.7 ± 0.2	0.0099 ± 2 × 10 <sup>-5</sup>
			6.3 ± 0.3	
	RAFT medium	440 ± 10	0.9 ± 0.3	0.0081 ± 1 × 10 <sup>-5</sup>
			7.0 ± 0.4	
	RAFT large	458 ± 10	0.5 ± 0.1	0.0082 ± 1 × 10 <sup>-4</sup>
			6.4 ± 0.2	

# Summery and Future Work

- It has been demonstrated that the Production of polyHIPEs using RAFT Reagents is possible and foams with low PDI are produced
- **Improvements and refinements**
  - ❑ Span 80 was used as a surfactant for the production of SMMA polyHIPE, However, SEM of SMMA PolyHIPE shows that there is some indication of emulsion breaking before polymerisation completed. Other surfactant, such as block co-polymers can be used which might considerably improve the polyHIPE structure of RAFT synthesised SMMA.
  - ❑ Using different RAFT concentrations to find the optimum PDI
  - ❑ Measurements of the strength of SMMA polyHIPE made using RAFT reagent and compare with SMMA polyHIPEs made by FRP to see whether the structural strength of SMMA polyHIPE has improved using RAFT reagents

# Acknowledgment

- Most of the synthetic work on RAFT was carried out by Kimberley Anderson and TDNMR work by Christopher Musgrave.
- We would like to thank all AWE characterisation team for carrying out GPC and SEM
- Special thanks to AWE for continuous financial support for High Energy Laser Materials Laboratory at St Andrews